Quantum Hall Edges Beyond Luttinger Liquid

Richard David Fern

Merton College

University of Oxford

A thesis submitted for the degree of

Doctor of Philosophy in Theoretical Physics

Trinity Term 2018

Quantum Hall Edges Beyond Luttinger Liquid

Richard David Fern

Merton College, University of Oxford

A thesis submitted for the degree of
Doctor of Philosophy in Theoretical Physics

Trinity Term 2018

Abstract

We consider a series of problems regarding quantum Hall edges, focusing on both dynamics and the mathematical structure of edge states.

We begin in Chapter 3 with a limiting case of the Laughlin state placed in a very steep confining potential, but which is weak compared to the interactions. We find that the eigenstates have a Jack polynomial structure and an energy spectrum which is extremely different from the well-known Luttinger liquid edge.

In Chapter 5 we analyse the inner products of edge state wavefunctions, using an effective description given by a large-N expansion ansatz proposed by J. Dubail, N. Read and E. Rezayi, PRB 86, 245310 (2012). As noted by these authors, the terms in this ansatz can be constrained using symmetry, a procedure we perform to high orders. We then check the conjecture by calculating overlaps exactly for small system sizes and comparing the numerics with our high-order expansion to find excellent agreement.

Finally, Chapter 6 considers the behaviour of quantum Hall edges close to the Luttinger liquid fixed point that occurs in the low energy, large system limit. We construct effective Hamiltonians using a local field theory description and then consider the effect of bulk symmetries on this edge. The symmetry analysis produces remarkable simplifications which allow for very accurate descriptions of the low-energy edge physics even relatively far away from the Luttinger liquid fixed point.

Acknowledgements

Books! And cleverness! There are more important things — friendship and bravery

— Hermione Granger [Harry Potter and the Philosopher's Stone, J.K. Rowling, 1997]

There are a number of people without whom this thesis would have been a great deal more difficult but it would have been impossible without my supervisor, Steve Simon, to whom I am extremely grateful. He has always been insightful, understanding, knowledgeable and patient and I wholeheartedly thank him for all the time and the many ideas he has shared with me over the course of these studies. I am also very grateful to Roberto Bondesan, with whom much of this work was completed in collaboration with. His insight, tutelage and encouragement were extremely valuable. Furthermore, I would like to thank Fabian Essler for steering me onto the path of Condensed Matter during my Masters studies and for his advice and good humour throughout.

I have been fortunate enough to share my time in Oxford with a number of excellent students and researchers. I am especially grateful to my various office mates during this time, including Dillon Liu for filling the office with amusement and the Moana soundtrack, Thomas Veness for his sage wisdom and all that climbing advice I apparently asked for and, of course, Stefan Groha, who has faced a full four-year term of my childishness with a caustic wit, but also a lot of geniality. I am also thankful to Jack Kemp and Yuri van Nieuwkerk for company in foreign lands and Fenner Harper, Zohar Ringel, Dmitry Kovrizhin and Adam Nahum for their valuable advice and support. I have also been lucky enough to enjoy a number of fruitful discussions with researchers from Oxford and further afield and so I thank, amongst others, Jérôme Dubail, Tom Price, Benoit Estienne, Nicolas Regnault, Hans Hansson and Paul Fendley for taking the time to listen and make important comments on my work.

I have also been supported by a number of friends during my time in Oxford and thank them all for their kindness. I am especially grateful to Samantha Love for long walks and life discussions and Alessandro Geraldini *per le stesse discussioni ma con più cibo Italiano e molto Lonely Island*. Finally, I would like to thank my parents and my sister. Your unending support through good times and bad has been invaluable.

The work presented in this thesis is based upon two publications[1, 2] and one submitted preprint[3]. This research was made possible in part by EPSRC grants EP/I031014/1 and EP/N01930X/1 and for this I would like to thank the British tax payer.

Contents

CHAPTER 1

Popular Science Background

Basic research is when I am doing what I don't know what I am doing.

— Wernher von Braun [New York Times, 1957]

The field within which this thesis fits is Theoretical Condensed Matter physics, which focuses on the description of large collections of objects which have been literally condensed into some phase of matter such as a solid or a liquid[4]. More specifically, the work is in quantum condensed matter, focusing on a particular phenomenon called the *Quantum Hall Effect*[5]. Quantum mechanics has proven incredibly useful in describing many properties of materials over the past century but its main utility is in explaining atomic-scale behaviour and how this affects what we see at our significantly larger scales[6]. However, the quantum Hall effect is a rare example of intrinsically quantum mechanical behaviour at our much larger scale.

The quantum Hall effect is also the archetypical example of a *topological* phase of matter[7]. Topology is an abstract field of mathematics which classifies how two shapes might be equivalent if one can be smoothly deformed, like putty, into the other[1][8] and the realisation that these concepts can be used to classify materials is a topic at the forefront of condensed matter physics today, credited with the Nobel Prize in Physics as recently as 2016[9]. The field has become

[1]For example, a sphere and a cube are equivalent but a sphere cannot be turned into a doughnut without tearing a hole in the centre.

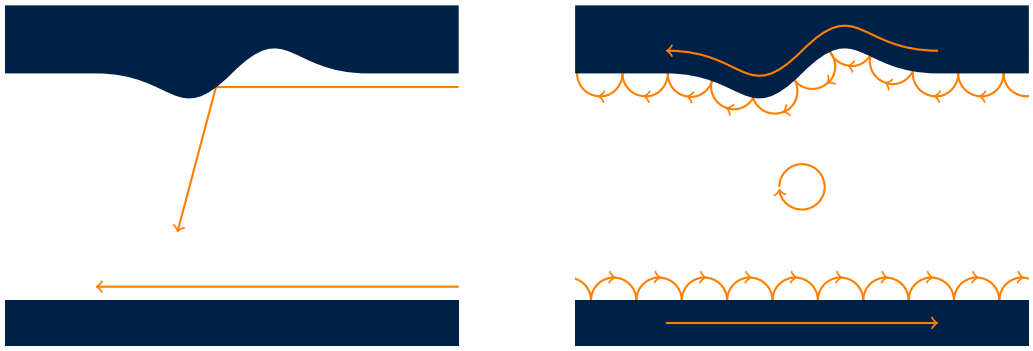

(a) (b)

Figure 1.1: In a magnetic field the charged electrons in a material move in circular orbits. Therefore, the electrons near the edge of our quantum Hall system end up bouncing along the boundary, generating a current along the edge of the system.

particularly exciting in recent years as efforts have been focused on using these remarkable phases of matter to build a quantum computer[10].

The particular focus of this work has been on describing the physics at the edges of quantum Hall systems. The quantum Hall effect is formed when an extremely thin piece of conducting material is exposed to an incredibly strong magnet and the exact way in which the current is transported through the material depends intimately on the edge of the system[11]. To understand this we first note that the electrical current is carried by charged electrons as they move through the material. When there are no magnets involved, electrons travel straight through the sample, as in Fig. 1.1a, until that motion is deviated by some imperfection or defect. This causes any current we try to push through the material to be resisted in much the same way that a stream of water encounters friction as it moves through a pipe.

However, in the presence of a magnet, charged particles are deflected and will move instead in circular paths[12]. Deep inside the material this is not so interesting but for the electrons near the edge something remarkable happens as the electrons try to move in their circular orbits but become continually deflected by the edge of the sample. This is demonstrated in Fig. 1.1b which shows that these

edge electrons find themselves bouncing along the edge, which in turn generates a current at the boundary. Note also that this current moves effortlessly around the dimple in the material and, given that the magnet only deflects the electrons into clockwise orbits, the current along the top edge can only move to the left whilst the current along the bottom edge can only move right.

We have used a variety of methods to try to better understand the behaviour at this edge. The picture presented above, whilst approximately correct, ignores a number of subtleties present in real systems. For example, we assumed that the electrons bounce against a hard boundary but, in truth, the edge might be significantly softer, more akin to trampoline than a brick wall. We have also ignored any interactions between the electrons. Therefore, this thesis considers a variety of problems to address these complications. In Chapter 3 we were able to exactly solve a particular extreme case for the edge softness, thus making some interesting links between quantum Hall edges and other condensed matter systems. In Chapter 5 we consider some of the mathematical structure necessary to calculate measureable quantities of these systems. Finally, in Chapter 6 we think of this edge as some quantum fluid and ask quite generally how it can move given the symmetries of the system as a whole. In doing so we are able to find how a more generic edge softness or inter-electron interactions cause simpler models to develop richer behaviour.

Part I

First Quantised Edges

CHAPTER 2

Introduction

There are no safe paths in this part of the world. Remember you are over the Edge of the Wild now, and in for all sorts of fun wherever you go.

— Gandalf the Grey [The Hobbit, J.R.R Tolkien, 1937]

The quantum Hall effect is the quintessential example of a topological phase of matter[9], containing many of the hallmark characteristics so omnipresent within this truly exciting field[13–17]. This single state of matter possesses macroscopic observables which are quantised to within a frightening degree of accuracy[5, 18], it supports quasiparticle excitations whose charges are some fraction of the fundamental electronic charge[19, 20] and whose exchange statistics correspond to neither bosons nor fermions[21–24] *and* it supports rich and interesting *topologically protected* edge states[11, 25] which we will analyse in great detail over the course of this thesis.

And yet, the quantum Hall effect is not simply a pin-up for the field. Perhaps the most exciting developments in topological matter during recent years have been the concerted efforts to build *topological quantum computers*[10, 26, 27]. A quantum computer relies on the high fidelity of its constituent qubits and in non-topological proposals errors due to small perturbations on the system constitute a considerable hurdle to be overcome[28]. However, by using the aforementioned quasiparticles with their unusual exchange statistics one could perform computations by braiding the worldines of these *anyons*. These computations are robust

to perturbations as they depend only on the topology of the paths travelled by the individual anyons so small deviations to the paths have no overall effect.

Much of this remarkable physics lies within the bulk of the system but equally amazing phenomena can be seen along the boundary. This edge constitutes the only low-energy degrees of freedom for these systems and supports dissipationless currents which move in one direction only[11, 29], therefore making it a prime example of a *chiral Luttinger liquid*[30, 31]. There is also an intriguing link to the bulk physics via *bulk-edge correspondence*[32, 33], which posits that the properties of the bulk are intrinsically related to the properties of the edge. This link is made more concrete in Chapter 4 where we discuss the construction of quantum Hall wavefunctions as correlation functions of a *conformal field theory*[22, 34, 35]. Furthermore, the edge is easy to measure[31, 36, 37]. On the other hand, certain properties of the bulk are difficult to measure conclusively[38–40] and therefore it has been suggested that experiments on the edges of quantum Hall systems might be used to infer bulk properties[41].

This thesis will be particularly focused on problems which are most applicable to potential future realisations of the quantum Hall effect in cold-atom settings. There are a variety of such proposals, some of the most promising of which involve only small numbers of particles[42–46]. However, the cold-atom setting gives unprecedented control over the confinement of and interactions between the constituent particles[47–49], which has led to a variety of discoveries in other areas of quantum condensed matter[50–52]. Therefore, one might hope for similar insights once the quantum Hall effect is realised in this setting.

Of course, a life on the edge begins with an appreciation of the bulk. Therefore, we begin this introductory chapter with a discussion of the integer quantum Hall effect in Section 2.1, focusing on the single particle picture before building up to the interacting case in Section 2.2 which spawns the fractional quantum Hall effect. We then discuss two ways to think about edge states, one of which is

often termed the microscopic picture in Section 2.3 before moving onto Wen's Hydrodynamic formulation[11] in Section 2.4.

2.1 The Integer Quantum Hall Effect

2.1.1 Two-Dimensional Particles

Consider a system of indistinguishable particles with electromagnetic charge q and effective mass m_q. The particles are placed into a trap defined by the potential $\mathcal{U}(x, y, z)$ and acted on by a magnetic field, $\boldsymbol{B}$. Ignoring interactions for the moment, the single-particle Hamiltonian for such a system is

$$\mathcal{H}_{3\mathrm{D}} = \frac{(\boldsymbol{\pi} - q\boldsymbol{\mathcal{A}})^2}{2m_q} + \mathcal{U}(x, y, z) \tag{2.1}$$

where $\boldsymbol{\pi} = (p_x, p_y, p_z)^{\mathrm{T}}$ is the particle's momentum vector and $\boldsymbol{\mathcal{A}}$ is the vector potential defined such that $\boldsymbol{B} = \nabla \times \boldsymbol{\mathcal{A}}$ [6, 12].

We are interested in two-dimensional physics and so design the confinement by splitting it into a relatively flat, isotropic part $U(x, y)$ and a deep valley in the perpendicular direction, $W(z)$. We also perform a gauge transformation on $\boldsymbol{\mathcal{A}}$ such that $\mathcal{A}_z = 0$, which leads the Hamiltonian to split naturally into two,

$$\mathcal{H}_{3\mathrm{D}} = \left[\frac{p_z^2}{2m_q} + W(z)\right] + \left[\frac{(\boldsymbol{p} - q\boldsymbol{A})^2}{2m_q} + U(x, y)\right] = \mathcal{H}_z + \mathcal{H} \tag{2.2}$$

where $\boldsymbol{p} = (p_x, p_y)^{\mathrm{T}}$ and $\boldsymbol{A} = (\mathcal{A}_x, \mathcal{A}_y)^{\mathrm{T}}$.

We now fix the magnetic field perpendicular to our planar system, $\boldsymbol{B} = B\hat{\boldsymbol{z}}$, which allows us to make $\boldsymbol{A}$ independent of z. Therefore, the original system decouples into two independent parts, $[\mathcal{H}_z, \mathcal{H}] = 0$, one existing in one dimension and the other in two. One can then consider constraining the locations of particles along z ever more precisely by creating an ever narrower potential, $W(z)$. This in turn increases the energy of excitations for motion along z and, once the first excitation energy is well above the thermal energy, the system always sits

in the zero-motion ground state of $\mathcal{H}_z$, thus making the system effectively two-dimensional.

2.1.2 In Magnetic Fields

Having restricted the problem to two-dimensions we may consider the physics of the integer quantum Hall effect[53–56]. Note that we will work on the plane throughout this thesis (as opposed to the cylinder or torus). In this planar case the problem is far simpler when working in the *symmetric gauge*, where the vector potential is taken to be $\boldsymbol{A} = \frac{B}{2}(-y, x)^{\mathrm{T}}$, giving

$$\mathcal{H} = \frac{1}{2m_q}\left(p_x + \frac{qBy}{2}\right)^2 + \frac{1}{2m_q}\left(p_y - \frac{qBx}{2}\right)^2 + U(x, y). \tag{2.3}$$

We will solve this perturbatively, taking $U(x, y)$ to be small and solving first for the kinetic term.

We begin by mapping the problem to the complex plane, $\mathbb{R}^2 \to \mathbb{C}$ via

$$z = x + iy, \qquad p = \frac{1}{2}(p_x - ip_y) \tag{2.4}$$

such that $p = -i\hbar\frac{\partial}{\partial z}$. Complex conjugate variables are denoted by $\bar{z}$ and $\bar{p}$. With these substitutions it can be shown that the Hamiltonian has the form

$$\mathcal{H} = \hbar\omega\left(a^\dagger a + \frac{1}{2}\right) \qquad \text{for} \qquad a^\dagger = \left(\frac{\ell_{\mathrm{B}}\sqrt{2}}{\hbar}\right)p + \left(\frac{i}{2\ell_{\mathrm{B}}\sqrt{2}}\right)\bar{z}, \tag{2.5}$$

where $\omega = \frac{qB}{m_q}$ is the cyclotron frequency and $\ell_{\mathrm{B}} = \sqrt{\frac{\hbar}{qB}}$ is the magnetic length[1]. Therefore, given that $a^\dagger$ is a ladder operator satisfying $[a, a^\dagger] = 1$, the Hamiltonian is that of a simple harmonic oscillator with energies $E_n = \hbar\omega\left(n + \frac{1}{2}\right)$ for principal quantum number $n \in \mathbb{Z}^+$. These levels are called *Landau Levels*[57].

[1]Note that to arrive at Eq. 2.5 we implicitly assumed that $qB > 0$. The result for $qB < 0$ is identical up to a constant and swapping variables, $(z, p) \leftrightarrow (\bar{z}, \bar{p})$.

2.1.3 Landau Levels

However, these ladder operators alone are not sufficient to determine the wavefunctions of the system. For this we construct a second set of ladder operators,

$$b^\dagger = \left(\frac{\ell_\mathrm{B}\sqrt{2}}{\hbar}\right)\bar{p} + \left(\frac{i}{2\ell_\mathrm{B}\sqrt{2}}\right)z, \tag{2.6}$$

which increment another quantum number, l. These have the property $[b, b^\dagger] = 1$ whilst both commuting with both a and $a^\dagger$ operators, and therefore the Hamiltonian. The full space of states is then constructed as

$$|\psi_{n,l}\rangle = \frac{\left(a^\dagger\right)^n\left(b^\dagger\right)^l}{\sqrt{n!l!}}|\psi_{0,0}\rangle \tag{2.7}$$

where the vacuum, $|\psi_{0,0}\rangle$, is the state annihilated by both a and b.

Throughout this thesis we will work in the lowest Landau level, $n = 0$. It is relatively straightforward to show that these are the states of the form

$$\psi_{0,l}(z,\bar{z}) = \left[\frac{1}{l!\left(2{\ell_\mathrm{B}}^2\right)^l}\right]^{\frac{1}{2}} z^l \exp\left(-\frac{z\bar{z}}{4\ell_B^2}\right), \tag{2.8}$$

[2]which describe rings of charge like those shown in Fig. 2.1. Higher Landau levels are reached by the repeated application of $a^\dagger$,

$$\left(a^\dagger\right)^n\psi_{0,l}(z,\bar{z}) \quad \propto \quad \left(\frac{\partial}{\partial z} - \frac{\bar{z}}{4{\ell_\mathrm{B}}^2}\right)^n\left(z^l e^{-\frac{z\bar{z}}{4{\ell_\mathrm{B}}^2}}\right) \tag{2.9}$$

which, using the Rodrigues representation for the *associated Laguerre polynomials*, $L_n^k(x) = e^x x^{-k}\frac{d^n}{dx^n}\left(x^{n+k}e^{-x}\right)$,[58] can be shown to have the form

$$\psi_{n,l}(z,\bar{z}) \quad \propto \quad z^{l-n}L_n^{l-n}\left(\frac{z\bar{z}}{2{\ell_\mathrm{B}}^2}\right)\exp\left(-\frac{z\bar{z}}{4{\ell_\mathrm{B}}^2}\right). \tag{2.10}$$

Finally, we note that angular momentum about the z-axis is a good quantum number of our system with the operator

$$L_z = xp_y - yp_x = i(zp - \bar{z}\bar{p}) \tag{2.11}$$

[2] Note that the normalisation given here depends on our choice of integration measure. We use $\int \mathrm{d}^2z/2\pi{\ell_\mathrm{B}}^2$ here, which simply scales all inner products by an overall constant.

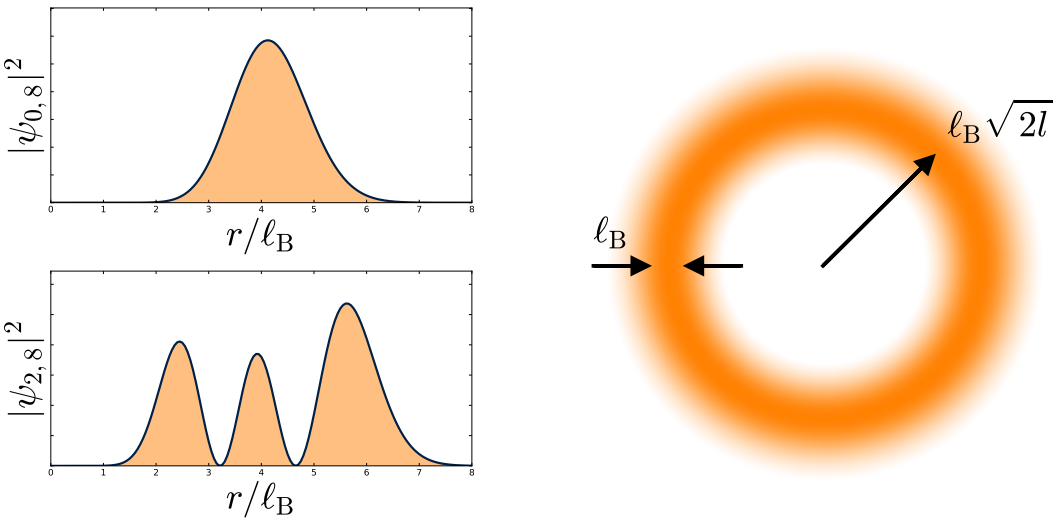

(a) (b)

Figure 2.1: The probability density of the wavefunctions $|\psi_{0,l}\rangle$ plotted (a) as function of the radius for the $n = 0$ and $n = 2$ Landau levels and (b) across the plane in the lowest Landau level.

commuting with our Hamiltonian. We can also phrase this in terms of the ladder operators as $L_z = \hbar\big(b^\dagger b - a^\dagger a\big)$ and therefore a given state has angular momentum

$$L_z|\psi_{n,l}\rangle = \hbar(l-n)|\psi_{n,l}\rangle. \tag{2.12}$$

2.1.4 Many Particles

We now wish to add N fermionic particles to the system. In the continued absence of confinement there is no unique ground state as there exists an infinite number of states in the lowest Landau level with ever higher angular momentum. However, consider restricting our particles to a region of area $A = \pi R^2$. Given that each wavefunction describes a distribution centered around the origin with a radius of $\ell_B\sqrt{2l}$, we see that only particles with $l < \frac{A}{2\pi{\ell_B}^2}$ are enclosed within our system. This gives each Landau level a degeneracy of $N_\Phi = \frac{\Phi}{\Phi_0}$ where Φ is the total magnetic flux through our sample and $\Phi_0 = \frac{h}{q}$ is the *magnetic flux quantum.*

Therefore, consider adding exactly enough particles to fill the lowest Landau

level. In this case all the orbitals from $l = 0$ to $l = N - 1$ are filled such that our (unnormalised) many-body wavefunction has the form

$$\Psi(z_1, \ldots, z_N) = \left| \begin{pmatrix} z_1^0 & \cdots & z_1^{N-1} \\ \vdots & \ddots & \vdots \\ z_N^0 & \cdots & z_N^{N-1} \end{pmatrix} \right| \exp\left(\sum_i \frac{|z_i|^2}{4{\ell_\mathrm{B}}^2} \right) \tag{2.13}$$

where $|X|$ denotes a Slater determinant of the matrix X. Therefore, the wavefunction is a polynomial of the z_i with total degree $\frac{N(N-1)}{2}$. By fermionic exclusion this polynomial must vanish whenever any two z_i are equal, implying that the polynomial has roots $(z_i - z_j)$ for all pairs i and j. Noting that there are $\frac{N(N-1)}{2}$ such pairs, the wavefunction must simply be

$$\Psi(z_1, \ldots, z_N) = \prod_{1 \le i < j \le N} (z_i - z_j) \exp\left(\sum_i \frac{|z_i|^2}{4{\ell_\mathrm{B}}^2} \right) \tag{2.14}$$

by power counting where $\Delta = \prod(z_i - z_j)$ is often called a *Jastrow factor*.

2.1.5 The System's Edge

The simple analysis provided above for the degeneracy of a given Landau level is adequate for the thermodynamic limit though belies some of the complexity of the situation. A real experimental system holds its electrons in with some confinement, which we will take to be rotationally symmetry, thus defining a circular sample. Therefore, each orbital is uplifted by an energy

$$U_{n,l} = \langle \psi_{n,l} | U | \psi_{n,l} \rangle = \int \mathrm{d}^2 z |\psi_{n,l}|^2 U(r) \tag{2.15}$$

where $r = |z|$ is the radial distance from the origin. The ground state then occupies those N orbitals for which $U_{n,l}$ is the smallest. Such a situation is given in Fig. 2.2a, which plots $U_{0,l}$ for particles confined in a circular well of height u_0. Given that the charge distributions are really smeared out, an orbital whose centre lies within the well can still be raised in energy, and this leads to a smooth transition from zero energy to u_0. Consequently, even though the bulk of the

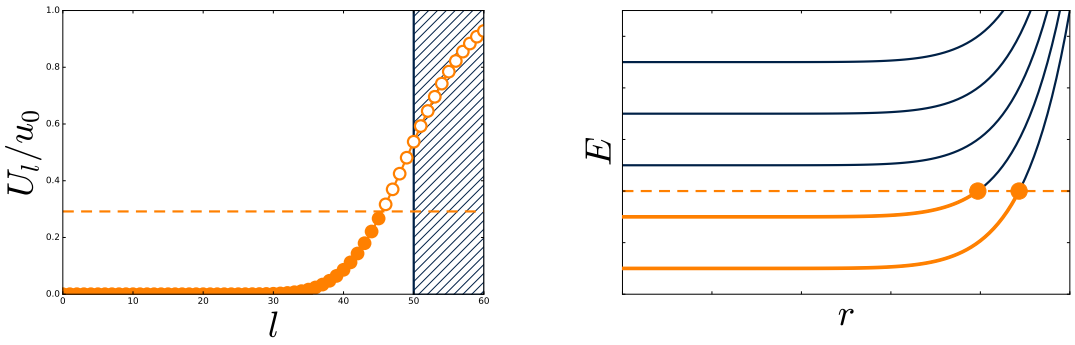

(a) (b)

Figure 2.2: (a) shows the cost of occupying orbital l in the lowest Landau level given confinement $U = u_0\Theta(r - 10\ell_B)$ where Θ is the Heaviside step function and r the radius from the origin. Those orbitals within the hatched region have their radius outside this confinement. Adding 45 particles would then fill all the states below the dashed line. In (b) we consider a coarse-grained picture including multiple Landau levels. States near the system's edge increase smoothly in energy such that there exist gapless edge excitations even when the chemical potential lies between Landau levels in the bulk[25].

system is gapped, there exists gapless edge excitations of the ground state which are localised near the edge of our system. This is also demonstrated in Fig. 2.2b where confinement causes the states localised near the edge of every Landau level to be raised in energy. Therefore, even when the chemical potential lies between two Landau levels, suggesting that the system might be gapped, we have gapless excitations at the edges of the system.

Aside 1

It is worth noting how this picture tends towards the thermodynamic limit, focusing on the case in Fig. 2.2a. Recall that the single-particle wavefunctions are rings of charge with a radius $\ell_B\sqrt{2l}$ and a width of around ℓ_B. Therefore, imposing a quantum well potential of depth u_0 at radius $R = \ell_B\sqrt{2l_0}$ will have little effect on all states at radii below $R - \ell_B$ and simply confer an energy u_0 to states at radii above $R + \ell_B$. However, the states from $l = l_0 - \sqrt{2l_0}$

to $l_0 + \sqrt{2l_0}$ sit within the smooth transition. Therefore, the total fraction of states near the edge varies as $\frac{1}{\sqrt{l_0}}$, thus validating the previous analysis when l_0 is large.

2.2 The Fractional Quantum Hall Effect

2.2.1 Interactions

The results of the preceding single-particle analysis are accurate when the number of Landau levels filled, ν, is at or near an integer. However, when a Landau level becomes partially filled the picture changes because we can no longer assume that the states are all degenerate. Instead one finds experimentally that new gaps appear in the spectrum[59, 60], and so we must search for something that might explain this broken degeneracy.

The obvious cause is the neglected interactions between particles. The full Hamiltonian we are interested in solving is not that given by Eq. 2.3 but

$$\mathcal{H} = \sum_{i=1}^{N} \frac{(\boldsymbol{p}_i - q\boldsymbol{A})^2}{2m_q} + \sum_{1\leq i<j\leq N} V(\boldsymbol{r}_i - \boldsymbol{r}_j) + \sum_{i=1}^{N} U(\boldsymbol{r}_i). \tag{2.16}$$

The solution of this Hamiltonian for arbitrary system sizes and for most typical interactions is exceedingly difficult. However, given that the single-particle analysis works so well for the majority of cases, we can perhaps consider the interactions as a perturbation, and this will simplify matters somewhat. In fact, in this thesis we will always work in a limit

$$\hbar\omega_c \gg V \gg U. \tag{2.17}$$

We therefore begin with a recap of the simple two-body problem in the lowest Landau level.

2.2.2 The Two-Body Problem

The solution of the kinetic term in Eq. 2.16 provides us with the orbitals in Eq. 2.8. Therefore, the two particle Hilbert space is made up of states

$$\langle z_1, z_2 | l_1, l_2 \rangle \quad \propto \quad z_1^{l_1} z_2^{l_2} \exp\left(-\frac{|z_1|^2 + |z_2|^2}{4{\ell_\mathrm{B}}^2} \right). \tag{2.18}$$

Throughout this thesis we will consider interactions which are both rotationally and translationally invariant, and therefore $V = V(|z_1 - z_2|)$. It is therefore more convenient to diagonalise V in a basis of states

$$\langle z_1, z_2 | l, L \rangle \quad \propto \quad z^l Z^L \exp\left(-\frac{|z|^2}{8{\ell_\mathrm{B}}^2} + \frac{|Z|^2}{2{\ell_\mathrm{B}}^2} \right). \tag{2.19}$$

where $z = z_1 - z_2$ and $Z = \frac{z_1 + z_2}{2}$ are the relative and centre-of-mass coordinates respectively. Therefore, the matrix elements of V in this basis are diagonal and independent of the centre-of-mass angular momentum, L, with

$$v_l = \langle l, L | V | l, L \rangle. \tag{2.20}$$

Example 1

For example, the matrix elements of the Coulomb interaction, $V(|z|) = \frac{v_\mathrm{c}}{|z|}$, are of the form

$$v_l[V] = \frac{v_\mathrm{C}}{l!(2\ell_\mathrm{B})^{2l+2}} \int \frac{\mathrm{d}^2 z}{\pi} |z|^{2l-1} e^{-\frac{|z|^2}{4{\ell_\mathrm{B}}^2}} = \frac{v_\mathrm{C}\sqrt{\pi}}{4\ell_\mathrm{B}} \frac{(2l-1)!!}{(2l)!!} \tag{2.21}$$

where $n!! = n(n-2)(n-4)\ldots$ is the double factorial. This is plotted in Fig. 2.3 alongside the same results for hard-core interactions. In the Coulomb case, v_l varies as $\frac{1}{\sqrt{l}}$ for large l, indicating that the interaction is smaller when the relative angular momentum is larger.

We can understand this variation when we realise that the state $|l, L\rangle$ describes particles z_1 and z_2 whose relative position is distributed as a ring of charge like that in Fig. 2.1b with a radius that varies at $\sqrt{l}$. Therefore, higher l separates the particles further.

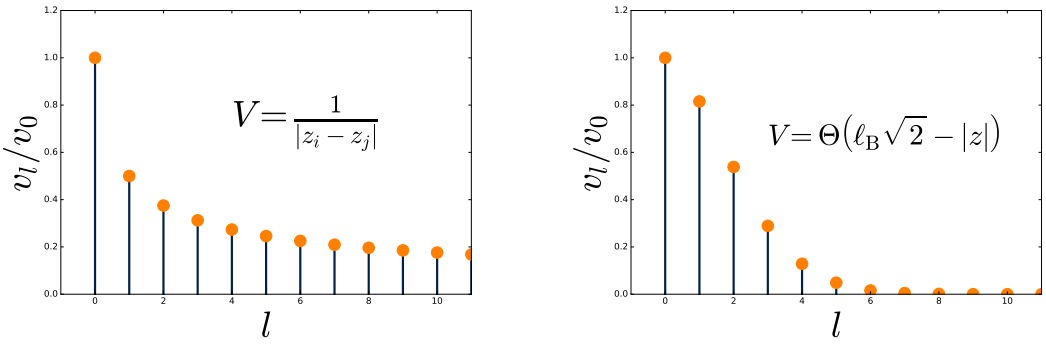

(a) (b)

Figure 2.3: (a) shows the size of the pseudopotentials of a Coulomb interaction as calculated in Eq. 2.21. We also show the pseudopotentials for a hard-core interaction in (b), which fall off quickly once the orbitals are centered outside the core.

Consider now that we can design some interactions, V_k, for which

$$v_l[V_k] = \delta_{l,k}. \tag{2.22}$$

These effective interactions are called the *Haldane pseudopotentials*[61] and can be used to replicate the matrix elements of any generic interaction V via

$$V(|z_1 - z_2|) = \sum_{k=0}^{\infty} v_k[V] V_k(|z_1 - z_2|). \tag{2.23}$$

An explicit construction of these $V_k(|z_i - z_j|)$ in a position representation is presented in Derivation 1 below.

Derivation 1

The Haldane pseudopotentials $V_k(|z|)$ are interactions defined such that

$$v_l[V_k] = \frac{1}{l!(2\ell_B)^{2l+2}} \int \frac{\mathrm{d}^2 z}{\pi} V_k(|z|)|z|^{2l} e^{-\frac{|z|^2}{4{\ell_B}^2}} = \delta_{l,k}. \tag{2.24}$$

Such an interaction can be constructed as

$$V_k(z,\bar{z}) = \left[\frac{4\pi {\ell_B}^2}{k!}\right] e^{\frac{|z|^2}{4{\ell_B}^2}} \left(4{\ell_B}^2 \partial\bar{\partial}\right)^k \left(\delta^{(2)}(z) e^{-\frac{|z|^2}{4{\ell_B}^2}}\right) \tag{2.25}$$

where $\partial = \frac{\partial}{\partial z}$. To check that this produces the required Kronecker-delta one first cancels the exponential factors and then integrates by parts. If $k > l$ then the integral evaluates to zero at this step. If $k \leq l$ we are left integrating $|z|^{2(l-k)}\delta^{(2)}(z)$, which evaluates to zero unless $k = l$.

Finally, this can be put into the more conventional form by commuting the exponential factors through the derivatives, leading to the result

$$V_k(z, \bar{z}) \propto L_k\big(-{\ell_\mathrm{B}}^2\nabla^2\big)\delta^{(2)}(z) \tag{2.26}$$

where $L_k(x)$ is the k^{th} Laguerre polynomial[62].

2.2.3 The Laughlin State

We have seen that the result of interactions is to maximise the relative angular momentum between pairs of particles, thus distancing them as much as possible. Therefore, consider a sample containing $N = N_\Phi/m$ particles where m is an integer[3], corresponding to filling only the lowest Landau level to $\nu = 1/m$. The confines of our system imply that the maximum angular momentum any particle can have is not far from mN. Therefore, we should design a wavefunction which maximises the minimum relative angular momentum between any pair of particles whilst remaining within this limit. The result is the Laughlin wavefunction,

$$\Psi^{(m)}(z_1, \ldots, z_N) = \prod_{1 \leq i < j \leq N} (z_i - z_j)^m \exp\left(\sum_i \frac{|z_i|^2}{4{\ell_\mathrm{B}}^2}\right), \tag{2.27}$$

a variational ansatz proposed by Robert Laughlin in 1983 to describe the then-called "anomalous quantum Hall effect" at filling $\nu = 1/3$ [19]. Whilst it is not the exact ground state of our full Hamiltonian it shows extremely good overlap with that state as found numerically and both are thought to be in the same

[3] Note that, unlike in the integer quantum Hall case, we will not force the particles to be fermionic. However, in the original problem considered by Laughlin, the particles were fermionic which we shall see requires m to be odd.

universality class[4][63].

Aside 2

Note that throughout this thesis we will use curly Dirac notation for many body states such as the Laughlin state in Eq. 2.27. Specifically, instead of $\Psi^{(m)}$ being expressed in the usual way as $\langle \boldsymbol{z} | \Psi^{(m)} \rangle$ we will use the notation

$$\Psi^{(m)}(z_1, \ldots, z_N) = \{ \boldsymbol{z} | \Psi^{(m)} \} \tag{2.28}$$

where $\boldsymbol{z} = (z_1, \ldots, z_N)$. The reason for this unconventional choice will be made clear in Part II of this thesis where we will need to make regular use of two distinct spaces of states, one of which will be many-body states such as the Laughlin state in Eq. 2.27 and another auxiliary space from *conformal field theory* which we will use to label these many-body states. It is hence important to make a clear notational distinction.

2.2.4 Parent Hamiltonians

Given this ansatz it is possible to work backwards and find the Hamiltonian for which this is the exact ground state[64, 65]. Such a Hamiltonian can be constructed with the Haldane pseudopotentials, recalling that V_k imposes a cost only on particles with relative angular momentum of k, i.e, states which vary as $(z_i - z_j)^k$. Therefore, one simply truncates the sum of Eq. 2.23 for general interactions, taking

$$V_m(\boldsymbol{r}_i - \boldsymbol{r}_j) = \sum_{k=0}^{m-1} v_k V_k(\boldsymbol{r}_i - \boldsymbol{r}_j) \tag{2.29}$$

where all $v_k > 0$. As we can see from Fig. 2.3, such a truncation is perhaps even natural for the case of hard-core interactions[5]. Taking these interactions leads to

[4] Note that the Laughlin wavefunction is antisymmetric with respect to an exchange of any two particles only when m is odd, corresponding to fermions. Conversely, the bosonic fractional quantum Hall effect is described by m even.

[5] Of course, this does not imply that such a truncation is unnatural for Coulomb interactions. Terms we neglect must be small compared to something and in this case we always have a

our parent Hamiltonian,

$$\mathcal{H}_m = \sum_{i=1}^{N} \frac{(\boldsymbol{p}_i - q\boldsymbol{A})^2}{2m_q} + \sum_{1\leq i<j\leq N} V_m(\boldsymbol{r}_i - \boldsymbol{r}_j), \tag{2.30}$$

which confers an energy cost to any wavefunction which vanishes slower than $(z_i - z_j)^m$. The maximally compressed ground state (i.e, the state which takes up the smallest area) of our parent Hamiltonian is then the Laughlin wavefunction, Eq. 2.27.

Aside 3

The quantum Hall effect has long been considered in two-dimensional electron gases within semiconductors[60]. Typically one sandwiches a thin layer of GaAs between two layers AlAs which, given the energy difference between the conduction bands of these two systems, creates a quantum well which the electrons fill[4]. When the GaAs layer in thin enough, this system becomes effectively two-dimensional as discussed in Section 2.1.1.

However, there has been significant recent interest in realising the quantum Hall effect in cold atom experiments[43, 45]. Freed from the messiness of crystalline samples and with significant control over the inter-particle interactions and confinement, these systems are an ideal location to observe many new and exciting phenomena in condensed matter physics. For quantum Hall physics this includes the possibility of realising a bosonic quantum Hall phase[42]. To do so, one could use uncharged particles, whose interactions are much closer to hard-core and so better approximated by pseudopotential interactions, but which also requires us to replace the Lorentz force with an equivalent, Coriolis force, as achieved by imparting rotational motion on the system[44].

balance between the interactions and the overall confinement. Therefore, if the confines of our system are such that the $\nu = \frac{1}{m}$ just fits inside then there will usually be no way of rearranging the wavefunction to satisfy the V_k for $k \geq m$ without expanding the wavefunction and incurring large confinement costs. Therefore, these remaining pseudopotentials are typically just a mean field energy shift to any possible ground state.

2.3 Edge States

2.3.1 States as Polynomials

It is worth noting that the Laughlin wavefunction is the unique *maximally compressed* ground state of $\mathcal{H}_m$ but it is not the only ground state. We have yet to impose any confinement on our system and so every single-particle orbital on the plane, $\psi_{0,l}$, has the same energy. Once the interactions are imposed we then realise that the ground states of our system are not only the Laughlin state, Eq. 2.27, but *any* holomorphic polynomial of the z_i which contains the factors $(z_i - z_j)^m$. Therefore, any

$$\Psi_{\mathcal{P}}^{(m)}(\boldsymbol{z}) = \mathcal{P}(\boldsymbol{z}) \prod_{1\leq i<j\leq N} (z_i - z_j)^m \exp\left(-\sum_{i=1}^{N} \frac{|z_i|^2}{4{\ell_{\mathrm{B}}}^2}\right) \tag{2.31}$$

is a ground state of $\mathcal{H}_m$ where $\mathcal{P}(\boldsymbol{z})$ is a symmetric polynomial of the positions $\boldsymbol{z} = (z_1, \ldots, z_N)$. Note that $\mathcal{P}$ must be symmetric to preserve the overall symmetry of the maximally compressed ground state.

We will call the polynomials, $\mathcal{P}$, *edge states*. This is because any polynomial will add an amount of angular momentum equal to its total degree, which we call ΔL, and this in turn pushes the particles further from the origin, thus expanding the state. Once the system is confined and the maximally compressed state becomes the ground state, these are then exactly the gapless edge states discussed in Fig. 2.2.

Example 2

Consider the $m = 1$ Laughlin state, which is identical to the integer quantum Hall effect at $\nu = 1$. In that case, the ground state (in confinement) can be represented by a series of filled orbitals as in Fig. 2.2a, with the ground state

given by a single slater determinant. We represent this by some *root state*,

$$|\cdots \mathbf{1}\,\mathbf{1}\,\mathbf{1}\,\mathbf{1}\,0\,0\,0\,0\} = \tag{2.32}$$

An excitation is formed by moving the fermions out to higher orbitals, the simplest $\Delta L = 1$ excitation being of the form

$$|\cdots \mathbf{1}\,\mathbf{1}\,\mathbf{1}\,0\,\mathbf{1}\,0\,0\,0\} = \tag{2.33}$$

As ΔL increases the number of ways to distribute the angular momentum amongst the particles also increases. For example, at $\Delta L = 5$ there are seven different options, one of which is given by

$$|\cdots \mathbf{1}\,\mathbf{1}\,0\,0\,\mathbf{1}\,0\,\mathbf{1}\,0\} = \tag{2.34}$$

2.3.2 Symmetric Polynomials

There exists an unending plethora of interchangeable bases with which to represent symmetric polynomials[66–69]. These include the power sums, the elementary symmetric polynomials, the Schur and Jack polynomials, the monomials and the complete homogenous symmetric polynomials. Each is a rich set of objects with a variety of intriguing properties. Within this thesis we will use the monomials, the power sums and the Jack polynomials (which include the Schur polynomials as a special case).

Monomials

The most fundamental of these bases are the monomials,

$$m_{\boldsymbol{\lambda}} = \mathbb{S}\big(z_1^{\lambda_1} z_2^{\lambda_2} \cdots\big), \tag{2.35}$$

where $\boldsymbol{\lambda}$ is a collection of positive integers $\boldsymbol{\lambda} = \{\lambda_1, \lambda_2, \ldots\}$ which we will order such that $\lambda_1 \geq \lambda_2 \geq \ldots$ and we use $\mathbb{S}$ to denote symmetrisation over all particles z_i. Therefore, when a single monomial $m_{\boldsymbol{\lambda}}$ multiplies the Laughlin state it adds λ_1 units of angular momentum to one particle, λ_2 to another and so on. The total added angular momentum is then the total degree of the polynomial, $\Delta L = |\boldsymbol{\lambda}| = \sum \lambda_i$.[6]

Power Sums

The simplest basis of symmetric polynomials are the power sums

$$p_n = \sum_i z_i^n \qquad \text{and} \qquad P_{\boldsymbol{\lambda}} = \prod_{\lambda_i} p_{\lambda_i}. \tag{2.36}$$

The individual p_n are simply the monomials, $m_{\{n\}}$, and they add n units of angular momentum to any one particle. Therefore, $P_{\boldsymbol{\lambda}}$ adds λ_1 units of angular momentum to any particle, then λ_2 units to any particle, and so on. This construction differs from the monomials in that the same particle could be bumped up multiple times.

Jack Polynomials

The Jacks are not so simple[70, 71]. We first require the concept of *lexicographical ordering*. Considering two partitions, $\boldsymbol{\lambda}$ and $\boldsymbol{\mu}$, we say that $\boldsymbol{\lambda} > \boldsymbol{\mu}$ if $\lambda_1 > \mu_1$. However, if $\lambda_1 = \mu_1$ then we compare the second element in each partition, and so on. So, for example, $\{5\} > \{4, 4, 4\}$ and $\{2, 2, 2\} > \{2, 2, 1, 1\}$.

Next, we must define an inner product on the power sums,

$$(P_{\boldsymbol{\lambda}}, P_{\boldsymbol{\mu}}) = \delta_{\boldsymbol{\lambda},\boldsymbol{\mu}} \zeta_{\boldsymbol{\lambda}} \alpha^{\ell(\boldsymbol{\lambda})}, \qquad \zeta_{\boldsymbol{\lambda}} = \prod_{n=1}^{\infty} m_n^{\boldsymbol{\lambda}}! n^{m_n^{\boldsymbol{\lambda}}} \tag{2.37}$$

where $m_n^{\boldsymbol{\lambda}}$ is the number of occurrences of the integer n within $\boldsymbol{\lambda}$ (so, for example, $m_2^{\{2,2\}} = 2$ and $m_1^{\{3,2\}} = 0$) and α is some free parameter. We also use the notation $\ell(\boldsymbol{\lambda})$ to denote the number of elements within the partition $\boldsymbol{\lambda}$ (with, for example,

[6] Within number theory, $\boldsymbol{\lambda}$ is often referred to as a *partition* of an integer, where that integer is the sum of the elements, $|\boldsymbol{\lambda}|$. So, for example, the partitions of 3 are $\{3\}$, $\{2, 1\}$ and $\{1, 1, 1\}$.

$\ell(\{2\}) = 1$ and $\ell(\{3,2,2\}) = 3$). Within the space defined by this inner product, the Jack polynomials, $J_{\boldsymbol{\lambda}}$, each indexed by a partition $\boldsymbol{\lambda}$, form a set of orthogonal polynomials such that

$$J^{(\alpha)}_{\boldsymbol{\lambda}} = m_{\boldsymbol{\lambda}} + \sum_{\boldsymbol{\mu}<\boldsymbol{\lambda}}^{|\boldsymbol{\mu}|=|\boldsymbol{\lambda}|} v_{\boldsymbol{\lambda},\boldsymbol{\mu}}(\alpha) m_{\boldsymbol{\mu}} \tag{2.38}$$

for some coefficients $v_{\boldsymbol{\lambda},\boldsymbol{\mu}}$ which depend on the parameter α.

Example 3

Consider $\Delta L = 1$ Jacks. There is only one partition of the integer 1, namely $\{1\}$. Therefore, we simply have $J^{(\alpha)}_{\{1\}} = m_{\{1\}}$.

The $\Delta L = 2$ subspace is more interesting, containing the partitions $\{2\}$ and $\{1,1\}$. To move between monomials and power sums one uses that $m_{\{2\}} = P_{\{2\}}$ and $m_{\{1,1\}} = \frac{1}{2}P_{\{1,1\}} - \frac{1}{2}P_{\{2\}}$. Therefore, the $\{1,1\}$ Jack is simple to write down as

$$J^{(\alpha)}_{\{1,1\}} = m_{\{1,1\}}. \tag{2.39}$$

We can then use the transformations to the power sums alongside the definition of the inner product to find that the polynomial orthogonal to $J_{\{1,1\}}$ under the inner product defined by Eq. 2.37 is

$$J^{(\alpha)}_{\{2\}} = m_{\{2\}} + \frac{2}{1+\alpha} m_{\{1,1\}}. \tag{2.40}$$

Going forward the process can be simplified as follows. The lexicographically most inferior Jack is simply $m_{\{1,1,\ldots\}}$. The next is the polynomial $J^{(\alpha)}_{\{2,1,\ldots\}} = m_{\{2,1,\ldots\}} + v(\alpha) m_{\{1,1,\ldots\}}$ where $v(\alpha)$ is chosen to make this orthogonal to $J^{(\alpha)}_{\{1,1,\ldots\}}$. We then keep adding the next most lexicographically inferior partition to the basis and finding the coefficients which ensure orthogonality.

The definition provided here for the Jack polynomials is one which is far more common in the mathematical literature despite these polynomials also being

present in certain physics problems[72, 73]. An alternative definition is that they are the eigenstates of the *Laplace-Beltrami operator* operator[74],

$$\mathcal{H}_{\mathrm{LB}}(\alpha) = \sum_i \left(z_i \frac{\partial}{\partial z_i} \right)^2 + \frac{1}{\alpha} \sum_{i<j} \frac{z_i + z_j}{z_i - z_j} \left(z_i \frac{\partial}{\partial z_i} - z_j \frac{\partial}{\partial z_j} \right), \tag{2.41}$$

which is intimately related to the *Calogero-Sutherland model*[75–79]. There has been much discussion in recent years about how Calogero-Sutherland might describe quantum Hall edge physics[80, 81] though such claims are still lacking rigorous derivations.

2.3.3 Full States vs. Edge States

For the majority of this thesis we will work with these polynomials as the edge states $\mathcal{P}$ which multiply the ground state wavefunction. However, the whole state itself, including the ground state wavefunction, is also a symmetric polynomial in the bosonic case. It is in fact possible to express the full wavefunctions as Jack polynomial with the following construction[82–94]. One begins by defining a *root partition*, $\mathbf{\Lambda}$, which must obey a *generalised Pauli principle*. For the $\nu = 1/m$ Laughlin state, the generalisation is that at most one orbital in any consecutive set of m orbitals can be occupied. One then takes a Jack parameter of $\alpha = -\frac{2}{m-1}$. Finally, to consider the fermionic case one can generate the Jack polynomial at $\nu = 1/(m-1)$ and multiply the result by a Jastrow factor[7].

Example 4

Let us see this in practice for a 5-particle Laughlin state at $\nu = 1/2$. The generalised Pauli principle is easier to visualise if we use the notation for states in Example 2. In that case the root partition for the ground state is

$$\mathbf{\Lambda}_0 = \{8, 6, 4, 2, 0\} \qquad \mapsto \qquad |\mathbf{1}\,0\,\mathbf{1}\,0\,\mathbf{1}\,0\,\mathbf{1}\,0\,\mathbf{1}\}. \tag{2.42}$$

[7] Note that we will also consider the *Moore-Read state* in Part II of this thesis which has a similar construction. At $\nu = 1/m$ the generalised exclusion principle is that at most two in any string of $2m$ consecutive orbitals can be occupied. One then uses a Jack parameter of $\alpha = -\frac{k+1}{m-1}$ with $k = 2$.

This is the most compressed state with at most 1 orbital occupied over any two consecutive orbitals. The full wavefunction is then $J^{(-2)}_{\mathbf{\Lambda}_0}$.

To form an edge excitation one simply adds angular momentum to the root partition, taking care to respect the generalised Pauli principle. So, for example, $|\mathbf{1}\,0\,\mathbf{1}\,0\,\mathbf{1}\,0\,0\,\mathbf{1}\,0\,0\,\mathbf{1}\}$ is an allowed root partition but $|\mathbf{1}\,0\,\mathbf{1}\,0\,\mathbf{1}\,0\,0\,0\,\mathbf{1}\,\mathbf{1}\}$ is not as the consecutive orbitals with $l = 8$ and $l = 9$ are occupied.

Note that it is still possible to represent the full-wavefunction Jack polynomials as some edge state polynomial multiplying the ground state with a closed-form expression existing for the Laughlin case[95][8]. To find the decomposition one must find the edge partition, $\boldsymbol{\lambda}$, which produces the root partition $\mathbf{\Lambda}$ from the root partition of the ground state, $\mathbf{\Lambda}_0$. Explicitly for the Laughlin state one must find the λ_i such that

$$\mathbf{\Lambda} = \{m(N-1) + \lambda_1,\ \ m(N-2) + \lambda_2, \ldots, m + \lambda_{N-1},\ \ 0 + \lambda_N\} \tag{2.43}$$

where the generalised Pauli principle ensures that $\lambda_1 \geq \lambda_2 \geq \ldots$. Then,

$$J^{\left(-\frac{2}{m-1}\right)}_{\mathbf{\Lambda}} = J^{\left(\frac{2}{m+1}\right)}_{\boldsymbol{\lambda}} \prod_{i<j} (z_i - z_j)^m. \tag{2.44}$$

2.4 Hydrodynamic Edges

2.4.1 The Quantum Hall Fluid

So far we have discussed the Laughlin state as a quantum wavefunction but we can also think about it as a semi-classical fluid. Therefore, we will first establish some key properties of the fluid's bulk before moving onto a discussion of the edge[53, 54, 63].

[8] However, for the Moore-Read state we consider in Part II of this thesis, an analogous closed form expression is lacking in the literature. Nevertheless, the decomposition can still be performed but must instead be considered on a case-by-case basis.

In thinking about our state as a fluid, the first claim we make is that the fluid has a uniform density throughout. For the integer quantum Hall effect ($\nu = 1$) we can see this by noting that the ground state wavefunction is that which occupies each orbital from $l = 0$ to $l = N - 1$. The number density of the resulting probability distribution function in the thermodynamic limit, $N \to \infty$, is then

$$n(z) = \frac{1}{2\pi {\ell_{\mathrm{B}}}^2} \sum_{l=0}^{N-1} \frac{1}{l!} \left(\frac{|z|^2}{2{\ell_{\mathrm{B}}}^2} \right)^l \exp\left(-\frac{|z|^2}{2{\ell_{\mathrm{B}}}^2} \right) \to \frac{1}{2\pi {\ell_{\mathrm{B}}}^2} \tag{2.45}$$

where the limit uses that this summation is simply the exponential $\exp\left(\frac{|z|^2}{2{\ell_{\mathrm{B}}}^2}\right)$. Therefore, the density is a constant value throughout.

The $\nu = 1/m$ Laughlin state has m times fewer particles contained within the same area and therefore a density of $n = \frac{\nu}{2\pi {\ell_{\mathrm{B}}}^2}$. However, to motivate that it is also uniform requires numerical checks or Laughlin's plasma analogy[19]. Within this analogy, one notices that the normalisation of the Laughlin wavefunction is

$$\mathcal{Z} \quad \propto \quad \int \prod_i \mathrm{d}^2 z_i \exp\left(-\beta E\right), \tag{2.46}$$

$$\text{for} \qquad \beta E = \sum_i \frac{|z_i|^2}{2{\ell_{\mathrm{B}}}^2} + 2m \sum_{i<j} -\ln|z_i - z_j|. \tag{2.47}$$

This is exactly the partition function for a classical two-dimensional plasma in the presence of a neutralising background and our state's most likely distributions will be given by the low-energy distributions of this plasma. If we conveniently interpret the results at $\beta = \frac{2}{m}$ then we find the particles in the plasma have charge of m and the neutralising has density $-\frac{1}{2\pi {\ell_{\mathrm{B}}}^2}$.[9] Numerical studies show that such a plasma sits in a screening phase for $m < m_c$ where $m_c \simeq 65$, above which the charges prefer a crystalline ordering[96]. This screening phase is characterised by a uniform density across the plane and so we expect the density of our fluid to closely mimic this result.

[9] To see this consider that $E = m\phi$ for some electrostatic potential ϕ. The charge distribution a given particle sees is then found via Gauss' law, $-\nabla^2\phi = 2\pi\rho$. The former term in Eq. 2.47 produces the constant background whilst the second term corresponds to an array of point-like charges of size m.

The second claim is that the fluid is also incompressible. We have already seen some hints of the incompressibility for the Laughlin state from the construction of our parent Hamiltonians, which force all low-energy states to vanish as $(z_i - z_j)^m$, meaning that our state has a radius of at least $R = \ell_B\sqrt{2mN}$ (because it will reach to at least the $l = m(N-1)$ orbital). More generally, the compressibility is

$$\kappa = -\frac{1}{V}\left(\frac{\partial V}{\partial p}\right)_N = \left[V\left(\frac{\partial^2 E}{\partial V^2}\right)_N\right]^{-1} \tag{2.48}$$

where p and V are the pressure and volume of the fluid. With energy per particle, ϵ and number density n yielding a total energy $E = n\epsilon V$ we then find

$$\frac{1}{\kappa} = n^2\frac{\partial \mu}{\partial n} \tag{2.49}$$

where $\mu = \left(\frac{\partial E}{\partial N}\right)_V$ is the chemical potential. However, if we begin with the Laughlin state and increase the density of particles then the filling fraction will increase above $\nu = 1/m$. This leads to a discontinuous jump in the chemical potential across the gap and therefore $\kappa \to 0$. Our state is therefore incompressible[10].

Therefore, the coarse-grained picture is of a quantum Hall fluid which is incompressible due to the interactions between particles (or Pauli exclusion for $\nu = 1$ fermions) and uniformly dense, behaving like a plasma. Recalling then that our system on the plane satisfies rotational symmetry, this fluid will form a circular droplet corresponding to the lowest energy configuration within some typical confinement. Then, as shown in Fig. 2.4, our edge modes are distortions of this droplet.

[10] Note, however, that this claim is dependent on exactly how the energy of the system varies with density. We have claimed that the chemical potential will jump as n is increased, which requires the total energy of a system of density $n = \frac{\nu}{2\pi\ell_B{}^2} + \delta n$ to approach zero linearly, as $E \sim \delta n$ for $\delta n > 0$ and $E = 0$ for $\delta n < 0$. This would make the chemical potential discontinuous at $\delta n = 0$. Whilst this seems eminently plausible, there is no rigorous proof of this statement. However, we can rely on a wealth of numerical and experimental evidence[61, 97–99].

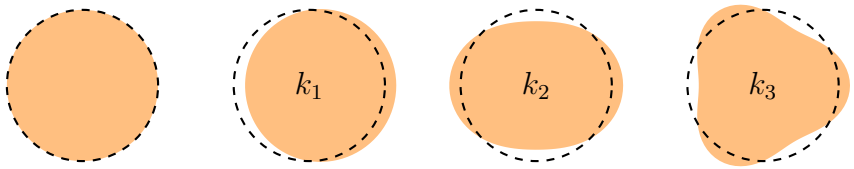

Figure 2.4: We show the first few modes of excitation for our circular droplet on the plane, which correspond to waves around the edge. Note that, being on a circle, these modes have automatic periodic boundary conditions so are quantised to have wavevector $k_n = \frac{n}{R}$.

2.4.2 The Classical Problem

We will now consider a semi-classical approach to finding the transport of these modes along the edge of our system, beginning with a discussion of the fully classical problem[12]. The equation of motion for our charges is

$$m_q \frac{\mathrm{d}\boldsymbol{v}}{\mathrm{d}t} = q\boldsymbol{E} + q\boldsymbol{v} \times \boldsymbol{B} \tag{2.50}$$

where $\boldsymbol{v}$ is the particle velocity at time t. In the absence of an electric field these particles simply execute circular motion in the form of cyclotron orbits. However, the electric field which contains these particles within the sample causes these orbits to drift, as demonstrated in Fig. 2.5a. This happens as the particle loses kinetic energy when it climbs up the potential gradient, thus making its motion slower at the top of the orbit and causing overall drift of $v = \frac{E}{B}$.[11]

Now consider that our edge is narrow enough that the electric field corresponding to the confinement of the particles is linear. Therefore, as shown in Fig. 2.5b, we would expect all the charges across the edge to set up a persistent current propagating at the same speed v, leading to an equation of motion

$$\frac{\partial h}{\partial t} + v\frac{\partial h}{\partial x} = 0 \tag{2.52}$$

[11] A simple method to find this drift is to make a Lorentz boost, $\boldsymbol{v}$, in the direction perpendicular to the electric field, which transforms the electric field to

$$\boldsymbol{E}' = \gamma(\boldsymbol{E} + \boldsymbol{v} \times \boldsymbol{B}). \tag{2.51}$$

Setting this to zero one finds that $v = \frac{E}{B}$.

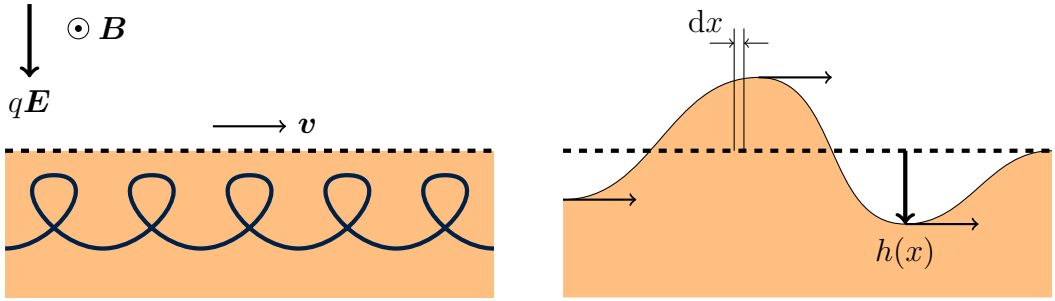

(a) (b)

Figure 2.5: In (a) we consider the motions of individual particles within the fluid and note that they develop an $\boldsymbol{E} \times \boldsymbol{B}$ drift. In (b) we consider the system as a fluid which, assuming that the edge is narrow enough to consider the electric field as linear, propagates all at the same velocity.

for the height, $h(x)$, of the fluid with respect to the ground state at position x along the edge. We now wish to quantise this theory and so we need to consider the energetics of the system.

2.4.3 Wen's Hydrodynamic Formulation

We begin by recalling that the fluid is incompressible with density n and so the one-dimensional density at position x is $\rho(x) = nh(x)$. Therefore, considering strips of charge like that shown in Fig. 2.5b, which have a total charge of $q\rho(x)\mathrm{d}x$ and feel an average potential of $\frac{1}{2}h(x)E$, the Hamiltonian for the system is[11]

$$H = \int \mathrm{d}x q\rho(x)\frac{h(x)E}{2} = \pi\hbar\frac{v}{\nu}\int \mathrm{d}x\rho(x)^2, \tag{2.53}$$

recalling that $n = \frac{\nu}{2\pi{\ell_\mathrm{B}}^2}$ and simplifying given the definition of ℓ_B. Working in momentum space, $\rho(x) = \sum_k \rho_k e^{-ikx}$, and taking $\rho_0 = 0$ (which just defines $h = 0$) our equation of motion, Eq. 2.52, and Hamiltonian, Eq. 2.53, become

$$\dot{\rho}_k = ivk\rho_k, \qquad H = 2\pi\hbar\frac{v}{\nu}\sum_{k>0}\rho_{-k}\rho_k. \tag{2.54}$$

We quantise this theory by identifying some generalised positions q_k and momenta p_k such that the equation of motion corresponds to Hamilton's equations[100] (i.e,

$\dot{\boldsymbol{q}} = \frac{\partial H}{\partial \boldsymbol{p}}$ and $\dot{\boldsymbol{p}} = -\frac{\partial H}{\partial \boldsymbol{q}}$) and then impose the canonical commutation relations, setting $[q_k, p_{k'}] = i\hbar\delta_{k,k'}$.

The result of this analysis is that $q_k = \rho_k$ and $p_k = \frac{2\pi\hbar}{k\nu} i\rho_{-k}$ for $k > 0$ only and

$$[\rho_k, \rho_{-k'}] = \left(\frac{\nu}{2\pi}\right) k\delta_{k,k'}. \tag{2.55}$$

This commutator defines the *U(1) Kac-Moody algebra*[101], which are the same modes that appear in the Tomonaga Luttinger liquid model[102]. Recalling then from Fig. 2.4 that the modes are quantised to $k_n = \frac{n}{R}$ by the automatic periodic boundary conditions around the circle, we can build generic distortions of the surface with the states

$$|\boldsymbol{\lambda}\rangle = \prod_{n \in \boldsymbol{\lambda}} \rho_{-k_n} |0\rangle \tag{2.56}$$

where $|0\rangle$ is the state annihilated by all ρ_{k_n} for $n > 0$ and $\boldsymbol{\lambda}$ is once again an integer partition.

Note that a given state may contain multiple copies of the same mode, implying that these edge modes are bosonic, and that the states have a linear energy spectrum, $E_{\boldsymbol{\lambda}} = v \sum_{n \in \boldsymbol{\lambda}} \hbar k_n$. These are the hallmark characteristics of a *linear Luttinger liquid*, a paradigmatic model of interacting fermions in quantum wires which happens to describe a large array of other one-dimensional systems[102–105]. However, in the usual Luttinger liquid model the excitations can travel in both directions whereas our modes propagate in one direction only. Therefore, this simple quantum Hall edge is an important example of a *chiral linear Luttinger liquid*.

Aside 4

We note that there is a one-to-one mapping between the space of edge states described by polynomials and these second quantised operators. This link will be explored in much greater detail in Part II of this thesis but for now we simply claim that, in the thermodynamic limit, the mapping from the operator

ρ_{-k_n} is to the polynomial p_n. This produces density density correlations of the form

$$\frac{\langle n|\rho(x)\rho(x')|n\rangle}{\langle n|n\rangle} = \frac{\nu k_n}{\pi}\cos\left(k_n(x-x')\right) \tag{2.57}$$

(where we implicitly normal order the operators in this expression). Therefore, the polynomials p_n correspond to the modes, k_n, shown in Fig. 2.4.

CHAPTER 3

Quantum Hall Edges with Hard Confinement

All right. Nobody move. I got a dragon here, and I'm not afraid to use it. I'm a donkey on the edge!

— Donkey [Shrek, 2001]

Within the realm of quantum Hall edges there exist very few exact solutions for the behaviour at the edge of a quantum Hall system, with Wen's hydrodynamic formulation being a rare exception. This solution is predicated on a smooth edge, which we can approximate as some linear potential that completely defines the velocity at which the modes propagate[11, 31]. More recently there has been significant focus on the deviation from linearity[41, 81, 105–107]. In this chapter we consider the complete opposite limit, where the confinement at the edge is so steep that the energy is determined entirely by the occupation of state's furthest out orbital. In this regime we add another rare exact solution to the annals of quantum Hall edges, whose energy spectrum is completely different from the usual Luttinger liquid and whose eigenstates correspond to Jack polynomials[71].

3.1 Extremely Steep Edges

3.1.1 The Steep Limit

We begin by taking the parent Hamiltonian for the Laughlin state, Eq. 2.30, and perturbing with some confinement, thus aiming to solve

$$\mathcal{H}_m = \sum_{i=1}^{N} \frac{(\boldsymbol{p}_i - q\boldsymbol{A})^2}{2m_q} + \sum_{1\leq i<j\leq N} V_m(\boldsymbol{r}_i - \boldsymbol{r}_j) + \sum_{i=1}^{N} U(\boldsymbol{r}_i), \tag{3.1}$$

in the lowest Landau level. We will therefore be working in the limit

$$\hbar\omega_c \gg V_m \gg U \tag{3.2}$$

throughout. Furthermore, we will take this confinement to obey the rotational symmetry of the underlying parent Hamiltonian, which therefore makes it diagonal in our basis of orbitals for the lowest Landau level, and so

$$U = \sum_{l=0}^{\infty} U_l \hat{n}_l, \tag{3.3}$$

where $\hat{n}_l$ is the operator which counts the occupation of the orbital $\psi_{0,l}$ (i.e, the z^l orbital defined in Eq. 2.8). Therefore, in order to satisfy our limit, Eq. 3.2, we will demand that U_l is much smaller than V_m for all the orbitals, l, that are occupied.

We are then interested in the solution to this problem in the extremely steep limit. Precisely, we define this by

$$\cdots \gg U_{l+1} \gg U_l \gg U_{l-1} \gg \cdots . \tag{3.4}$$

It was noted previously in Ref. [41] that there is a great simplification in this limit: the energy of a state should be determined entirely by the largest-l orbital which is occupied, and eigenstates can be constructed by successively orthogonalizing the root states (i.e, the Jack polynomial states $J_{\boldsymbol{\Lambda}}^{(-\frac{2}{m+1})}$ discussed in Section 2.3.3 where $\boldsymbol{\Lambda}$ is the root partition). We use this intuition to construct a fully analytic solution.

Aside 5

It should be noted that this limit does not correspond to any experimental system created thus far. However, it should in principle be possible to construct such a trap in cold atom realisations[44, 45] of the fractional quantum Hall effect *for small particle numbers* (see below). Furthermore, it is in these experiments where the pseudopotential interactions, V_m, are more likely to constitute a reasonable approximation to the real interactions, which are typically hard-core as opposed to long-range Coulomb.

However, to approach this limit we also require the system size to be small. Consider for example the step function edge considered in Fig. 2.2a, which did not confer an instant jump in U_l but a smooth transition over a range $\sqrt{l_0}$ where $l_0 \simeq mN$ is the outermost orbital. The issue we must surmount is that the spacing between subsequent orbitals varies as $1/\sqrt{l}$ at high angular momentum so we would need a confinement which grows, and continues to grow, over very short distance scales. If we were to take $U(r) \sim r^{2\gamma}$ for example then the energies of the orbitals would vary as $U_l \sim \frac{(\gamma+l)!}{l!}$. Therefore, to satisfy our limit at the edge (around l_0) we would require $\gamma \gg mN$.

3.1.2 Convenient Bases

Given the rotational symmetry of the problem we can diagonalise U in sectors of well-defined total angular momentum. We then require a suitable basis of states with which to perform this diagonalisation. As building blocks we will use the normalised power sum basis, with $q_n = \sum_i \left(\frac{z_i}{R}\right)^n$. We have already seen a hint that this basis is orthogonal as these power sums correspond to the Kac-Moody generators, ρ_{-k_n}, encountered in Section 2.4.3. Specifically, we will take the states to be of the form $\{\boldsymbol{z}|Q_{\boldsymbol{\lambda}}\} = Q_{\boldsymbol{\lambda}}\Psi^{(m)}/\sqrt{\mathcal{Z}_N}$, where $\mathcal{Z}_N = \{1|1\}$ is the normalisation of the ground state Laughlin wavefunction and $Q_{\boldsymbol{\lambda}}$ are defined exactly equivalently

to the $P_{\boldsymbol{\lambda}}$ given in Eq. 2.36 (but now in terms of these normalised power sums, q_n). Then, the states have overlaps of the form[34]

$$\{Q_{\boldsymbol{\lambda}}|Q_{\boldsymbol{\mu}}\} = \delta_{\boldsymbol{\lambda},\boldsymbol{\mu}}\zeta_{\boldsymbol{\lambda}}\nu^{\ell(\boldsymbol{\lambda})} + \mathcal{O}\big(N^{-1}\big), \qquad \zeta_{\boldsymbol{\lambda}} = \prod_{n=1}^{\infty} m_n^{\boldsymbol{\lambda}}! n^{m_n^{\boldsymbol{\lambda}}}. \tag{3.5}$$

We will say a great deal about this orthogonality in Part II of this thesis but for now we simply take the result in $N \to \infty$ limit. In that limit, this inner product is exactly equivalent to Eq. 2.37 with Jack parameter $\alpha = \nu$. Therefore, the Jack polynomials, $J_{\boldsymbol{\lambda}}^{(\nu)}$, also form an orthogonal basis which we could use to diagonalise U.

Given these two bases, we will choose the more convenient, which happens to be the Jack polynomials. To see this, consider using the power sums in the sector $\Delta L = |\boldsymbol{\lambda}|$. Each $Q_{\boldsymbol{\lambda}}$ can add all ΔL units of angular momentum to a single particle and so the highest occupied orbital of $Q_{\boldsymbol{\lambda}}\Psi^{(m)}$ will be the $(l_0 + |\boldsymbol{\lambda}|)^{\text{th}}$. Naïvely one might assume that diagonalisation will therefore produce three states with energy of order $U_{l_0+\Delta L}$. However, this is not the case as we can construct states such as $(Q_{\boldsymbol{\lambda}} - Q_{\boldsymbol{\mu}})$ or $(Q_{\boldsymbol{\lambda}} - 3Q_{\boldsymbol{\mu}} + 2Q_{\boldsymbol{\gamma}})$ which no longer have $l_0 + \Delta L$ as the highest occupied orbital, and so these states have energy of order $U_{l_0+\Delta L-1}$ or below. Therefore, we require a basis for which the maximum power added follows a strict hierarchy, which is exactly the case for the Jack polynomials. The Jacks have built-in the property that they add at most λ_1 units of angular momentum to a single particle and are constructed such that no linear combination of $J_{\boldsymbol{\lambda}}$ with λ_1 matching will remove this leading addition of angular momentum (i.e, the general combination $\alpha J_{\boldsymbol{\lambda}} + \beta J_{\boldsymbol{\mu}}$ for $\boldsymbol{\lambda} \neq \boldsymbol{\mu}$ where $\lambda_1 = \mu_1$ will always have a leading power of z^{λ_1}).

Aside 6

The Jacks will make it easier to diagonalise U but, as we have already seen, they are not simple objects like the power sums. Here we discuss their nor-

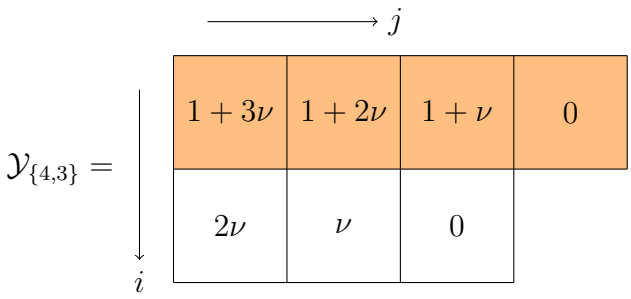

Figure 3.1: The Young tableau for the partition $\{4, 3\}$, including the hook lengths associated with each box, which count the number of cells below plus ν multiples of the number of cells to the right. We highlight the uppermost row as we will shortly see that this completely determines the spectrum of U.

malisation. The Jack polynomials are orthogonal with[71]

$$\left\{ J_{\boldsymbol{\lambda}}^{(\nu)} \middle| J_{\boldsymbol{\mu}}^{(\nu)} \right\} = j_{\boldsymbol{\lambda}}(\nu)\delta_{\boldsymbol{\lambda},\boldsymbol{\mu}} \tag{3.6}$$

where this normalisation, $j_{\boldsymbol{\lambda}}(\nu)$ can be phrased in terms of *Young Tableaux*[108]. These tableaux, $\mathcal{Y}_{\boldsymbol{\lambda}}$, are combinatorial objects which represent a particular partition, $\boldsymbol{\lambda}$, as a collection of boxes arranged in rows. There are λ_1 boxes in the first row, λ_2 in the second row and so on. The box at position (i, j) is in the i^{th} row and j^{th} column. We then ascribe *hook lengths*, $h_{\boldsymbol{\lambda}}(i, j)$, to each box, which equal the number of boxes underneath plus ν multiples of the number of boxes to the right. An example is given in Fig. 3.1. The normalisation can then be phrased in terms of these hook lengths as

$$j_{\boldsymbol{\lambda}}(\nu) = \prod_{(i,j)\in\mathcal{Y}_{\boldsymbol{\lambda}}} (h_{\boldsymbol{\lambda}}(i, j) + 1)(h_{\boldsymbol{\lambda}}(i, j) + \nu). \tag{3.7}$$

3.2 Analytic Solution

3.2.1 Method of Solution

We now proceed to diagonalise U in the basis of Jack polynomials, $\left|J_{\boldsymbol{\lambda}}^{(\nu)}\right\}$. The matrix elements are

$$U_{\boldsymbol{\mu},\boldsymbol{\lambda}} = \frac{\left\{J_{\boldsymbol{\mu}}^{(\nu)}\middle|U\middle|J_{\boldsymbol{\lambda}}^{(\nu)}\right\}}{\sqrt{j_{\boldsymbol{\mu}}(\nu)j_{\boldsymbol{\lambda}}(\nu)}} \tag{3.8}$$

where $j_{\boldsymbol{\lambda}}(\nu)$ is the normalisation of the Jack discussed in Aside 6. Since U is rotationally invariant we need only consider sectors in which $|\boldsymbol{\lambda}| = |\boldsymbol{\mu}| = \Delta L$. The key simplification of $U_{\boldsymbol{\mu},\boldsymbol{\lambda}}$ stems from the steep edge condition, Eq. 3.4 which, to leading order, implies that we need only identify the highest angular momentum orbital which is occupied, say z^l, and we can focus only on the potential from this orbital, U_l. Given the structure of the Jacks this will be the $l = l_0 + \lambda_1$ orbital.

We now introduce the notation $[z_k^n]$ to mean "factoring out everything which includes the n^{th} power of z_k". For example, $[x^2](\alpha_3 x^3 + \alpha_2 x^2 + \alpha_1 x) = \alpha_2 x^2$. We then apply this to the holomorphic polynomial representing the edge state (ignoring the Gaussian factors) to find how much of the state has particle k in the $l_0 + \lambda_1$ orbital. Therefore, we can find how much of a particular state, Ψ occupies orbital l by considering

$$\langle n_l \rangle = \int \prod_i \left(\frac{\mathrm{d}^2 z_i}{2\pi {\ell_{\mathrm{B}}}^2}\right) \bar{\Psi}(\boldsymbol{z}) \sum_{k=1}^{N} [z_k^l]\Psi(\boldsymbol{z}). \tag{3.9}$$

The subsequent Gaussian integral will then produce the same factorisation on the bra-state (i.e, any part of $\bar{\Psi}$ which varies like $z_k^{l'}$ where $l' \neq l$ will vanish in this integral) and so

$$\langle n_l \rangle = \sum_{k=1}^{N} \int \prod_i \left(\frac{\mathrm{d}^2 z_i}{2\pi {\ell_{\mathrm{B}}}^2}\right) \left|[z_k^l]\Psi(\boldsymbol{z})\right|^2. \tag{3.10}$$

A similar result also holds for the off-diagonal elements of n_l.

3.2.2 Diagonalisation

Applying the factorisation to $J^{(\nu)}_{\boldsymbol{\lambda}}\Psi^{(m)}$ we find

$$[z_k^{l_0+\lambda_1}]J^{(\nu)}_{\boldsymbol{\lambda}}\Psi^{(m)} = \left([z_k^{\lambda_1}]J^{(\nu)}_{\boldsymbol{\lambda}}\right)\left([z_k^{l_0}]\Psi^{(m)}\right) \tag{3.11}$$

since the only way we can factorise $z_k^{l_0+\lambda_1}$ is by saturating the contributions from both the Jack polynomial and the Jastrow factors within the Laughlin wavefunction. At this point we invoke a remarkable identity of the Jack polynomials from Ref. [71], which states

$$[z_k^{\lambda_1}]J^{(\nu)}_{\boldsymbol{\lambda}}(\boldsymbol{z}) = \left(\frac{z_k}{R}\right)^{\lambda_1} d_{\boldsymbol{\lambda}}(\nu)J^{(\nu)}_{\boldsymbol{\lambda}^-}(\boldsymbol{z}_{\not k}). \tag{3.12}$$

Note that the z_k is normalised by R because our Jacks are composed of the normalised power sums, functions of z_k/R. We have defined $\boldsymbol{z}_{\not k}$ to be the particle positions without z_k and the new partition $\boldsymbol{\lambda}^-$ is exactly the original partition with the first element removed, $\boldsymbol{\lambda}^- = \{\lambda_2, \ldots\}$. Finally, the function $d_{\boldsymbol{\lambda}}(\nu)$ is a combinatorial factor closely related to the normalisation $j_{\boldsymbol{\lambda}}(\nu)$.

Aside 7

Specifically, this factor $d_{\boldsymbol{\lambda}}(\nu)$ be expressed with the help of the partition's Young tableau. It can be expressed, similar to the normalisation, as a product of hook lengths, though this time only those over the first row,

$$d_{\boldsymbol{\lambda}}(\nu) = \prod_{j=1}^{\lambda_1}(h_{\boldsymbol{\lambda}}(1,j)+1). \tag{3.13}$$

Hence, as illustrated in Fig. 3.1, the first row of the tableau will be important.

Similarly, we apply the factorisation to the Jastrow factors,

$$[z_k^{l_0}]\prod_{i<j}(z_i - z_j)^m = (-1)^{m(k-1)} z_k^{l_0} \prod_{i<j\neq k}(z_i - z_j)^m \tag{3.14}$$

and therefore arrive at the result that

$$[z_k^{l_0+\lambda_1}]J_{\boldsymbol{\lambda}}^{(\nu)}\Psi^{(m)} = \left(\left(\frac{z_k}{R}\right)^{\lambda_1} d_{\boldsymbol{\lambda}}(\nu) J_{\boldsymbol{\lambda}^-}^{(\nu)}(\boldsymbol{z}_{\not k})\right)\left((-1)^{m(k-1)} z_k^{l_0} e^{-\frac{|z_k|^2}{4\ell_{\mathrm{B}}{}^2}} \Psi^{(m)}(\boldsymbol{z}_{\not k})\right). \tag{3.15}$$

To find the individual matrix elements we then perform the same manipulation on the bra-state, $J_{\boldsymbol{\mu}}^{(\nu)}$, and take the inner product with the result

$$U_{\boldsymbol{\mu},\boldsymbol{\lambda}} = U_{l_0+\lambda_1}\left[\frac{N\mathcal{Z}_{N-1}\left(2\ell_{\mathrm{B}}{}^2\right)^{l_0+\lambda_1}(l_0+\lambda_1)!}{\mathcal{Z}_N R^{2\lambda_1}}\right]\delta_{\mu_1,\lambda_1}\frac{d_{\boldsymbol{\mu}}(\nu)d_{\boldsymbol{\lambda}}(\nu)}{\sqrt{j_{\boldsymbol{\mu}}(\nu)j_{\boldsymbol{\lambda}}(\nu)}}\left\{J_{\boldsymbol{\mu}^-}^{(\nu)}\middle|J_{\boldsymbol{\lambda}^-}^{(\nu)}\right\} \tag{3.16}$$

with corrections of order $U_{l_0+\lambda_1-1}$. Recall in this expression that $\mathcal{Z}_N$ is the normalisation of the Laughlin wavefunction, defined as $\mathcal{Z}_N = \{1|1\}$. It is at this point that the power of the identity in Eq. 3.12 becomes apparent as the states $J_{\boldsymbol{\mu}^-}^{(\nu)}$ and $J_{\boldsymbol{\lambda}^-}^{(\nu)}$ will also be orthogonal[1], leading to the result that our perturbation is diagonal in this Jack basis with

$$U_{\boldsymbol{\mu},\boldsymbol{\lambda}} = U_{l_0+\lambda_1}\mathcal{N}(N,\nu,\lambda_1)\delta_{\boldsymbol{\mu},\boldsymbol{\lambda}}\frac{(d_{\boldsymbol{\lambda}}(\nu))^2 j_{\boldsymbol{\lambda}^-}(\nu)}{j_{\boldsymbol{\lambda}}(\nu)}, \tag{3.17}$$

where $\mathcal{N}(N,\nu,\lambda_1)$ is the overall normalisation factor in square brackets in Eq. 3.16. We can then apply the results from Asides 6 and 7 for the factors $j_{\boldsymbol{\lambda}}(\nu)$ and $d_{\boldsymbol{\lambda}}(\nu)$ to find that

$$\boxed{E_{\boldsymbol{\lambda}} = U_{l_0+\lambda_1}\mathcal{N}(N,\nu,\lambda_1)\prod_{j=1}^{\lambda_1}\frac{h_{\boldsymbol{\lambda}}(1,j)+1}{h_{\boldsymbol{\lambda}}(1,j)+\nu}} \tag{3.18}$$

where $h_{\boldsymbol{\lambda}}(1,j)$ are the *hook lengths* (from only the top row of the Young tableau) which can be shown to have the form

$$h_{\boldsymbol{\lambda}}(1,j) = (\lambda_1 - j)\nu + \left(\sum_{n=j}^{\lambda_1} m_n^{\boldsymbol{\lambda}} - 1\right) \tag{3.19}$$

where recall we defined $m_n^{\boldsymbol{\lambda}}$ as the frequency of the integer n in the partition $\boldsymbol{\lambda}$.

[1] However, note that these Jacks are part of an $(N-1)$-particle many-body state. Therefore, we should renormalise the z_i such that correspond to the new radius of the state, $R = \ell_{\mathrm{B}}\sqrt{2m(N-1)}$. However, given that we work in the thermodynamic limit, $N \to \infty$, this discrepancy is negligible.

Aside 8

The scale factor $\mathcal{N}(N,\nu,\lambda_1)$ contains the sole unknown within our energy spectrum due to the unknown form of the Laughlin wavefunction's normalisation, $\mathcal{Z}_N$. Nevertheless, there exists a large-N expansion[109] which can be used to constrain $\mathcal{N}$ up to a single constant factor. We begin by taking the $N\to\infty$ limit of $\mathcal{N}$, working also with $\lambda_1 \ll N$,

$$\mathcal{N}(N,\nu,\lambda_1) = \frac{N\mathcal{Z}_{N-1}\left(2{\ell_\mathrm{B}}^2\right)^{l_0} l_0!}{\mathcal{Z}_N}. \tag{3.20}$$

Into this we can insert the large-N expansion for $\mathcal{Z}_N$ taken from Ref. [109],

$$\ln\frac{\mathcal{Z}_N}{(2{\ell_\mathrm{B}}^2)^{\frac{mN(N-1)}{2}}} = \frac{mN^2}{2}\ln(mN) - \frac{3}{4}mN^2 + N\ln(mN) + \kappa(\nu)N + \dots \tag{3.21}$$

where the constant $\kappa(\nu)$ is unknown except at $\nu = 1$ and recall that $\nu = 1/m$. Therefore,

$$\mathcal{N}(N,\nu) = \alpha(mN)^{\frac{1-m}{2}} \tag{3.22}$$

where $\alpha = \frac{\sqrt{2\pi}}{m}e^{-m-\kappa}$, which equals 1 when $\nu = 1$. This coefficient, α can then be fit using either Monte-Carlo integration[110] or more simply by comparing the spectrum in Eq. 3.18 with exact diagonalisation.

3.3 Results

3.3.1 Energy Spectra

We now turn to consider the physics of this result. First, we note that the spectrum breaks into branches having different values of λ_1, with the corresponding piece having energy proportional to $U_{l_0+\lambda_1}$. The ratio of energies between the branches is determined by the structure of the confining potential, U, and is non-universal. Secondly within each branch, we find that the highest energy cor-

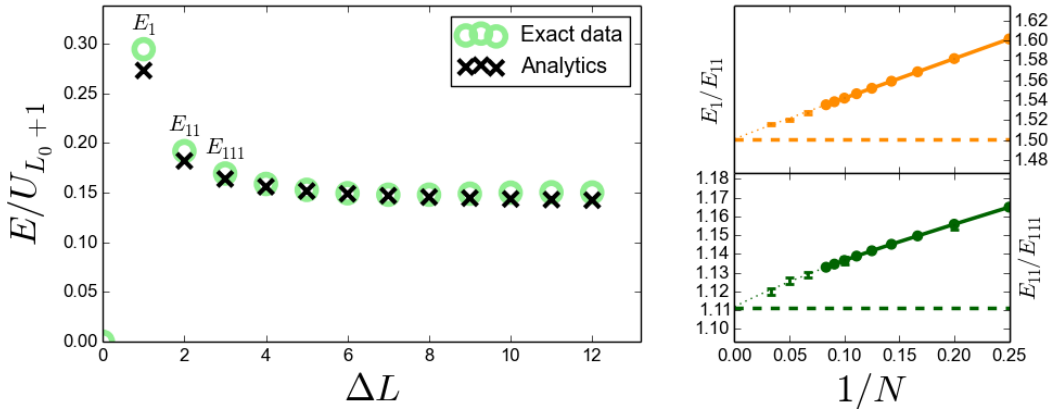

Figure 3.2: A comparison of exact diagonalisation data and our analytic result for filling fraction $\nu = 1/2$ and system size $N = 12$ in the $\lambda_1 = 1$ branch. On the left we fit $\mathcal{Z}_{N-1}/\mathcal{Z}_N$ using this data (and check the form against Monte Carlo integration). On the right we demonstrate the convergence of ratios of certain energies (which should be exact without the problematic $\mathcal{Z}_{N-1}/\mathcal{Z}_N$ factors). Circles represent exact diagonalisation data and dumbbells represent Monte Carlo data with a size corresponding to the total error in the result. We extrapolate to $N = \infty$ by including the first two sub-leading corrections (i.e, we fit the data to $a + b/N + c/N^{3/2}$). The horizontal dashed lines are the 'exact' predictions for the thermodynamic limit behaviour.

responds to the smallest angular momentum (we will describe a case of this in detail below and consider the physics of it) in strong contrast to the traditional Luttinger liquid picture. Nor do the energies bear any resemblance to that of the Calogero Sutherland model, the alternative model for the edge[80, 81] which also has Jack polynomials as its eigenstates.

In Figs. 3.2 and 3.3 we show the lowest two branches of the excitation spectrum for $\nu = 1/2$. In these numerics we work in the limit $U_{l+1} \gg U_l$ but at finite size. Therefore, as we will see in Part II of this thesis, there should be corrections to this result initially of order N^{-1} and sub-leading corrections of order $N^{-3/2}$. However, despite a system size of only $N = 12$, our analytic results are in almost perfect agreement with exact diagonalisation. For example, the lowest branch of excitations with $\lambda_1 = 1$ and corresponding to the partitions $\boldsymbol{\lambda} = \{1^{\Delta L}\}$ (i.e, 1 is reproduced ΔL times in this partition) are shown in Fig. 3.2. Here, the maximum

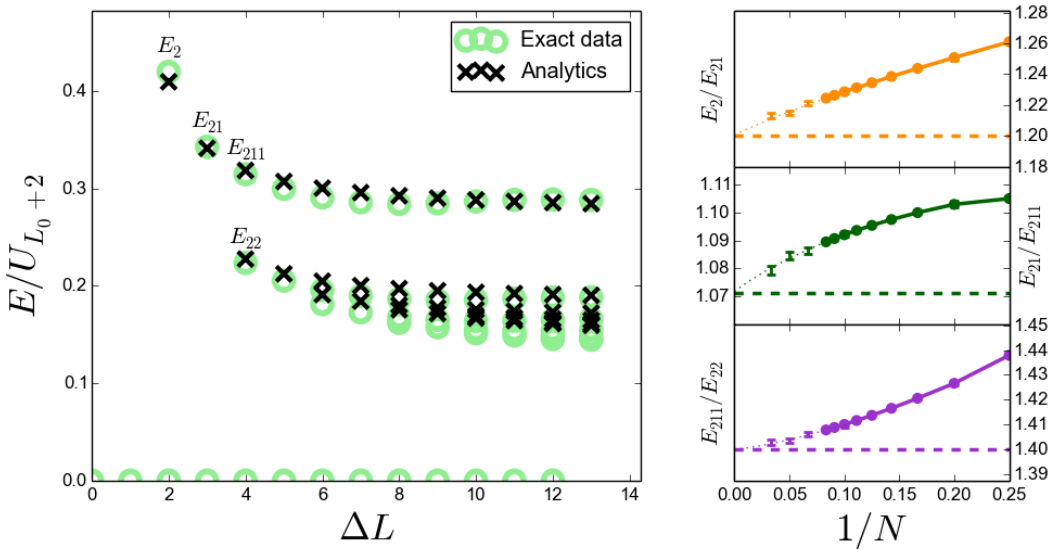

Figure 3.3: A comparison of exact diagonalisation and our analytic result for the $\lambda_1 = 2$ band at $\nu = 1/2$ and $N = 12$ alongside the finite size scaling of energy ratios. As for Fig. 3.2, the $N \to \infty$ extrapolation is a fit of the first two subleading corrections (and in this case the $N^{-3/2}$ corrections are large enough to be important).

---

amount of angular momentum added to any one particle is 1, giving an energy spectrum of the form

$$E_{\{1^{\Delta L}\}} = U_{l_0+1}\mathcal{N}(N,\nu,1)\frac{\Delta L}{\Delta L+\nu-1}. \tag{3.23}$$

The second branch with $\lambda_1 = 2$ has modes at an energy scale of U_{l_0+2} and partitions of the form $\{2^a, 1^b\}$ where $a > 0$ and $b \geq 0$. These states add angular momentum $\Delta L = 2a + b$ to the ground state and produce the spectrum shown in Fig. 3.3.

Aside 9

Note that when one calculates similar spectra for smaller filling fractions, $\nu = 1/3$ and $\nu = 1/4$, one again finds good agreement with exact diagonalisation, although with larger finite size errors. For example, at $N = 10$, the finite size error in E_1/E_{11} is 2.1% for $\nu = 1/2$, rising to 4.5% for $\nu = 1/3$, and 5.6%

for $\nu = 1/4$. In all cases, however, the convergence to the analytic result as $N \to \infty$ is clear.

3.3.2 Physical Explanation

As shown in the figures for each branch, the energy is largest for the smallest angular momentum, suggesting both that the system prefers to be in a state of higher angular momentum (though the lowest energy state remains the ground state) and that the velocity of modes at the edge is in fact negative. To understand this we consider first the case of $\nu = 1$ which can be considered within a single-particle framework. The ground state is simply a single Slater determinant of all orbitals filled up to angular momentum l_0. For the lowest branch of excitations (the U_{l_0+1} branch) one electron is pushed into the angular momentum $l_0 + 1$ orbital, leaving a single hole in one of the previously filled orbitals. Therefore, the states are of the form

$$|\cdots \mathbf{1}\,\mathbf{1}\,\mathbf{1}\,0\,\mathbf{1}\,0\,0\,0\} = \tag{3.24}$$

$$|\cdots \mathbf{1}\,\mathbf{1}\,0\,\mathbf{1}\,\mathbf{1}\,0\,0\,0\} = \tag{3.25}$$

$$|\cdots \mathbf{1}\,0\,\mathbf{1}\,\mathbf{1}\,\mathbf{1}\,0\,0\,0\} = \tag{3.26}$$

and so on. However, given the steep edge condition (and therefore neglecting all U_l for $l \leq l_0$), the occupancy of any orbitals other than the $l_0 + 1$ orbital has a negligible bearing on the energy. Therefore, given that the occupancy of the l_0+1 orbital is exactly 1 for each of these states, the hole can be placed anywhere within the bulk and the energy of the excitation will therefore be independent of the total angular momentum to leading order. This can be seen in the spectrum, Eq. 3.18 where at $\nu = 1$ the energy of any state will be simply $E_{\boldsymbol{\lambda}} = U_{l_0+\lambda_1}$.

In the case of $\nu = 1/m$ with $m > 1$ we can think in a similar manner by considering the *composite fermion* picture[111]. Within this picture one notes

that the Laughlin wavefunction can be constructed as a Slater determinant of orbitals $z_i^l \prod_{j\neq i}(z_i - z_j)^{\frac{m-1}{2}}$. Therefore, each orbital has a correlation factor built in which keeps the other particles sufficiently separated to satisfy the interactions.

Thinking in this way, one might first guess that placing a single hole somewhere in the bulk would, as in the integer case, excite only one particle to the l_0+1 orbital and therefore lead to the conclusion that the energy is once again independent of the angular momentum of the hole (and therefore the angular momentum of the state as a whole). However, one should remember that in the fractional case orbitals are typically neither completely filled nor completely empty, and it is, in fact, the density of particles in the l_0+1 orbital which completely determines the energy of the state. Clearly when the hole is well inside the bulk its exact angular momentum matters little, and hence we see the flattening of the bands at high ΔL. However, as the hole approaches the edge, corresponding to smaller ΔL, the correlation factors become important and begin to increase the average occupancy of the $l_0 + 1$ orbital (as the particles of would like to be close to a hole of opposite charge). Thus the energy is highest when the hole is as close to the edge as possible, i.e, when the angular momentum is at its lowest.

Aside 10

As already mentioned in Aside 5, achieving this steep limit in experiment is likely to be extremely difficult, with the only realistic avenue in cold atom systems. Within these systems extremely hard wall confinements of the form $U(r) \sim r^\gamma$ with exponents as high as $\gamma = 20$ have already been demonstrated[49, 112]. However, to achieve the limit $\gamma \gg mN$ as stipulated in Aside 5 would require something *even steeper* for any more than a handful of particles.

Nevertheless, whilst the exact limit is perhaps beyond what is reasonable, the result remains important as a limiting case which exhibits novel behaviour,

particularly with regards to the putative negative edge velocity. Therefore, as the confinement steepens one should expect the velocity to diminish with the eventual limit of changing sign. In fact, for a system of size $N = 10$ a potential of r^{20} is already sufficient to see a negative edge velocity, albeit at higher angular momentum with a maximum energy for the U_{l_0+1} branch at $\Delta L = 3$. The shift occurs because we can no longer ignore the energy of the hole when it sits close to the edge. However, once the hole is sufficiently within the bulk, the previous arguments relating to correlation factors diminishing the occupancy of the furthest out orbitals are once again valid and the edge velocity turns around.

3.4 Further Work

The methods introduced in this paper can be extended in several ways. For example, with more analytic effort corrections to some of the results can be obtained which keep sub-leading terms in orders of U_{l-1}/U_l. In this case when U_{l-1}/U_l is not strictly zero the dispersion develops additional structure, although the feature of negative edge mode velocity is fairly robust at least for ΔL not too small. The technique may also be applied to the edge excitations of the other quantum Hall states, such as the Moore-Read state (which will be discussed in Part II), although analysis of these excitations does not appear to result in a closed form expression for the energy spectrum. Finally, it is interesting to think about how $1/N$ corrections might play a role in our results.

Part II

Second Quantised Edges

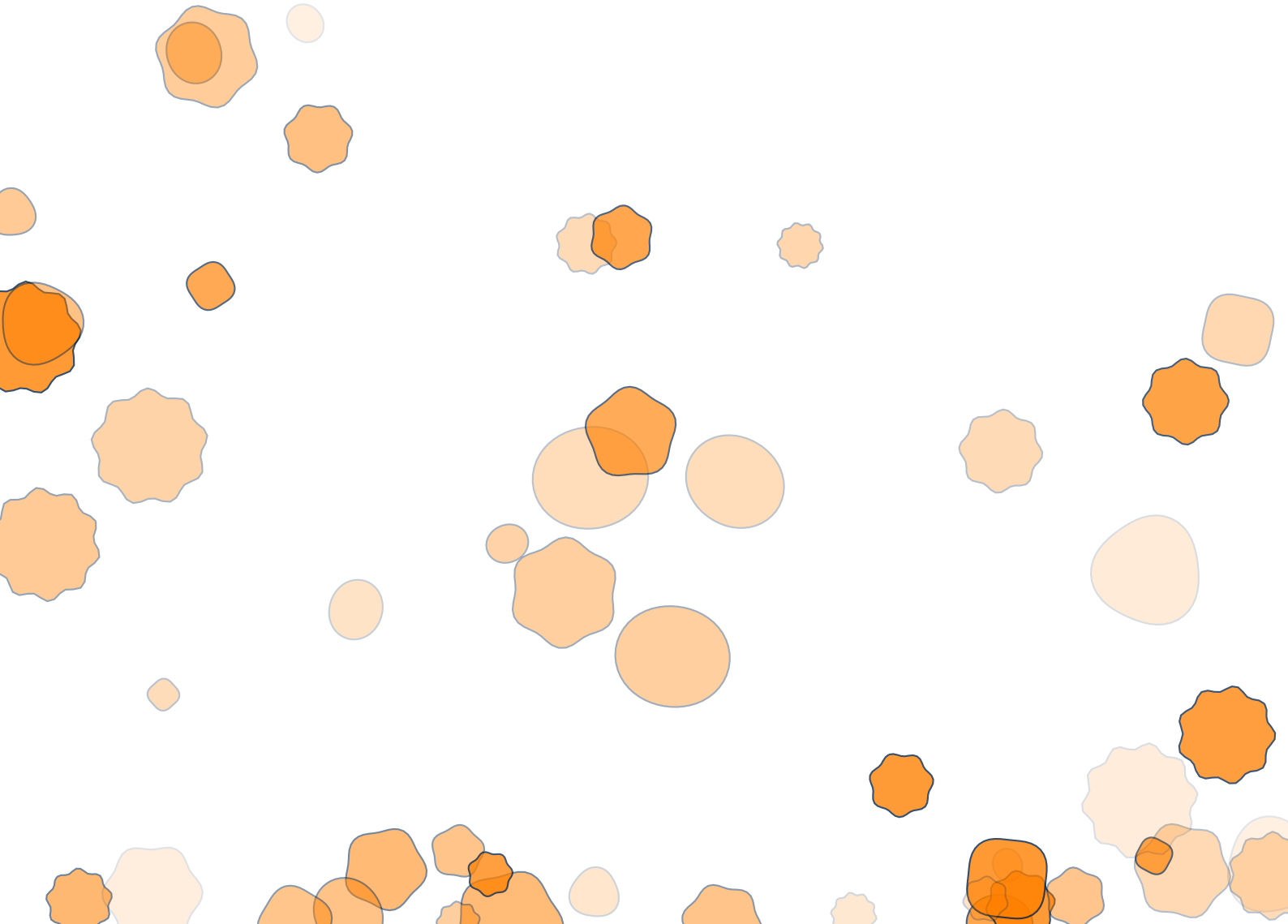

CHAPTER 4

Theoretical Background

You're off the edge of the map, mate. Here there be monsters.

— Hector Barbossa [Pirates of the Caribbean: The Curse of the Black Pearl, 2003]

In Part I we mainly dealt with the Laughlin wavefunction as a polynomial. However, as alluded to in Section 2.4.3, there exists an incredibly powerful method to express these wavefunctions in second-quantised language, which in turn also allows for the construction of additional trial wavefunctions to describe quantum Hall behaviour. The tool for this method is *Conformal Field Theory* (CFT) [35, 113, 114].

4.1 Conformal Field Theory

4.1.1 Conformal Operators

Conformal field theories are invariant under *conformal transformations*, which are any transformation that preserves angles, as shown in Fig. 4.1. Such a stringent symmetry makes these field theories especially tractable, forcing correlation functions to behave in particular ways and making the operators within the theories obey a variety of convenient identities which make them useful for all manner of problems in physics. In the quantum Hall effect these operators are exploited in a remarkable manner that was discovered by Moore and Read[22]; they noted that

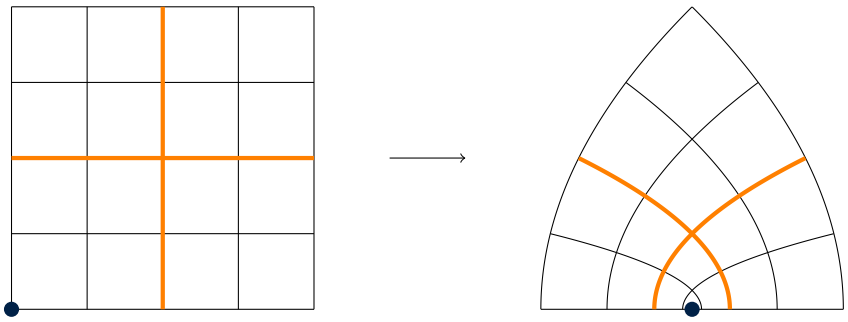

Figure 4.1: An example of a conformal transformation. Specifically, where the domain is the complex plane, z, the image is the complex plane $w = z^2$. The origin in both cases is given by the blue dot. Note that in two-dimensions any holomorphic transformation $w = f(z)$ is conformal.

the N-particle wavefunctions we have seen so far can be expressed as correlation functions of N *chiral* operators from some CFT. The authors were subsequently able to generalise this construction to produce new trial wavefunctions and there now exists a smorgasbord of such trial states including the Read-Rezayi series[23], the Haffnian[115], the Gaffnian[116] and the NASS state[117].

In this part of the thesis we will focus on two wavefunctions; the Laughlin state which we have already encountered and the Moore-Read wavefunction mentioned above. In order to understand the construction of these states in terms of CFT we will begin with introductions to the free boson and free fermion conformal field theories[35]. We will then introduce the specific construction of trial states in terms of the operators from these theories in Section 4.2[22, 34].

4.1.2 Free Bosons

Basic Solution

The conformal field theory for free bosons in two dimensions has an action of the form

$$\mathcal{S} = \frac{1}{8\pi} \int \mathrm{d}^2\boldsymbol{x}\ \partial_\mu \phi(\boldsymbol{x}) \partial^\mu \phi(\boldsymbol{x}). \tag{4.1}$$

Note that in this two-dimensional world this real scalar Bose field, $\phi(\boldsymbol{x})$, is dimensionless — it has a *scaling dimension* of zero. More generally, if the dimension of some operator $\mathcal{O}$ is ℓ^{-d} (where ℓ is some dimension of length and we work in natural units, $c = \hbar = 1$, throughout this chapter) then we say that the operator has a scaling dimension of d.

Within a path integral formulation, the two-point correlation function of fields $\phi(\boldsymbol{x})$ and $\phi(\boldsymbol{y})$ within this theory can be found by evaluating the Green's function, $G(\boldsymbol{x}, \boldsymbol{y})$, defined by

$$-\frac{1}{4\pi}\nabla^2_{\boldsymbol{x}} G(\boldsymbol{x}, \boldsymbol{y}) = \delta(\boldsymbol{x} - \boldsymbol{y}). \tag{4.2}$$

By conformal invariance this correlator can only depend on the relative position, $|\boldsymbol{x} - \boldsymbol{y}|$, which implies that, up to an overall constant

$$\langle \phi(\boldsymbol{x})\phi(\boldsymbol{y})\rangle = -\ln|\boldsymbol{x} - \boldsymbol{y}|^2. \tag{4.3}$$

Quantisation

Taking a Minkowski metric, $g_{\mu\nu} = \mathrm{Diag}(-1, 1)$ and $\boldsymbol{x} = (x, t)$, the action in Eq. 4.1 describes a one-dimensional system supported on the line, x, evolving in time, t. We will take periodic boundary conditions, $\phi(x + L, t) = \phi(x, t)$, thus placing the system on a cylinder of circumference L. We may therefore decompose the field in Fourier modes,

$$\phi(x, t) = \sum_n \phi_n(t) e^{i\frac{2\pi n}{L}x} \tag{4.4}$$

where $\phi_n^\dagger = \phi_{-n}$. Inserting this into the Lagrangian allows one to identify the generalised momenta of the theory as $\pi_n = \frac{L}{4\pi}\dot{\phi}_{-n}$, where $\dot{\phi}_n = \frac{\partial \phi_n}{\partial t}$, and hence we can construct the system's Hamiltonian, which is

$$H = \frac{2\pi}{L}\sum_n \left(\pi_n \pi_{-n} + \left(\frac{n}{2}\right)^2 \phi_n \phi_{-n}\right). \tag{4.5}$$

This Hamiltonian describes a collection of oscillators with frequency $\omega_n = \frac{2\pi}{L}|n|$. We canonically quantise, taking $[\phi_n, \pi_m] = i\delta_{n,m}$, and can then define

ladder operators for each oscillator,

$$a_n = \pi_{-n} - \frac{in}{2}\phi_n, \qquad \bar{a}_n = \pi_n - \frac{in}{2}\phi_{-n}, \tag{4.6}$$

which satisfy $a_n^\dagger = a_{-n}$ and obey the commutation relations

$$[a_n, a_m] = n\delta_{n+m,0}, \qquad [a_n, \bar{a}_m] = 0, \qquad [\bar{a}_n, \bar{a}_m] = n\delta_{n+m,0}. \tag{4.7}$$

Furthermore, one finds that $[H, a_{-n}] = \frac{2\pi n}{L} a_{-n}$ and similar for $\bar{a}_{-n}$ so we can identify a_{-n} and $\bar{a}_{-n}$ for $n > 0$ as the raising operators of the theory, which increase the energy of a given state by $\frac{2\pi n}{L}$. Likewise, we can identify the a_n and $\bar{a}_n$ for $n > 0$ as lowering operators and therefore define the vacuum state, $|0\rangle$, as the state which is annihilated by all a_n and $\bar{a}_n$ for $n \geq 0$.

The operators remaining with which to generate the full Fock space include a_{-n} and $\bar{a}_{-n}$ for $n > 0$, each of which increase the energy of the state. However, our field theory also contains a symmetry which produces an extra degeneracy due to the operators a_0 and ϕ_0. Within the action, Eq. 4.1, this symmetry manifests itself as the invariance of $\mathcal{S}$ under the transformation $\phi(\boldsymbol{x}) \to \phi(\boldsymbol{x}) + \text{constant}$. For the Hamiltonian, the symmetry is $[H, a_0] = 0$ where a_0 is the operator that counts this charge. We may then define states of zero energy but charge C by

$$|C\rangle = e^{iC\phi_0}|0\rangle, \tag{4.8}$$

such that $a_0|C\rangle = C|C\rangle$. As a corollary note that states $|C\rangle$ with differing charge are orthogonal[1]. Therefore, a general state in the theory is of the form

$$|\psi\rangle = e^{iC\phi_0} \prod_i a_{-n_i} \prod_j \bar{a}_{-\bar{n}_j}|0\rangle \tag{4.10}$$

for any sets of positive integers n_i and $\bar{n}_j$.

[1] To prove this note that $a_0^\dagger = a_0$. Therefore, consider the matrix element

$$\langle C_1|a_0|C_2\rangle = C_1\langle C_1|C_2\rangle = C_2\langle C_1|C_2\rangle, \tag{4.9}$$

which implies that, unless $C_1 = C_2$, the overlap of any two states must be zero.

Mode Expansion

We now consider the structure of the field itself, which will be of crucial importance in the construction of trial wavefunctions. To do so, note that $\phi_n(t) = \frac{i}{n}[a_n(t) - \bar{a}_{-n}(t)]$ where the time dependence of these ladder operators can be extracted using a Heisenberg picture, conjugating with the evolution operator, e^{-iHt}, to find

$$a_n(t) = a_n(0)e^{-i\frac{2\pi n}{L}t}. \tag{4.11}$$

This gives us the time dependence of all $\phi_n(t)$ except for $\phi_0(t)$, which does not appear in the definition of any ladder operators. However, using the canonical commutation relations it is simple to show that

$$\phi_0(t) = \varphi_0 + \frac{4\pi}{L}a_0 t \tag{4.12}$$

where $\varphi_0 = \phi_0(0)$.

Using these results we can now express the field with the time dependence explicit. With all operators now implicitly time-independent, the field in terms of ladder operators has the form

$$\phi(x,t) = \varphi_0 + \frac{4\pi}{L}a_0 t + i\sum_{n\neq 0}\frac{1}{n}\Big(a_n e^{-i\frac{2\pi n}{L}(t-x)} + \bar{a}_n e^{-i\frac{2\pi n}{L}(t+x)}\Big). \tag{4.13}$$

By inspection we note that can be split into two chiral fields, $\phi(x,t) = \varphi(t-x) + \varphi(t+x)$, one of which corresponds to right-moving bosons and the other corresponding to left-movers. We will find it useful to phrase this chirality in terms of complex coordinates on the plane, $z = e^{\frac{2\pi}{L}(\tau - ix)}$ and $\bar{z} = e^{\frac{2\pi}{L}(\tau + ix)}$ where $\tau = it$ is the *Euclidean time*. This mapping is shown in Fig. 4.2. Therefore, we can express $\phi(x,t)$ as the sum of a holomorphic part, $\varphi(z)$, and an anti-holomorphic part, $\bar{\varphi}(\bar{z})$. We then take

$$\varphi(z) = \varphi_0 - ia_0\ln(z) + i\sum_{n\neq 0}\frac{1}{n}a_n z^{-n}. \tag{4.14}$$

as the subsequent mode expansion.

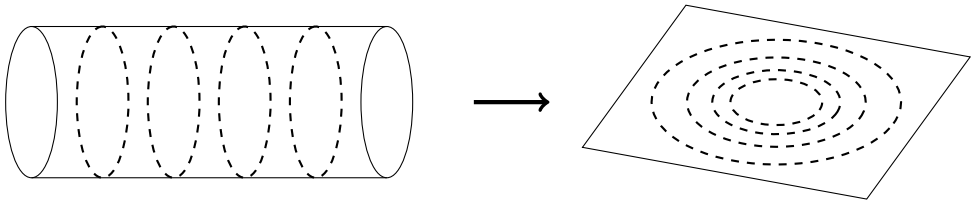

Figure 4.2: The mapping $z = e^{\frac{2\pi}{L}(\tau - ix)}$ which maps rings at constant Euclidean time, τ, on the cylinder onto rings over the plane.

Aside 11

Note that the mode expansion in Eq. 4.14 is not quite as advertised. Assuming an equivalent definition for $\bar{\varphi}(\bar{z})$ one would find that $\varphi(z) + \bar{\varphi}(\bar{z}) = \phi(z, \bar{z}) + \varphi_0$, which includes an extra zero mode. We rectify this using a procedure called *compactification*, which places the range of ϕ onto a circle so that ϕ is identified with $\phi + 2\pi Q$ where Q is some integer called the *compactification radius*. This introduces another zero mode into the expansion of ϕ due to the possible winding of the field (i.e, $\phi(x, t)$ can now include some linear term $a_0' x$). In this way we note that the symmetry $\phi \to \phi + \text{const}$ is a U(1) symmetry with an associated U(1) charge measured by a_0. The extra zero modes make Eq. 4.14 exact, though complicate the energetics so have been omitted here for simplicity.

Identities for the Bose Field

We now consider crucial identities for the chiral Bose field given by the mode expansion, Eq. 4.14. We have already seen the two-point correlator for the full field $\phi(z, \bar{z})$ in Eq. 4.3 and, given the decoupling into $\varphi(z)$ and $\bar{\varphi}(\bar{z})$ it is no surprise that

$$\langle \varphi(z)\varphi(w) \rangle = -\ln(z - w). \tag{4.15}$$

Another extremely important result we will need from the free boson theory

is the concept of *Vertex operators*. Given that $\varphi(z)$ is dimensionless it can be exponentiated without introducing a new scale by defining

$$\mathcal{V}_\alpha(z) =: e^{i\alpha\varphi(z)} : \tag{4.16}$$

for some number α and where the notation $: X :$ refers to the *normal ordering* of operator X[2]. This operator has a U(1) charge of α and a scaling dimension of $\frac{\alpha^2}{2}$. An important identity for this operator which we will require later pertains to the product of two such operators. The Baker-Campbell-Hausdorff formula gives the result that

$$: e^{\Phi_1} :: e^{\Phi_2} :=: e^{\Phi_1+\Phi_2} : e^{\langle\Phi_1\Phi_2\rangle}, \tag{4.17}$$

where Φ_1 and Φ_2 are operators of a harmonic oscillator as in the case of our free boson. Therefore,

$$\mathcal{V}_\alpha(z)\mathcal{V}_\beta(w) = (z-w)^{\alpha\beta} : e^{i(\alpha\varphi(z)+\beta\varphi(w))} : . \tag{4.18}$$

4.1.3 Free Fermions

Basic Solution

We now consider free Majorana fermions in two dimensions. The field in this case is made from two Grassmann fields, $\Psi = (\psi, \bar{\psi})^{\mathrm{T}}$ and, in terms of complex coordinates, has an action of the form

$$\mathcal{S} = \frac{1}{2\pi}\int \mathrm{d}^2 z\big(\bar{\psi}\partial\bar{\psi} + \psi\bar{\partial}\psi\big). \tag{4.19}$$

Note that the fields ψ and $\bar{\psi}$ have scaling dimension of $\frac{1}{2}$. Note however that this theory contains a *parity symmetry* due to the Grassmann nature of the fields. Effectively, one notes that observables and the action must be real which, due to the nature of Grassmann variables, requires them to be some product of an even number of fields.

[2] Normal ordering is the process of removing unwanted infinities by moving all annihilation operators to the right of the expression or, equivalently, by defining $: X := X - \langle 0|X|0\rangle$.

The classical equations of motion relating to the free fermion action are $\partial\bar{\psi} = \bar{\partial}\psi = 0$. Therefore, as in the bosonic case, we have a "left-mover", $\psi(z)$ and a "right-mover", $\bar{\psi}(\bar{z})$. To find the correlation functions we once again look for Green's functions, defined by the equations

$$\begin{pmatrix} \frac{1}{\pi}\bar{\partial}_z & 0 \\ 0 & \frac{1}{\pi}\partial_z \end{pmatrix} \begin{pmatrix} \langle\psi(z,\bar{z})\psi(w,\bar{w})\rangle & \langle\psi(z,\bar{z})\bar{\psi}(w,\bar{w})\rangle \\ \langle\bar{\psi}(z,\bar{z})\psi(w,\bar{w})\rangle & \langle\bar{\psi}(z,\bar{z})\bar{\psi}(w,\bar{w})\rangle \end{pmatrix} = \mathbb{1}\delta^{(2)}(z-w), \quad (4.20)$$

where $\mathbb{1}$ is the 2×2 identity. We can then make use of the result[3] that $\bar{\partial}z^{-1} = \partial\bar{z}^{-1} = \pi\delta^{(2)}(z)$ to see that

$$\langle\psi(z,\bar{z})\psi(w,\bar{w})\rangle = \frac{1}{z-w}, \quad (4.21)$$

$$\langle\bar{\psi}(z,\bar{z})\bar{\psi}(w,\bar{w})\rangle = \frac{1}{\bar{z}-\bar{w}}, \quad (4.22)$$

$$\langle\psi(z,\bar{z})\bar{\psi}(w,\bar{w})\rangle = 0. \quad (4.23)$$

Mode Expansion

Much like in the bosonic case, the Majorana field has a well-defined mode expansion, which on the plane takes the form

$$\psi(z) = \sum_k \psi_k z^{-k-\frac{1}{2}}, \quad (4.24)$$

and similar for $\bar{\psi}(\bar{z})$. The power of $-\frac{1}{2}$ is included as the scaling dimension of the field is $\frac{1}{2}$, hence making the dimensionality explicit. However, to ensure that the field is single-valued on the plane the allowable values of k are therefore restricted to the half-integers, $k \in \mathbb{Z} + \frac{1}{2}$.

These modes satisfy the anti-commutation relations

$$\{\psi_k, \psi_p\} = \delta_{k+p,0}, \qquad \{\psi_k, \bar{\psi}_p\} = 0, \qquad \{\bar{\psi}_k, \bar{\psi}_p\} = \delta_{k+p,0}. \quad (4.25)$$

Furthermore, the modes ψ_k and $\bar{\psi}_k$ for $k > 0$ can once again be interpreted as annihilation operators and ψ_{-k} and $\bar{\psi}_{-k}$ as creation operators. The vacuum is

[3] This can be checked by integrating a holomorphic test function and applying Gauss' law.

therefore the state defined by $\psi_k|0\rangle = \bar{\psi}_k|0\rangle = 0$ for all $k > 0$, which leads to a full Fock space containing any state of the form

$$|\psi\rangle = \prod_i \psi_{-k_i} \prod_j \bar{\psi}_{-\bar{k}_j}|0\rangle, \tag{4.26}$$

where k_i and $\bar{k}_j$ are any positive half-integers. However, due to fermionic exclusion there can be no duplicates (i.e, the state $\psi_{\frac{1}{2}}\psi_{\frac{1}{2}}|0\rangle$ is not allowed because $\psi^2_{\frac{1}{2}} = 0$). Using this technology it is relatively simple to check that $\langle 0|\psi(z)\psi(w)|0\rangle = \frac{1}{z-w}$.

4.1.4 Energy-Momentum

In both of these theories, a special operator is the energy-momentum tensor, which is a conserved Noether current arising from conformal invariance. For the free boson and free fermion theories the holomorphic part of this current has the form

$$T^{\varphi}(z) = \frac{1}{2} : (i\partial\varphi(z))^2 : \tag{4.27}$$

$$\text{and} \qquad T^{\psi}(z) = -\frac{1}{2} : \psi(z)\partial\psi(z) : \tag{4.28}$$

respectively where, as before, :: corresponds to normal ordering of the operators. Much like the fields themselves, these $T(z)$ also admit their own mode expansions of the form

$$T(z) = \sum_n L_n z^{-n-2} \tag{4.29}$$

where the L_n are the modes of the *Virasoro algebra* and correspond to particular facets of the set of conformal transformations. For example, L_{-1} is the generator of translations whilst L_0 generates dilations and rotations on the plane. The operator L_0 is particularly special as it makes up the Hamiltonian with $H \propto L_0 + \bar{L}_0$. The eigenvalue of L_0 is called the *conformal dimension* of the state and for both of our theories effectively counts the numbers of modes weighted by their mode number, i.e, $[L_0, a_{-n}] = na_{-n}$ and $[L_0, \psi_k] = k\psi_k$.

4.2 Trial Wavefunctions as Conformal Blocks

4.2.1 General Construction

We now introduce the remarkable result that trial wavefunctions can be written as correlation functions of chiral operators from a conformal field theory[22, 23, 34, 118]. The relevant CFTs will always be made up of two *sectors*, being supported in some

$$\mathrm{CFT} = \mathrm{CFT}_{\mathrm{U}(1)} \otimes \mathrm{CFT}_{\chi}, \tag{4.30}$$

where the U(1) sector always corresponds to the chiral part of the free boson theory and CFT_{χ} is the *statistics sector*, some other chiral CFT which contains the holomorphic field $\chi(z)$. In this way we will construct operators from the building blocks of the CFT which represent the individual particles in a manner similar to *bosonisation*[103, 104].

Specifically, we represent any given particle at position z by the operator

$$\mathcal{A}_m(z) = \chi(z) : e^{i\sqrt{m}\varphi(z)} :, \tag{4.31}$$

which has a U(1) charge of magnitude $\sqrt{m}$ given by the vertex operator of $\varphi(z)$. The quantum Hall wavefunction on the plane at filling fraction $\nu = 1/m$ can then be expressed as the correlation function

$$\Psi_{\langle v|}(\boldsymbol{z}) = \langle v| c_m^N \mathcal{A}_m(z_1) \dots \mathcal{A}_m(z_N) |0\rangle, \tag{4.32}$$

where c_m^N is the *background charge*, $|0\rangle = |0\rangle_{\mathrm{U}(1)} \otimes |0\rangle_{\chi}$ is the vacuum of the full CFT and $|v\rangle$ is some neutral state of the full CFT (i.e, a state containing zero U(1) charge). Note that in the absence of the background charge, this correlator would evaluate to zero, as the N particle operators provide a total charge of $N\sqrt{m}$. The background charge is a neutralising operator of the form

$$c_m^N = e^{-iN\sqrt{m}\varphi_0}, \tag{4.33}$$

and hence the correlator is non-vanishing.

Aside 12

Note that our particular choice for the background charge in Eq. 4.33 is not unique. Physically, this choice corresponds to placing a U(1) charge of $-N\sqrt{m}$ at infinity but alternative methods exist in which the charge is instead spread out over the droplet[118]. We place our charge at infinity because it is significantly simpler to work with but we note that, unlike some other choices, it will lead to wavefunctions $\Psi_{\langle v|}(\boldsymbol{z})$ which do *not* include the Gaussian factors, $\exp\left(-\frac{|z|^2}{4{\ell_{\mathrm{B}}}^2}\right)$, usually attached to each orbital. However, given the constancy of these factors it is exceedingly simple to include them within our integration measure instead of directly attached to each state. Therefore, we will define the overlap of two quantum Hall wavefunctions as

$$\left\{\Psi_{\langle v|}\middle|\Psi_{\langle w|}\right\} = \int_{\mathbb{C}^N} \mathrm{D}\boldsymbol{z}\ \bar{\Psi}_{\langle v|}(\boldsymbol{z})\Psi_{\langle w|}(\boldsymbol{z}), \tag{4.34}$$

where the integration measure has the form

$$\mathrm{D}\boldsymbol{z} = \prod_i \left[\mathrm{d}^2 z_i \exp\left(-\frac{|z_i|^2}{2{\ell_{\mathrm{B}}}^2}\right)\right]. \tag{4.35}$$

Note that $\Psi_{\langle v|}(\boldsymbol{z})$ describes edge states with the auxiliary state, $|v\rangle$ corresponding to the particular edge excitation. In fact, Ψ can be considered as some linear mapping from a CFT state to a physical wavefunction,

$$\Psi : |v\rangle \mapsto \Psi_{\langle v|}(\boldsymbol{z}). \tag{4.36}$$

For the case $|v\rangle = |0\rangle$, the wavefunction is that of the ground state. More generally we recall that each edge excitation has an associated quantum number, ΔL, which corresponds to the amount of angular momentum each edge state has with respect to the ground state. The analogue in the CFT is the conformal dimension of the state $|v\rangle$ with $L_0|v\rangle = \Delta L|v\rangle$.

4.2.2 The Laughlin State

The Laughlin state has a trivial statistics sector, i.e, $\chi = \mathbb{1}$, making its CFT solely that of the free boson, $\mathrm{CFT}_{\mathrm{U}(1)}$. The particle operator for this case is then simply the vertex operator. Therefore, we can use the identity for products of vertex operators given in Eq. 4.18 to see that

$$\Psi_{\langle 0|}(\boldsymbol{z}) = \langle 0| : e^{i\sqrt{m}\left(\sum_i \varphi(z_i) - N\varphi_0\right)} : |0\rangle \prod_{i<j}(z_i - z_j)^m = \prod_{i<j}(z_i - z_j)^m \tag{4.37}$$

as required for the Laughlin wavefunction.

Now consider some non-trivial auxiliary state, $|v\rangle$. This state must be neutral such that it does not add any particles but can otherwise be any state from the $\mathrm{CFT}_{\mathrm{U}(1)}$. We can label the states as

$$|\boldsymbol{\lambda}\rangle = \prod_{n\in\boldsymbol{\lambda}} a_{-n}|0\rangle \tag{4.38}$$

where $\boldsymbol{\lambda} = \{\lambda_1, \lambda_2, \ldots\}$ is an integer partition containing any collection of integers greater than zero. These states have conformal dimension $L_0|\boldsymbol{\lambda}\rangle = \sum_i \lambda_i |\boldsymbol{\lambda}\rangle$, which corresponds to the amount of angular momentum added by the particular excitation.

The mapping to a first quantised wavefunction can be found by noting that

$$[a_n, \mathcal{A}_m(z)] = \sqrt{m} z^n \mathcal{A}_m(z). \tag{4.39}$$

Therefore, it is straightforward to see that the a_n modes correspond to unnormalised power sums,

$$\Psi_{\langle\boldsymbol{\lambda}|}(\boldsymbol{z}) = m^{\frac{\ell(\boldsymbol{\lambda})}{2}} P_{\boldsymbol{\lambda}}(\boldsymbol{z}) \prod_{i<j}(z_i - z_j)^m, \tag{4.40}$$

where the individual p_n are taken to be unnormalised, i.e, $p_n = \sum_i z_i^n$, and recall that the notation $\ell(\boldsymbol{\lambda})$ refers to the number of elements in the partition $\boldsymbol{\lambda}$. Therefore, as claimed, the state $\Psi_{\langle\boldsymbol{\lambda}|}$ does indeed have angular momentum $\Delta L = \sum_i \lambda_i$ with respect to the ground state[4].

[4] We can now contrast this picture in terms of a CFT with the modes of the density we

4.2.3 The Moore-Read State

The statistics sector for the Moore-Read wavefunction is that of a free Majorana fermion with field $\chi(z) = \psi(z)$. Before we construct the trial wavefunctions which follow from this CFT it is worth recalling that the fermionic CFT contains a parity symmetry, which forces the correlation function of an odd number of fermionic fields to vanish. Therefore, the construction differs slightly between odd and even particle numbers, and we shall focus initially on the even case. In this case the vacuum, $|0\rangle$, corresponds to the ground state, which has the form

$$\Psi_{\langle 0|}(\boldsymbol{z}) = \langle \psi(z_1) \dots \psi(z_N) \rangle \prod_{i<j} (z_i - z_j)^m. \tag{4.41}$$

To the many-body fermion correlator one can apply Wick's theorem to find the Moore-Read (Pfaffian) wavefunction,

$$\Psi_{\langle 0|}(\boldsymbol{z}) = \mathrm{Pf}\left(\frac{1}{z_i - z_j}\right) \prod_{i<j} (z_i - z_j)^m, \tag{4.42}$$

where this extra term, Pf(...), is called the Pfaffian, and is an antisymmetrised sum over all products of the fractions $\frac{1}{z_i - z_j}$,

$$\mathrm{Pf}\left(\frac{1}{z_i - z_j}\right) = \mathbb{A}\left(\frac{1}{z_1 - z_2}\frac{1}{z_3 - z_4} \cdots \frac{1}{z_{N-1} - z_N}\right) \tag{4.43}$$

where $\mathbb{A}$ refers to the antisymmetrisation over all the indices $1, \dots, N$. Once again, note the absence of Gaussian factors in Eq. 4.42, which we once again place within the integration measure, whose form is once again given by Eq. 4.35.

Aside 13

We claim that the Moore-Read wavefunction describes the quantum Hall effect at filling $\nu = 1/m$. To see this note that the maximum angular momentum of any one particle in the Moore-Read ground state is $m(N-2)$.

considered in Section 2.4.3. By comparing the resulting space of states and the commutation relations of the modes we see that the two pictures are equivalent with $\rho_{k_n} = \sqrt{\frac{\nu}{2\pi R}} a_n$, where we recall that $k_n = \frac{n}{R}$.

Therefore, for large system sizes we see that, indeed, there are N particles filling approximately mN orbitals. It is then proposed that this state or its particle-hole conjugate, the *anti-Pfaffian* describes the true ground state of the quantum Hall state at filling fraction $\nu = 5/2$ (i.e, with two inert lower Landau levels and an additional half-filled, spin-polarised level)[119–124].

Furthermore, note that there also exist parent Hamiltonians for the Moore-Read state[125, 126]. However, the interactions necessary to realise the exact form in Eq. 4.42 are three-body interactions which impose energy costs unless the wavefunction vanishes sufficiently fast as $z_i \to z_j \to z_k$.

Consistent with the Laughlin state, we excite edge modes by applying the positive modes of the fields in our CFT on the vacuum. In this case, we have two branches of excitations, one of which is an exact replica of the bosonic excitations from the Laughlin state and another arising due to the fermionic field. This second branch is more restricted than for the bosons because the individual states must obey parity symmetry and satisfy fermionic exclusion. As such, general states have the form

$$|\boldsymbol{\lambda}; \boldsymbol{\mu}\rangle = \prod_{n \in \boldsymbol{\lambda}} a_{-n} \prod_{l \in \boldsymbol{\mu}} \psi_{-l} |0\rangle \tag{4.44}$$

where $\boldsymbol{\lambda}$ is once again any integer partition but $\boldsymbol{\mu}$ is an ordered $(\mu_1 > \mu_2 > \ldots)$ set of positive half-integers $(\mu_i \in \mathbb{Z}^+ + \frac{1}{2})$. Parity symmetry then forces the number of elements within the set $\boldsymbol{\mu}$ to be even. Furthermore, given that the ψ_l anti-commute we must also enforce an ordering on this product and we choose to order the ψ_l with the smallest l at the right-most position, i.e,

$$\left|\emptyset; \frac{3}{2}, \frac{1}{2}\right\rangle = \psi_{\frac{3}{2}} \psi_{\frac{1}{2}} |0\rangle \tag{4.45}$$

where $\emptyset$ refers to an empty set containing no elements. Despite the extra complexity of these states, they once again raise the angular momentum by an amount

equal to the conformal dimension of the state, which in this case is

$$\Delta L = \sum_i \lambda_i + \sum_j \mu_j. \tag{4.46}$$

Therefore, there must once again be some function of the z_i multiplying the ground state with a total degree of ΔL and it has the form

$$\mathcal{P}_{\boldsymbol{\lambda},\boldsymbol{\mu}} = m^{\frac{\ell(\boldsymbol{\lambda})}{2}} P_{\boldsymbol{\lambda}}(\boldsymbol{z}) \frac{\left\langle \left(\prod_{l\in\boldsymbol{\mu}} \psi_l\right) \psi(z_1)\cdots\psi(z_N)\right\rangle}{\langle \psi(z_1)\cdots\psi(z_N)\rangle} \tag{4.47}$$

where these correlation functions can be evaluated by Wick's theorem to give similar Pfaffians to Eq. 4.43 (see Ref. [34] for an explicit example).

Aside 14

Finally, we consider the case when N is odd. The picture is almost identical but, due to parity symmetry, we must be careful to ensure that the total number of fermionic operators within any given correlator is even despite an odd number of particle operators. This discrepancy is made up for by the edge states, which are identical to those in Eq. 4.44 except that $\boldsymbol{\mu}$ must contain an odd number of elements. This even holds for the ground state, which is instead defined by the CFT state $\psi_{\frac{1}{2}}|0\rangle$. Furthermore, an odd particle number leads to a different counting of states to the even Moore-Read state. For example, at $\Delta L = 1$ the only edge state when N is even is $|1;\emptyset\rangle$ but when N is odd we can have both $\left|\emptyset;\frac{3}{2}\right\rangle$ and $\left|1;\frac{1}{2}\right\rangle$.

4.2.4 "Ward Identities" for Trial States

In the following two chapters we will consider the effects of various symmetries in the first-quantised space of quantum Hall wavefunctions and their effects on this auxiliary CFT space. To do so, we will need to be able to map a number of operators acting on $\Psi_{\langle v|}(\boldsymbol{z})$ to operators which act directly on the auxiliary state,

$|v\rangle$. We have already seen a number of these in the form of the edge states,

$$\left(\sum_i z_i^n\right)\Psi_{\langle v|}(\boldsymbol{z}) = \Psi : \langle v|\frac{a_n}{\sqrt{m}}. \tag{4.48}$$

What follows is a series similar mappings for some important operators, some of which are reminiscent of the *Ward identities*[35], which are a set of differential equations for correlators in a CFT arising due to conformal symmetry.

The Number Operator

Consider first the action of the number operator, $\hat{N}$. Recall that each particle is represented by the operator $\mathcal{A}_m(z)$ and these carry a U(1) charge of $\sqrt{m}$. Given that this charge must accompany every particle we surmise that the operator $a_0/\sqrt{m}$ will count particles. Therefore,

$$\hat{N}\Psi_{\langle v|}(\boldsymbol{z}) = \langle v|c_m^N\left(\frac{a_0}{\sqrt{m}}\right)\mathcal{A}_m(z_1)\cdots\mathcal{A}_m(z_N)|0\rangle. \tag{4.49}$$

However, the job is not complete as this operator does not act directly on our auxiliary state but instead on $|v\rangle$ through the background charge. To find the action directly on the state $|v\rangle$ we must then commute it through this background charge, which has the effect that $a_0 \to a_0 + N\sqrt{m}$ throughout. This produces the result that

$$\hat{N}\Psi_{\langle v|}(\boldsymbol{z}) = \Psi : \left(N + \frac{a_0}{\sqrt{m}}\right)|v\rangle. \tag{4.50}$$

The Dilation Operator

We next consider the action of the generator of dilations,

$$\mathcal{L}_0 = \sum_i z_i\partial_i \tag{4.51}$$

on our state. Acting on a holomorphic polynomial, this operator simply counts the total degree of that polynomial. Therefore, it should be immediately obvious that its mapping into the CFT will be as L_0 plus some constant relating to the total angular momentum of the ground state.

Assuming we do not know the rest angular momentum we can use the result that

$$[L_0, \mathcal{A}_m(z)] = \left(z\partial + \frac{\tilde{m}}{2}\right)\mathcal{A}_m(z) \tag{4.52}$$

where $\tilde{m} = m$ for the Laughlin wavefunction and $m+1$ for the Moore-Read state. Therefore, we can replace the action of $\mathcal{L}_0$ with

$$\sum_i z_i \partial_i \Psi_{\langle v|}(\boldsymbol{z}) = \langle v| c_m^N \left(L_0 - \frac{\tilde{m}N}{2}\right)\mathcal{A}_m(z_1)\ldots\mathcal{A}_m(z_N)|0\rangle. \tag{4.53}$$

As a final step we must once again commute this operator through the background charge. To do so we note that conjugating the bosonic field by c_m^N has the effect

$$c_m^N i\partial\varphi(z) c_m^{-N} = i\partial\varphi(z) + \frac{N\sqrt{m}}{z} \tag{4.54}$$

but has no effect on the statistics sector. Therefore, given that $L_0 = L_0^{\varphi} + L_0^{\psi}$ and the operator from the statistics sector commutes with the charge, it can be shown that

$$\mathcal{L}_0 \Psi_{\langle v|}(\boldsymbol{z}) = \Psi : \left(L_0 + a_0 N\sqrt{m} + \frac{(mN - \tilde{m})N}{2}\right)|v\rangle. \tag{4.55}$$

For our neutral states the a_0 term will evaluate to zero and this constant is usually unimportant, leaving solely L_0. Note however that this constant does indeed reproduce the expected total angular momentum of the ground state, $\frac{mN(N-1)}{2}$ for the Laughlin state and $\frac{mN(N-2)}{2}$ for Moore-Read.

The Translation Operator

We conclude with a mapping of the generator of translations into the CFT,

$$\mathcal{L}_{-1} = \sum_i \partial_i. \tag{4.56}$$

Once again, it is perhaps unsurprising that the operator in the CFT language which replicates the action of the translation operator on the full wavefunction is in fact the generator of translations, L_{-1}. To see this we note that

$$[L_{-1}, \mathcal{A}_m(z)] = \partial\mathcal{A}_m(z), \tag{4.57}$$

and therefore we can map the derivative directly into the CFT as

$$\sum_i \partial_i \Psi_{\langle v|}(\boldsymbol{z}) = \langle v| c_m^N (L_{-1}) \mathcal{A}_m(z_1) \dots \mathcal{A}_m(z_N) |0\rangle. \tag{4.58}$$

We once again wish to commute this through the background charge and therefore, using the result for the conjugation of the field by the charge given in Eq. 4.54, find that the action of a derivative directly on the state is

$$\mathcal{L}_{-1} \Psi_{\langle v|}(\boldsymbol{z}) = \Psi : \left(L_{-1} + N\sqrt{m} a_{-1}\right)^\dagger |v\rangle. \tag{4.59}$$

Projection to the Lowest Landau Level

We conclude this section with an identity which will make it far easier to map certain terms in the space of polynomial wavefunctions into the CFT by converting them into differential operators. The procedure is called *Projection to the lowest Landau level*[127] and relies on the fact that the wavefunctions we work with will always be holomorphic polynomials with some unchanging Gaussian factors. Therefore, consider the matrix element of a single power of the anti-holomorphic coordinate, $\bar{z}_i$, between the states labelled by auxiliary states $|v\rangle$ and $|w\rangle$. This is defined as

$$(\bar{z}_i)_{v,w} = \int \mathrm{D}\boldsymbol{z} \bar{\Psi}_{\langle v|}(\bar{\boldsymbol{z}}) \bar{z}_i \Psi_{\langle w|}(\boldsymbol{z}), \tag{4.60}$$

where we recall the existence of the Gaussian factors in the integration measure, Eq. 4.35. Therefore, in any such matrix element we can replace the power of $\bar{z}_i$ by a derivative acting on the Gaussian factor within the integration measure,

$$(\bar{z}_i)_{v,w} = \int 2{\ell_\mathrm{B}}^2 \partial_i (\mathrm{D}\boldsymbol{z}) \bar{\Psi}_{\langle v|}(\bar{\boldsymbol{z}}) \Psi_{\langle w|}(\boldsymbol{z}). \tag{4.61}$$

We then integrate by parts, using that the Gaussian factors cause the integrand to vanish at infinity, and therefore conclude that, within the space of states of lowest Landau level wavefunctions, we are at liberty to make the substitution,

$$\bar{z}_i \to 2{\ell_\mathrm{B}}^2 \partial_i. \tag{4.62}$$

In this way we will be able to consider the action of the anti-holomorphic coordinates on the holomorphic wavefunctions.

CHAPTER 5

Inner Products

O, what may man within him hide, Though angel on the outward side!

— Duke Vincentio [Measure for Measure, William Shakespeare, 1603]

Calculating the overlaps of the strongly correlated trial wavefunctions in the quantum Hall effect is a very difficult problem Nevertheless, the problem is of great importance for finding the energy and entanglement spectra of quantum Hall systems, as well as for computing observables. Recent works have made progress by using the aforementioned description of wave functions in terms of CFT correlation functions[34, 128], as we can work with the much simpler space of states from the auxiliary CFT space. We will closely follow the description in Ref. [34] where the authors provide powerful constraints on the structure of the inner products of these trial states by appealing to the underlying symmetries of qH states.

In Ref. [34] the structure of these edge state inner products was used to analyze the particle and real-space entanglement spectra of quantum Hall states[129, 130]. However, the exact form for the inner product is a conjecture. Therefore, even though the conjecture is extremely well motivated, being based on an exact calculation for the trial wave functions of a $p_x + ip_y$ superconductor and having a strong physical basis, the authors do not provide a derivation of this result. Specifically, the authors of Ref. [34] use the ansatz that the inner product form is the exponential of a local action, S_N, which is very difficult to prove in general,

and we can only do so for the integer quantum Hall case, as demonstrated in a future publication[131]. Therefore, it is important to further check the validity of this powerful result, and this constitutes the main outcomes of this chapter as we provide extensive numerical evidence in support of these claims. We also use the constraints proposed in Ref. [34] to calculate S_N to very high orders. In Chapter 6 we will build on these results to study effective Hamiltonians for the quantum Hall effect.

We begin in Section 5.1 with an overview of the general form for inner products and an introduction to the constraints provided by the symmetries of quantum Hall states in the CFT. In Section 5.2 we provide high order expansions calculated for S_N in the Laughlin and Moore-Read cases. Finally, we provide numerical evidence in support of the conjectures made by Ref. [34] in Section 5.3.

5.1 Symmetries of the Inner Product

In this section we will introduce the notation and general structure of inner products of edge state wave functions in the quantum Hall effect. We will then review the conjecture and symmetry analysis of Ref. [34] before using these symmetries to constrain the form of this inner product as much as possible.

5.1.1 CFT Formulation

For the purposes of inner products we will use curly Dirac notation for states in the physical space of holomorphic polynomials to distinguish them from the states in the conformal field theory, i.e.,

$$\left\{\boldsymbol{z}\middle|\Psi_{\langle v|}\right\} = \Psi_{\langle v|}(\boldsymbol{z}). \tag{5.1}$$

We are interested in finding the overlaps of such states, as defined by the integration measure in Eq. 4.35. Using our previous definitions of quantum Hall states

in terms of conformal blocks we may now rewrite this inner product in the Hilbert space of the CFT as

$$\left\{\Psi_{\langle v|}\middle|\Psi_{\langle w|}\right\} = \int \mathrm{D}\boldsymbol{z}\langle w|c_m^N\mathcal{A}_m(z_1)\dots\mathcal{A}_m(z_N)|0\rangle\langle 0|{\mathcal{A}_m}^\dagger(\bar{z}_N)\dots{\mathcal{A}_m}^\dagger(\bar{z}_1)c_m^{-N}|v\rangle. \tag{5.2}$$

Therefore, we can define the inner product, G_N, within the space of the CFT as

$$G_N = \int \mathrm{D}\boldsymbol{z}c_m^N\mathcal{A}_m(z_1)\dots\mathcal{A}_m(z_N)|0\rangle\langle 0|{\mathcal{A}_m}^\dagger(\bar{z}_N)\dots{\mathcal{A}_m}^\dagger(\bar{z}_1)c_m^{-N} \tag{5.3}$$

which produces a mapping from an inner product in the physical space into the CFT language of the form

$$\left\{\Psi_{\langle v|}\middle|\Psi_{\langle w|}\right\} = \langle w|G_N|v\rangle. \tag{5.4}$$

If we could evaluate Eq. 5.3 we would then have the exact form for overlaps of quantum Hall edge states. Unfortunately this proves to be an extremely difficult problem.

Instead we consider what the generic form of G_N could be. By definition, G_N is a Hermitian and positive definite operator so we can write it in the form

$$G_N = \mathcal{Z}_N R^{2L_0} e^{-S_N}, \tag{5.5}$$

where recall that $\mathcal{Z}_N$ is the N-particle normalisation of the ground state (i.e, defined such that $\left\{\Psi_{\langle 0|}\middle|\Psi_{\langle 0|}\right\} = \mathcal{Z}_N$) and R is the radius of the quantum Hall droplet. L_0 is the zero mode of the Virasoro algebra. This equation defines the action, $S_N = S_N^\dagger$ and is the form proposed in Ref. [34], in which the authors argue that S_N is a local action on the boundary of the droplet; it is a massive perturbation to the full CFT.

By itself, Eq. 5.5 is just a definition of some operator S_N onto which we shift our ignorance about the exact form of G_N. However, the crucial simplification lies with the claim that S_N is local. This is a conjecture based on exact calculations for the trial states of $p_x + ip_y$ superconductors, a kind of toy model for trial

wavefunctions with many similarities to quantum Hall trial wavefunctions, and also on the assumption of charge screening within the bulk of the droplet. This conjecture is one of the major constraints we impose upon S_N which allows one to make progress. However, as it is not a rigorous statement it is important that we check its validity. This, as well as computing the explicit form for S_N, is the main motivation for this work with Section 5.3 providing numerical evidence in support of this ansatz.

5.1.2 The Symmetries of S_N

We begin with a short discussion on the conjecture of locality made by Ref. [34]. This claim is motivated partly by the fact that, for trial states of a $p_x + ip_y$ superconductor, the inner product operator equivalent to G_N can be calculated exactly and it has the form claimed in Eq. 5.5 for a local action, S_N. Another motivation is provided by the generalized screening hypothesis, the idea that all correlation functions within the bulk of the droplet should be short range.

For the Laughlin state, this screening can be understood in terms of the plasma analogy, which we have already seen in Section 2.4.1. Recall that this system is in a screening phase for $m < m_c$ where $m_c \simeq 65$, meaning that correlation functions decay exponentially[53, 96]. A similar (though much more in-depth) analysis is also possible for the Moore-Read state with a similar conclusion[132]. As such, we expect that all the important physics in at least these two systems should be due to local interactions[133].

This idea of screening suggests that the degrees of freedom at one point in the system will not interact significantly with degrees of freedom at another location. Given that the relevant degrees of freedom for the overlaps of edge states (which are localized on the boundary) will be located on the edge we surmise that the action will exist only at the boundary. Furthermore, it can include only local terms which do not generate interactions between well-separated regions along

the edge. As such, one may take an ansatz for S_N which is local, of the form

$$S_N = \sum_a \tilde{s}_a \int \mathrm{d}x \; \tilde{\Phi}_a(x), \tag{5.6}$$

where x is the coordinate along the circumference of the droplet at radius R (i.e., at $z = Re^{ix/R}$) and we sum over all possible local operators, $\tilde{\Phi}_a$, which have a priori unknown coupling coefficients $\tilde{s}_a$.

It is important to understand which terms in this sum remain relevant as the system size increases. The variation of each term becomes clear when we perform a change of variables from the circle x to the plane z. Under this substitution

$$\tilde{\Phi}_a(x) = \left(\frac{iz}{R}\right)^{d_a} \tilde{\Phi}_a(z) = \frac{1}{R^{d_a}} \Phi_a(z) \tag{5.7}$$

where the second equality defines a new operator $\Phi_a(z) = (iz)^{d_a} \tilde{\Phi}_a(z)$. Note that d_a is the scaling dimension of the field Φ_a and recall that $R = \ell_{\mathrm{B}}\sqrt{2mN}$ is the radius of the droplet where ℓ_{B} is the magnetic length. This maps the action to

$$S_N = \sum_a \frac{2\pi \tilde{s}_a}{R^{d_a - 1}} \oint \frac{\mathrm{d}z}{2\pi i} z^{-1} \Phi_a(z). \tag{5.8}$$

Having rephrased the action we note that the contour integral can be freely deformed and is a scale invariant quantity. Based on the previous heuristics, we also expect the coefficients to vary as $\tilde{s}_a \sim {\ell_{\mathrm{B}}}^{d_a - 1}$ where ℓ_{B} is roughly the UV cutoff in the theory. As such, we define dimensionless coefficients, s_a which we expect to be of order unity via $2\pi\tilde{s}_a = s_a\big(\ell_{\mathrm{B}}\sqrt{2m}\big)^{d_a - 1}$ such that

$$S_N = \sum_a \frac{s_a}{\sqrt{N}^{d_a - 1}} \oint \frac{\mathrm{d}z}{2\pi i} z^{-1} \Phi_a(z). \tag{5.9}$$

Therefore, we see that the action is an expansion in $\sqrt{N}^{-1}$ and so, for N large enough, we can restrict our attention to only those operators where d_a is small.

5.1.3 Number Conservation

We now begin to make rigorous observations about the structure of the inner product. Firstly, we note that particle number is conserved, which is a simple

statement that the scalar product between any two states must be zero if the number of particles is not the same. We have already seen that the operator which counts the particle number is $a_0/\sqrt{m}$ where a_0 is the zero mode of the Bose field and counts the total charge. Therefore this constraint can be imposed by $[a_0, S_N] = 0$.

As such, number conservation precludes any terms in S_N which contain φ_0 and this imposes a strong constraint on the U(1) sector of the field theory. It prevents the inclusion of any vertex operators, $: e^{i\alpha\varphi(z)} :$ and requires any mention of the bosonic field to be as a derivative, i.e., the current $i\partial\varphi(z)$ or a descendant of it. This does not imply any constraint on terms arising from the statistics sector.

5.1.4 Rotational Invariance

The next rigorous constraint is a result of rotational invariance. In a rotationally invariant environment, Quantum Hall states have well-defined angular momenta and the scalar product of any two excited states with different angular momenta must be zero. The operator which measures angular momentum in the CFT language is L_0, (which we note contains a contribution from both the charge and statistics sectors, $L_0 = L_0^{\varphi} + L_0^{\psi}$). Therefore rotational invariance forces us to conclude that $[L_0, S_N] = 0$.

This constraint happens to be rather powerful. So far the structure of S_N is one of polynomials of the fields and their derivatives multiplied by any a priori arbitrary function of z. For example, in the Laughlin case all terms have the form

$$\Phi_a(z) = f(z)(i\partial\varphi(z))^{m_1}\left(i\partial^2\varphi(z)\right)^{m_2}\cdots \tag{5.10}$$

where m_j are integer which give the operator's scaling dimension as $d_a = \sum_j jm_j$. This function of $f(z)$ is then an a priori completely arbitrary function. However, if we impose rotational invariance then this constrains it to be simply $f(z) \propto z^{d_a}$.

An analogous result exists for any other trial quantum Hall state constructed as a CFT correlator in this manner.

5.1.5 Translational Invariance

The final constraint is the most powerful as it allows many of the coefficients in the proposed expansion of S_N to be fixed. It is a consequence of the translational invariance of the Laughlin wave function and leads to the conclusion that the action must satisfy[34]

$$[e^{-S_N}, a_{-1}] = \frac{1}{N\sqrt{m}} L_{-1} e^{-S_N} \tag{5.11}$$

where L_{-1} is the generator of translations in our Virasoro algebra. This allows us to fix the coefficients of all operators which have some nontrivial commutation relation with the a_{-1} mode of the U(1) field.

To derive Eq. 5.11 we will analyze how translational symmetry can help us make exact statements about the inner products of edge states containing p_1 edge modes (where these modes correspond physically to a small shift of the whole droplet). Consider the inner product,

$$\left\{\Psi_{\langle v|a_1}\middle|\Psi_{\langle w|}\right\} = \langle w|G_N a_{-1}|v\rangle = \int \mathrm{D}\boldsymbol{z}\bar{p}_1\bar{\Psi}_{\langle v|}\Psi_{\langle w|}. \tag{5.12}$$

Within this integral we can use the procedure outlined Section 4.2.4 for projecting anti-holomorphic terms onto the holomorphic wavefunction in the lowest Landau level, using the substitution $\bar{z}_i \to 2{\ell_\mathrm{B}}^2\partial_i$. Applying this substitution we find

$$\langle w|G_N a_{-1}|v\rangle = \int \mathrm{D}\boldsymbol{z}\bar{\Psi}_{\langle v|}2{\ell_\mathrm{B}}^2\sqrt{m}\mathcal{L}_{-1}\Psi_{\langle w|} \tag{5.13}$$

where recall that $\mathcal{L}_{-1} = \sum_i \partial_i$ is the generator of translations. We have also already seen how this operator maps into the CFT in Derivation 4.2.4 and therefore find that

$$\langle w|G_N a_{-1}|v\rangle = 2{\ell_\mathrm{B}}^2\sqrt{m}\langle w|\big(N\sqrt{m}a_{-1} + L_{-1}\big)G_N|v\rangle, \tag{5.14}$$

which holds for all states $|w\rangle$ and $|v\rangle$. Therefore, we have that

$$R^{2L_0}e^{-S_N}a_{-1} = R^2\left(a_{-1} + \frac{1}{N\sqrt{m}}L_{-1}\right)R^{2L_0}e^{-S_N}. \tag{5.15}$$

We can then use that $[L_0, a_{-1}] = 1$ and tidy up the remaining terms to find exactly the identity given in Eq. 5.11.

5.2 Results for the inner product

5.2.1 The Laughlin State

A Basis of Operators

We begin by summarising the consequences of the conditions of locality, number conservation and rotational invariance for operators allowed in S_N from the U(1) sector. A general basis of terms which satisfies all three conditions is given by

$$T_{\mathbf{\Gamma}} = \oint \frac{\mathrm{d}z}{2\pi i} z^{|\mathbf{\Gamma}|-1} \prod_{\gamma_i \in \mathbf{\Gamma}} i\partial^{\gamma_i}\varphi(z) \tag{5.16}$$

where we take $\mathbf{\Gamma} = \{\gamma_1, \gamma_2, \ldots\}$ as a semi-ordered set of positive integers $\gamma_1 \geq \gamma_2 \geq \ldots \geq 0$ of weight $|\mathbf{\Gamma}| = \sum_i \gamma_i$ which corresponds to the term's scaling dimension, i.e, $d_{\mathbf{\Gamma}} = |\mathbf{\Gamma}|$. Using this basis we may generate any local action.

Note that the basis defined by Eq. 5.16 is over-complete. To see this, consider T_{21}, which we can integrate by parts to give

$$T_{21} = \oint \frac{\mathrm{d}z}{2\pi i} z^2 \frac{1}{2}\partial\big((i\partial\varphi(z))^2\big) = -T_{11}. \tag{5.17}$$

Therefore, one must be careful to use a basis of $T_{\mathbf{\Gamma}}$ which includes only 'unique' $\mathbf{\Gamma}$ (i.e, linearly independent $T_{\mathbf{\Gamma}}$). At low orders it is sufficient to find these 'unique' $\mathbf{\Gamma}$ simply by the integration by parts procedure described above, though for higher orders it may be necessary to decompose the subsequent terms into bosonic modes and analyse whether the individual matrices are linearly independent.

It is worth noting an apparent oddity in Eq. 5.17. On the left hand side we have T_{21} with scaling dimension 3 and on the right hand side T_{11}, whose scaling dimension is 2. The source of this contradiction is really just notation. From scaling arguments we do not really expect $(\partial\varphi)^2$ to appear at scaling dimension $d_a = 3$. We only expect $\partial^2\varphi\partial\varphi$ at this order (and also $(\partial\varphi)^3$ and $\partial^3\varphi$). However, given that we want to use a convenient basis it makes little sense to keep careful track of both T_{21} and T_{11} in the action if they are simply the same operator. Therefore, it is more convenient to simply throw away T_{21} and allow T_{11} to appear at both scaling dimension 2 and 3, which means more generally that any $T_{\mathbf{\Gamma}}$ in the final basis can appear at scaling dimension $d_{\mathbf{\Gamma}}$ *and any scaling dimension higher*. This further implies that the coefficients will vary as $s_a \sim c\sqrt{N}^{1-d_a} + c'\sqrt{N}^{-d_a} + \ldots$ for some constants c, c' and so on.

Once we rid ourselves of these extraneous terms we are left with a linearly independent basis up to scaling dimension 7 (or R^{-6}) given in table 5.1. Note that we do not consider the scaling dimension $d_{\mathbf{\Gamma}} = 1$ as the sole term here is $T_1 = a_0$ and we work with states $|\boldsymbol{\lambda}\rangle$ which have U(1) charge of zero (i.e, $a_0|\boldsymbol{\lambda}\rangle = 0$ for all $|\boldsymbol{\lambda}\rangle$). Therefore, this term and others like it are trivial.

Aside 15

Let us see in greater detail how the table of 'unique' terms in Table 5.1 was constructed. As mentioned already, the $d_a = 1$ sector is somewhat trivial. It does give us T_1, but this operator is null ($T_1 = a_0 = 0$). Therefore, the first nontrivial case arises at $d_a = 2$. Here, there are two partitions, T_2 and T_{11}. The former can be integrated by parts and gives us back our null operator. The latter, however, is distinct, containing two bosonic modes. Thus, at scaling dimensions $d_a = 2$ a full, linearly independent basis is given by

$$T_{\mathbf{\Gamma}} \in \{T_{11}\}. \tag{5.18}$$

We then move onto $d_a = 3$, where the possibilities are T_3, T_{21}, and T_{111}.

$d_{\mathbf{\Gamma}}$	Unique terms
2	T_{11}
3	T_{111}
4	T_{22}, T_{1111}
5	T_{221}, T_{11111}
6	$T_{33}, T_{222}, T_{2211}, T_{111111}$
7	$T_{331}, T_{2221}, T_{22111}, T_{1111111}$
⋮	⋮

Table 5.1: A table of some of the first few linearly independent terms from which H can be constructed. Note that the choices made for $\mathbf{\Gamma}$ are not unique. For example, as we have already seen T_{11} and T_{21} are exactly equivalent up to an overall sign and so to keep notation simpler we replace T_{21} with T_{11}, though must then allow part of the coefficient of T_{11} to vary as $R^{1-d_{21}}$.

Once again, the first case is a couple of integrations by parts away from our null operator, T_1. The last case, T_{111}, is a distinct operator, containing three bosonic modes, and so indescribable by a linear combination of any other terms which are all two bosons or fewer. Finally, the middle case, T_{21} can be integrated by parts to give $-T_{11}$ as we have already seen. Therefore, this is not new. Our linearly independent basis of operators for $d_a = 3$ is

$$T_{\mathbf{\Gamma}} \in \{T_{11}, T_{111}\}. \tag{5.19}$$

Going forward, the view is much the same. We continue to add partitions, $\mathbf{\Gamma}$, of higher scaling dimension and attempt to phrase them in terms of basis operators we already have. To do so, we choose to reduce the size of the maximal derivatives in that term, i.e., given some term T_{311} our first priority should be to integrate away the 3. However, this is a choice and other approaches would work equally well.

Nevertheless, the situation becomes slightly more complex. At scaling

dimension $d_a = 4$ the term T_4 is once again trivial. The term T_{31} when integrated by parts is equal to a sum of T_{11} and T_{22}. The former, T_{11}, is already in our basis but the latter arises at this scaling dimension. Therefore, we can take T_{31} or T_{22} and elect for T_{22}. Finally, T_{211} can be expressed in terms of T_{111} and T_{1111} is a necessarily new term. Therefore, we claim that up to $d_a = 4$

$$T_{\mathbf{\Gamma}} \in \{T_{11}, T_{111}, T_{1111}, T_{22}\}. \tag{5.20}$$

However, one should note that, whilst T_{22} cannot be expressed in terms of T_{11} by integrating by parts, one may still worry that the two terms, being bilinears, might be equivalent. To fully convince oneself of the contrary one can check the matrix elements of the two operators to see that they are indeed independent.

Therefore, a general, efficient method for finding unique $T_{\mathbf{\Gamma}}$ is one of integration by parts to phrase $T_{\mathbf{\Gamma}}$ in terms of other $T_{\mathbf{\Gamma}}$ with at least the first two integers γ_1 and γ_2 being equal. Such terms are difficult to reduce further integrating by parts so one must see if the resulting terms are linearly independent by other means, for example by considering individual matrix elements or by taking a commutator.

Laughlin Action

Given our basis of operators we may now express the action as

$$S_N = \sum_{\text{unique } \mathbf{\Gamma}} \frac{s_{\mathbf{\Gamma}}}{\sqrt{N}^{|\mathbf{\Gamma}|-1}} T_{\mathbf{\Gamma}}. \tag{5.21}$$

We can then apply our translational invariance condition, Eq. 5.11 at each order (corresponding to increasing scaling dimensions) to fix the individual coefficients,

$s_{\mathbf{\Gamma}}$. We find the final form up to 6^{th} order (scaling dimension of 7) to be

$$\begin{aligned} S_N = &- \frac{1}{6\sqrt{m}N} T_{111} + \frac{s_{22}}{N^{3/2}} T_{22} + \frac{1}{24mN^2} T_{1111} \\ &- \left(\frac{s_{22}}{2\sqrt{m}N^{5/2}} - \frac{1}{144m\sqrt{m}N^3} \right) (3T_{221} - 2T_{111}) \\ &+ \frac{s_{33}}{N^{5/2}} T_{33} - \frac{1}{60m\sqrt{m}N^3} T_{11111} + \mathcal{O}\left(N^{-7/2}\right) \end{aligned} \tag{5.22}$$

where s_{22} and s_{33} are undetermined coupling coefficients which cannot be fixed by translational invariance as they commute with the a_{-1} mode. By scaling arguments we expect these coefficients to have sub-leading corrections of order $\sqrt{N}^{-1}$, i.e,

$$\frac{s_{22}}{N^{3/2}} = \frac{s_{22}^{(3)}}{N^{3/2}} + \frac{s_{22}^{(4)}}{N^{4/2}} + \dots \tag{5.23}$$

and similar for s_{33}. We will now sketch an explicit derivation of the form of Eq. 5.22 up to 3^{rd} order.

Derivation 2

We begin by expanding S_N in powers of $\sqrt{N}^{-1}$ as

$$S_N = S^{(0)} + \frac{S^{(1)}}{\sqrt{N}} + \frac{S^{(2)}}{\sqrt{N}^2} + \cdots . \tag{5.24}$$

To fix $S^{(0)}$ we simply note that our ground state must be normalised. This is the condition that

$$\langle 0 | R^{2L_0} e^{-S_N} | 0 \rangle = 1 \tag{5.25}$$

and so $S^{(0)}|0\rangle = 0$. Given that the only term with a scaling dimension of zero is $T_1 = a_0$ and a_0 will always evaluate to zero on our neutral states we simply discard it as set $S^{(0)} = 0$.

We can also quickly convince ourselves that $S^{(1)} = 0$. The only terms allowed at this order are $T_1 = a_0 = 0$ and T_{11}, the latter of which has a nontrivial commutation with a_{-1}. However, translational invariance, Eq. 5.11,

requires that the commutator of $S^{(1)}$ with a_{-1} be zero, and so the coupling coefficient s_{11} must be zero.

The first nontrivial term arises at order N^{-1}. At this order our translational invariance condition reads

$$[S^{(2)}, a_{-1}] = -\frac{1}{\sqrt{m}} L_{-1}. \tag{5.26}$$

By noting that

$$[i\partial\varphi(z), a_{-1}] = z^{-2} \tag{5.27}$$

we see straight away that the term T_{111} has commutation relation

$$[T_{111}, a_{-1}] = 3 \oint \frac{\mathrm{d}z}{2\pi i} : [i\partial\varphi(z)]^2 : = 6L_{-1}. \tag{5.28}$$

Therefore, we may conclude that $s_{111} = -\frac{1}{6\sqrt{m}}$ at this order whilst all other coefficients vanish.

At order $N^{-3/2}$ our translational invariance condition tells us that

$$[S^{(3)}, a_{-1}] = 0. \tag{5.29}$$

The smallest set of non-vanishing linearly independent operators we are allowed at this order are $T_{11}, T_{111}, T_{1111}$ and T_{22}. The first three have a non-trivial commutation relation with a_{-1} so their coupling coefficients at this order must vanish. T_{22} however, commutes with a_{-1} and so we can say nothing about its coupling coefficient. As such,

$$S_N = -\frac{1}{6\sqrt{m}N} T_{111} + \frac{s_{22}}{N^{3/2}} T_{22} + \mathcal{O}\big(N^{-2}\big). \tag{5.30}$$

Beyond these orders the picture becomes more involved but can still be approached in a manner similar to that presented here. The only extra concern to consider is that S_N is hermitian and is therefore made up only of hermitian operators. As it transpires, some of the terms, $T_{\mathbf{\Gamma}}$, are neither hermitian nor can be made hermitian in combination with other $T_{\mathbf{\Gamma}}$. The first casualty of this condition is T_{222}, which we conclude cannot be present in the action.

5.2.2 The Moore-Read State

A Basis of Operators

We proceed exactly as before, beginning with a definition of the basis we can use to express any local Hamiltonian constructed from these two fields, $\varphi(z)$ and $\psi(z)$, which are relevant to the problem. These will now be labelled by a pair of partitions, $\mathbf{\Gamma} = \{\gamma_1, \gamma_2, \ldots\}$ and also $\mathbf{\Xi} = \{\xi_1, \xi_2, \ldots\}$, one for the bosonic sector and one for the fermionic sector,

$$T_{\mathbf{\Gamma},\mathbf{\Xi}} = \oint \frac{\mathrm{d}z}{2\pi i} z^{|\mathbf{\Gamma}|+|\mathbf{\Xi}|+\frac{l(\mathbf{\Xi})}{2}-1} \prod_{\gamma_i \in \mathbf{\Gamma}} i\partial^{\gamma_i}\varphi(z) \prod_{\xi_i \in \mathbf{\Xi}} \partial^{\xi_i}\psi(z). \tag{5.31}$$

There are a few things to note about this definition. Firstly, $\mathbf{\Gamma}$, relating to the bosonic fields, is as before; it is a partition of positive integers which we order such that $\gamma_1 \geq \gamma_2 \geq \ldots$. The new, fermionic partition, $\mathbf{\Xi}$, is also a set of integers though it cannot contain any integer twice (due to fermionic exclusion) and it must have an even number of elements (due to parity symmetry). We denote the number of elements by $l(\mathbf{\Xi})$ so, for example, $l(\{0,1\}) = 2$ and $l(\{0,1,2,3\}) = 4$. Furthermore, it can also contain 0 as an entry ($i\partial^0\varphi$ is excluded due to number conservation though no such symmetry prevents $\partial^0\psi$). To further distinguish this partition from $\boldsymbol{\gamma}$ we will also order it in reverse, with $\xi_1 < \xi_2 < \ldots$. Finally, the product over the elements, ξ_i, must have a specific ordering, as permutations bring about an overall sign change, so we define this product such that

$$\prod_{\xi_i \in \mathbf{\Xi}} \partial^{\xi_i}\psi = \partial^{\xi_1}\psi\partial^{\xi_2}\psi\ldots. \tag{5.32}$$

Note that in both the bosonic and fermionic cases the empty set, $\emptyset$, refers to no contributions from that sector. So for example $T_{\mathbf{\Gamma},\emptyset}$ are all the purely bosonic terms which we found when considering the Laughlin state and include no fermionic fields.

Once again, there is a large degeneracy in this definition of basis elements.

$d_{\mathbf{\Gamma},\mathbf{\Xi}}$	Unique terms
2	$T_{11,\emptyset}, T_{\emptyset,01}$
3	$T_{111,\emptyset}, T_{1,01}$
4	$T_{22,\emptyset}, T_{1111,\emptyset}, T_{2,01}, T_{11,01}, T_{\emptyset,12}$
5	$T_{221,\emptyset}, T_{11111,\emptyset}, T_{3,01}, T_{21,01}, T_{111,01}, T_{1,12}$
⋮	⋮

Table 5.2: A table of some of the first few linearly independent terms we can use to construct the action in the Moore-Read case. The number of possibilities grows much quicker with the scaling dimension than it did in the Laughlin case.

For example,

$$\begin{aligned} T_{\emptyset,02} &= \oint \frac{\mathrm{d}z}{2\pi i} z^2 \psi \partial^2 \psi \\ &= -\oint \frac{\mathrm{d}z}{2\pi i} \partial(z^2\psi)\partial\psi = -2T_{\emptyset,01}. \end{aligned} \tag{5.33}$$

Therefore, we must once again weed out these duplicate entries, and so we provide a particular choice of a linearly independent basis of terms in table 5.2 for the first few scaling dimensions, where the scaling dimension of a given term is $d_{\mathbf{\Gamma},\mathbf{\Xi}} = |\mathbf{\Gamma}| + |\mathbf{\Xi}| + \frac{l(\mathbf{\Xi})}{2}$.

Moore-Read Action

As in the Laughlin case, we generate an action which is a sum over all the uniquely defined labels, $\mathbf{\Gamma}$ and $\mathbf{\Xi}$ and constrain whatever coefficients we can by translational symmetry. We find that the action has the form

$$\begin{aligned} S_N = &\frac{s_{\emptyset,01}}{N^{1/2}} T_{\emptyset,01} - \frac{1}{6\sqrt{m}N} T_{111,\emptyset} + \frac{\left(1 - s_{\emptyset,01}/N^{1/2} + s_{\emptyset,01}^2/3N\right)}{2\sqrt{m}N} T_{1,01} \\ &+ \frac{s_{22,\emptyset}}{N^{3/2}} T_{22,\emptyset} + \frac{s_{\emptyset,12}}{N^{3/2}} T_{\emptyset,12} + \frac{1}{24mN^2} T_{1111,\emptyset} - \frac{1}{4mN^2} T_{11,01} \\ &+ \frac{s_{3,01}}{N^2}(T_{3,01} + 3T_{2,01}) + \mathcal{O}\left(N^{-5/2}\right) \end{aligned} \tag{5.34}$$

where $s_{\emptyset,01}, s_{22,\emptyset}, s_{\emptyset,12}$ and $s_{3,01}$ are all undetermined constants assumed to be of order unity but with potential corrections of order $\sqrt{N}^{-1}$ etc. Once again, we sketch a short proof of the lower orders of this result.

Derivation 3

As was the case for the Laughlin state, we expand S_N in powers of $\sqrt{N}^{-1}$ and apply the translational invariance constraint, Eq. 5.11, order by order. We first note that $S^{(0)} = 0$ for exactly the reasons presented in the Laughlin calculation. We then note that $S^{(1)}$ can be made up of only two non-trivial terms, namely $T_{11,\emptyset}$ and $T_{\emptyset,01}$. As we saw in the Laughlin case, the non-vanishing commutation relation which $T_{11,\emptyset}$ satisfies with a_{-1} disqualifies it but the fermionic term, $T_{\emptyset,01}$ commutes with a_{-1}, and therefore might appear with any coefficient. Therefore, we surmise that

$$S^{(1)} = s_{\emptyset,01} T_{\emptyset,01} \tag{5.35}$$

where $s_{\emptyset,01}$ is an unknown. We note that this first term is, up to an overall factor, simply the stress-energy for the statistics sector,

$$S^{(1)} = -2 s_{\emptyset,01} \oint \frac{\mathrm{d}z}{2\pi i} z T^{\psi}(z) \tag{5.36}$$

where $T^{\psi}(z)$ is the holomorphic component of the stress-energy tensor.

At the next order our constraint is of the form

$$\left[-S^{(2)} + \frac{\left(S^{(1)}\right)^2}{2}, a_{-1} \right] = \frac{1}{\sqrt{m}} L_{-1}. \tag{5.37}$$

We have just seen that $S^{(1)}$ commutes with a_{-1} so the contribution involving this vanishes whilst $S^{(2)}$ must produce L_{-1}. The terms allowed by this order are those we saw at order $\sqrt{N}^{-1}$ and also

$$T_{111,\emptyset} = \oint \frac{\mathrm{d}z}{2\pi i} z^2 : (i\partial\varphi(z))^3 :, \tag{5.38}$$

$$T_{1,01} = \oint \frac{\mathrm{d}z}{2\pi i} z^2 : i\partial\varphi(z)\psi(z)\partial\psi(z) : . \tag{5.39}$$

Therefore, given that the generator of translations in the Virasoro algebra of the full CFT has the form

$$L_{-1} = \frac{1}{2}\oint \frac{\mathrm{d}z}{2\pi i} : \left((i\partial\varphi(z))^2 - \psi(z)\partial\psi(z)\right) :, \tag{5.40}$$

and recalling the identity in Eq. 5.27, it is straightforward to see that

$$S^{(2)} = -\frac{1}{6\sqrt{m}}T_{111,\emptyset} + \frac{1}{2\sqrt{m}}T_{1,01}. \tag{5.41}$$

Beyond this point the calculation once again progresses in a very similar manner with operators which commute with our a_{-1} mode being assigned a priori unknown coefficients and the remaining terms being fixed by translational invariance. We must also pay attention to hermiticity which first excludes $T_{2,01}$ appearing by itself as we might expect it to in $S^{(3)}$.

5.3 Numerical Analysis

The major aim of this chapter is to test that the conjectured form for inner products proposed in Ref. [34] agrees with the true overlaps of quantum Hall edge states. We calculate these overlaps exactly by generating the edge states in a single-particle basis of monomials, making use of the description of these states in terms of Jack polynomials as pioneered in Refs. [82–84]. We must then perform a basis transformation on these Jack polynomial states to produce the edge states generated by the CFT modes, a procedure which is well understood for the Laughlin case[95] but must be considered on a case-by-case basis for Moore-Read states[1].

Unfortunately, this method limits us to quite modest values of N as the Hilbert

[1] Recall that the Jack polynomials can be expressed as a sum of linearly independent monomials. Similarly, a general edge state $\Psi_{\langle \boldsymbol{\lambda};\boldsymbol{\mu}|}$ can also be expanded in terms of monomials. Therefore, by comparing the coefficients attached to monomials within these expanded states we are able to find the relevant change of basis between the $\Psi_{\langle \boldsymbol{\lambda};\boldsymbol{\mu}|}$ and the Jack polynomials.

space dimension quickly becomes too large to store individual states. For the Laughlin case this limits us to $N = 12$ whilst for the Moore-Read case the size of the Hilbert space in this monomial basis is more limited and only grows too large for our methods above $N = 18$. However, given that the effects we are trying to observe are as small as $1/N^3$ it is crucial that our method is exact as the errors on a similar implementation with Monte Carlo, for example, would be unlikely to converge without enormous computer time. Furthermore, the fact that N is small makes the corrections we are looking for more clearly visible and makes the subsequent excellent agreement all the more impressive.

5.3.1 The Laughlin State

Fitting the coefficients of S_N

In order to evaluate the accuracy of the ansatz, Eq. 5.5, we must first find suitable fits for the coefficients we were unable to constrain by symmetry arguments alone. To do this we minimise the Frobenius norm of the matrix corresponding to deviations between the exact data and this ansatz, $G_N(s_{22}, s_{33}) = R^{2L_0} e^{-S_N(s_{22},s_{33})}$ where S_N is defined in Eq. 5.22. So, given a matrix of overlaps calculated exactly, $(O_N)_{i,j} = \left\{\Psi_{\langle i|}\middle|\Psi_{\langle j|}\right\}$, we set the values of the coefficients s_{22} and s_{33} such that the "error",

$$e_N = \|G_N(s_{22}, s_{33}) - O_N\|_F \,, \tag{5.42}$$

is minimised, where $\|X\|_F = \mathrm{Tr}\left(XX^\dagger\right)$ denotes the Frobenius norm of the matrix X.

To perform this minimisation we use a process of simulated annealing[134]. The aim of the process is to minimise our loss function, $e_N(s_{22}, s_{33})$, but this unfortunately contains a number of local minima in which typical minimisation processes can get stuck. Therefore, we minimise e_N with random moves $s_{22}^{(i)}, s_{33}^{(i)} \rightarrow$

$s_{22}^{(i+1)}, s_{33}^{(i+1)}$ which we accept with a probability

$$p_{i,i+1} = \min\left[1,\ \exp\left(-\frac{e_N^{(i+1)} - e_N^{(i)}}{T}\right)\right] \tag{5.43}$$

for some 'temperature', T. Within the simulated annealing process, this temperature begins large and is then steadily decreased to close to zero.

Aside 16

We expect this description to be most accurate for lower angular momentum states, as we discuss in the following subsection. Therefore we restrict the basis of states $|i\rangle$ in which we perform this minimisation procedure to be only those in the $\Delta L = 4$ subspace. Furthermore, we work with states $|i\rangle$ which are normalised. Given that the individual normalisations of the states (Eq. 4.38) vary quite significantly (for example, $\langle 11111|11111\rangle = 120$ whilst $\langle 41|41\rangle = 4$), this normalisation ensures that diagonal matrix elements of O_N and G_N are each close to unity. This is important as the Frobenius norm only cares about the magnitude of the deviations, and so this normalisation ensures that each matrix element is weighted roughly equally during the minimisation procedure.

Recall that we truncate G_N to be a sixth order expansion with errors of order $N^{-7/2}$. Therefore, we should expect that e_N is of the same order and this introduces some uncertainty in the values we fit for s_{22} and s_{33}. For example, because we a priori expect s_{22} to appear as a third order contribution, any fit using our sixth order expansion of G_N will have some error of order N^{-2} as compared with an infinite-order expansion of G_N. Similarly, our fit to s_{33} will suffer errors of order N^{-1}.

We could, of course, reduce this error by expanding G_N to higher orders, a procedure which is algorithmically simple and so could be delegated to a computer. However, we have chosen to truncate at sixth order because the seventh

order contribution includes three new coefficients which cannot be constrained by translational symmetry. As such, if one continues to expand G_N to higher and higher orders one is forced to accept more and more fit coefficients. Whilst this would no doubt increase the accuracy of G_N, it somewhat diminishes the utility and results in over-fitting the data.

Therefore, we simply fit the values of s_{22} and s_{33} such that G_N as expanded to sixth order provides the optimal description of the data, O_N (a selection of this data for the largest case of $N = 12$ is provided in tables 5.3 and 5.4). We plot the results of these fits in Fig. 5.1 for filling $\nu = 1/2$ and $\nu = 1/3$. Firstly we note that the scaling of s_{22} appears to be as expected, tending towards some constant value in both cases. This is strong evidence in support of the scaling arguments from Ref. [34]. The scaling of s_{33} is less clear and suggests that the term T_{33}, to which this coefficient is associated, may appear at order N^{-3} or higher, instead of the $N^{-5/2}$ we expect. Nevertheless, this does not contradict the scaling arguments as we expect each coefficient to include such sub-leading corrections. The only surprise is that the leading term may vanish. As such, this is still supporting evidence that this scaling analysis is valid.

However, it is also interesting to note the strong similarity between the data for $\nu = 1/2$ and $\nu = 1/3$. Firstly, the large-N value of the coefficient, $s_{22}^{(3)}$, appears to be the same, or very similar, in both cases. The sub-leading correction, $s_{22}^{(4)}$ also contains a remarkable coincidence. For the integer qH effect at $\nu = 1$ it is straightforward to show[131] that this sub-leading contribution is $s_{22}^{(4)} = -1/24$ and so it is interesting to note that the values for these fractional cases are extremely close to $-1/24\sqrt{m}$ (where $m = 1$ for the integer case). In the $\nu = 1/2$ case we find $s_{22}^{(4)} = -0.0286$ as compared with $-1/24\sqrt{m} = -0.0295$ and for the case at $\nu = 1/3$ we have $s_{22}^{(4)} = -0.0230$ as compared with -0.0241.

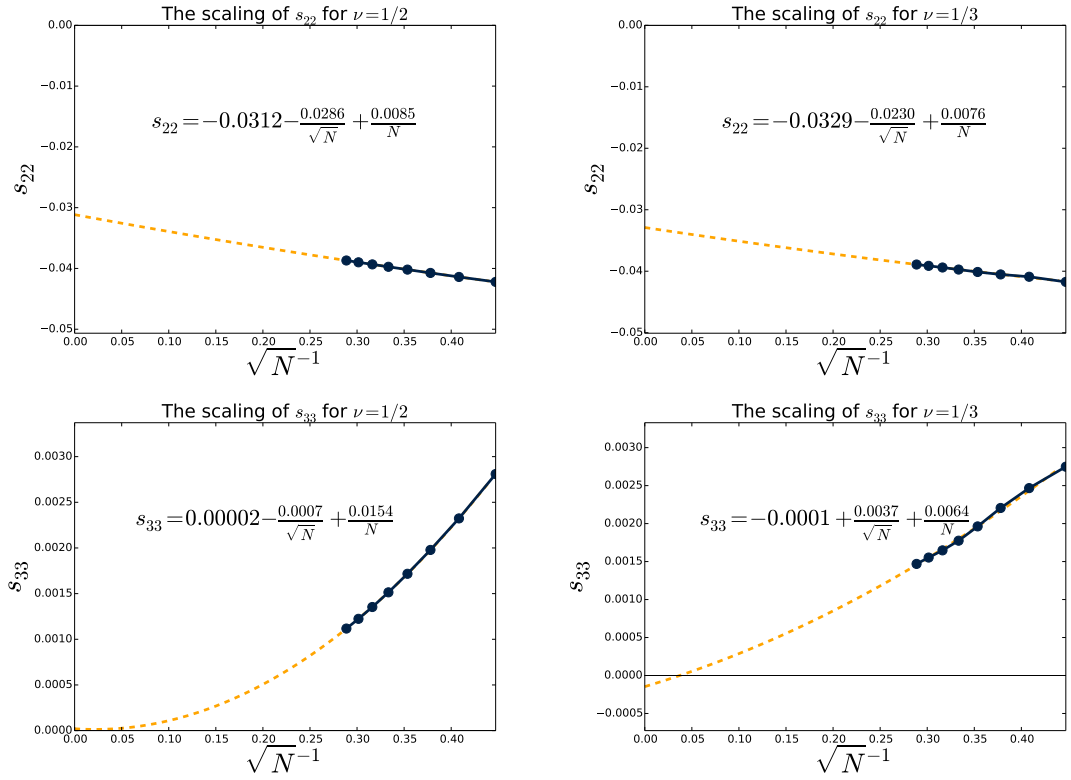

Figure 5.1: We calculate the values for the coupling coefficients s_{22} and s_{33} which best describe the data for the Laughlin state at filling $\nu = 1/2$ and $\nu = 1/3$ as shown by the dark blue points in the figures. We then perform a weighted least-squares fit of the variation of these coefficients with $\sqrt{N}^{-1}$ and find the forms given in each plot, as shown by the orange dashed curve. Although the points are calculated exactly, the weighting of each point assumes that the errors due to truncation on s_{22} are of order N^{-2} and of order N^{-1} for s_{33}. Specifically the fit is obtained by minimising the sum $s = \sum_i (y_i - f(x_i))^2/e_i^2$ where y_i are our data points, $f(x_i)$ our fit function with variable $x_i = \sqrt{N}^{-1}$ and e_i this assumed "error".

Aside 17

For filling fractions $\nu = 1/m$ where $m > 3$ the structure is less clear. Firstly, these states live in a larger single-particle Hilbert space as they have a larger total angular momentum, which makes storing the state difficult. Secondly, we find that the convergence, even at comparable system sizes, is much worse, in much the same way that the data for $\nu = 1/3$ is slightly less smooth than

that at $\nu = 1/2$. Nevertheless, we can perform the same analysis for $\nu = 1/4$ and $\nu = 1/5$ up to system sizes of $N = 10$. Whilst the resulting data is far noisier than that presented in Fig. 5.1, a simple linear fit is potentially consistent with the cases above. We find that $s_{22}^{(3)} = -0.030$ and -0.027 in the $\nu = 1/4$ and $\nu = 1/5$ states respectively, similar to the values we fit in Fig. 5.1. Furthermore, we find that the slopes are $s_{22}^{(4)} = -0.0206$ and -0.0190 as compared to our guess, $-1/24\sqrt{m}$, which evaluates to approximately -0.0208 and 0.0186 respectively.

These coincidences, as well as the suggestion that the leading contributions to s_{33} vanish in both cases, seem to suggest deeper structure in this form for the inner product which it might be possible to access analytically. For example, it may be possible to derive further identities like Eq. 5.11 which encode other, non-obvious symmetries of the problem. One might also be able to use the large-N expansions of generating functions for the 2D Dyson gas presented in Ref. [128]. Furthermore, it is conceivable that the Matrix Product State description of these states, as pioneered in Refs. [135, 136], might also be used to make exact statements about some or all of these coefficients.

Accuracy of the S_N expansion

Most important is that the form of G_N accurately describes the overlaps of qH edge states. Therefore, we input the fits for s_{22} and s_{33} shown in Fig. 5.1 into the inner product operator, $G_N(s_{22}, s_{33})$ and calculate the form of inner products of edge states, once again for filling fractions $\nu = 1/2$ and $\nu = 1/3$. Some results for 12-particle systems are presented in Tables 5.3 and 5.4 where we show the overlaps matrices in the $\Delta L = 5$ sub-space (where recall ΔL is the amount of angular momentum added by the edge excitation). The inner product as calculated by G_N agrees extremely well with the exact data for every overlap.

$\nu = 1/2$	$\Psi_{\langle 1,1,1,1,1\rvert}$	$\Psi_{\langle 2,1,1,1\rvert}$	$\Psi_{\langle 2,2,1\rvert}$	$\Psi_{\langle 3,1,1\rvert}$	$\Psi_{\langle 3,2\rvert}$	$\Psi_{\langle 4,1\rvert}$	$\Psi_{\langle 5\rvert}$
$\Psi_{\langle 1,1,1,1,1\rvert}$	120.0000 **120.0000**	7.0711 **7.0711**	0.4167 **0.4167**	0.4167 **0.4167**	0.0246 **0.0246**	0.0246 **0.0246**	0.0014 **0.0000**
$\Psi_{\langle 2,1,1,1\rvert}$	7.0711 **7.0711**	12.2628 **12.2626**	1.4206 **1.4205**	2.1187 **2.1185**	0.1660 **0.1667**	0.2482 **0.2500**	0.0243 **0.0246**
$\Psi_{\langle 2,2,1\rvert}$	0.4167 **0.4167**	1.4206 **1.4205**	8.0167 **8.0177**	0.2482 **0.2500**	1.4073 **1.4072**	0.9355 **0.9352**	0.2699 **0.2778**
$\Psi_{\langle 3,1,1\rvert}$	0.4167 **0.4167**	2.1187 **2.1185**	0.2482 **0.2500**	6.0461 **6.0472**	0.3635 **0.3635**	1.3812 **1.3805**	0.2013 **0.2083**
$\Psi_{\langle 3,2\rvert}$	0.0246 **0.0246**	0.1660 **0.1667**	1.4073 **1.4072**	0.3635 **0.3635**	5.9861 **5.9940**	0.2425 **0.2500**	1.6569 **1.6528**
$\Psi_{\langle 4,1\rvert}$	0.0246 **0.0246**	0.2482 **0.2500**	0.9355 **0.9352**	1.3812 **1.3805**	0.2425 **0.2500**	3.8653 **3.8709**	1.0914 **1.0878**
$\Psi_{\langle 5\rvert}$	0.0014 **0.0000**	0.0243 **0.0246**	0.2699 **0.2778**	0.2013 **0.2083**	1.6569 **1.6528**	1.0914 **1.0878**	4.3703 **4.3855**

Table 5.3: We show a table calculating the overlaps of Laughlin-type edge states numerically and with our expression G_N at filling $\nu = 1/2$ and system size $N = 12$. The entries in the row i and column j correspond to $\left\{\Psi_{\langle i\rvert}\middle|\Psi_{\langle j\rvert}\right\}/R^{2\Delta L}$ where the upper entry is the value we find by taking exact overlaps numerically and the lower entry (in bold) is the value we find when we use G_N.

However, the data also shows that the agreement is worse for inner products involving large-n modes, a_n, with one of the worst agreements being the calculation of the normalisation of the $\Psi_{\langle 0|a_5}$ state. That the agreements become worse for larger n modes is not unexpected. Consider, for example, the operator T_{mm} which we expect to appear at order $N^{-(2m-1)/2}$. The expectation of this operator in the state $a_{-n}|0\rangle$ for large n varies as

$$\langle 0|a_n(T_{mm})a_{-n}|0\rangle \sim n^{2m-1}. \tag{5.44}$$

As such, if such an operator were to appear in the action, S_N, then it's leading contribution to the normalisation of the state $\Psi_{\langle 0|a_n}$ would vary as $\sim s_{mm}(n/\sqrt{N})^{2m-1}$

$\nu = 1/3$	$\Psi_{\langle 1,1,1,1,1\rvert}$	$\Psi_{\langle 2,1,1,1\rvert}$	$\Psi_{\langle 2,2,1\rvert}$	$\Psi_{\langle 3,1,1\rvert}$	$\Psi_{\langle 3,2\rvert}$	$\Psi_{\langle 4,1\rvert}$	$\Psi_{\langle 5\rvert}$
$\Psi_{\langle 1,1,1,1,1\rvert}$	120.0000 **120.0000**	5.7735 **5.7735**	0.2778 **0.2778**	0.2778 **0.2778**	0.0134 **0.0134**	0.0134 **0.0134**	0.0006 **0.0000**
$\Psi_{\langle 2,1,1,1\rvert}$	5.7735 **5.7735**	12.1301 **12.1299**	1.1539 **1.1538**	1.7241 **1.7240**	0.1104 **0.1111**	0.1653 **0.1667**	0.0132 **0.0134**
$\Psi_{\langle 2,2,1\rvert}$	0.2778 **0.2778**	1.1539 **1.1538**	7.9512 **7.9520**	0.1653 **0.1667**	1.1423 **1.1421**	0.7563 **0.7562**	0.1794 **0.1852**
$\Psi_{\langle 3,1,1\rvert}$	0.2778 **0.2778**	1.7241 **1.7240**	0.1653 **0.1667**	5.9398 **5.9407**	0.2897 **0.2897**	1.1193 **1.1189**	0.1337 **0.1389**
$\Psi_{\langle 3,2\rvert}$	0.0134 **0.0134**	0.1104 **0.1111**	1.1423 **1.1421**	0.2897 **0.2897**	5.8779 **5.8836**	0.1611 **0.1667**	1.3393 **1.3371**
$\Psi_{\langle 4,1\rvert}$	0.0134 **0.0134**	0.1653 **0.1667**	0.7563 **0.7562**	1.1193 **1.1189**	0.1611 **0.1667**	3.7585 **3.7629**	0.8784 **0.8765**
$\Psi_{\langle 5\rvert}$	0.0006 **0.0000**	0.0132 **0.0134**	0.1794 **0.1852**	0.1337 **0.1389**	1.3393 **1.3371**	0.8784 **0.8765**	4.2072 **4.2189**

Table 5.4: As in table 5.3 we show a comparison of exact calculations of Laughlin state overlaps found numerically (upper entry) with our approximation using G_N (lower entry in bold) for $N = 12$. This data is at filling $\nu = 1/3$.

where s_{mm} would be its associated coupling constant (which we would be unable to fix using translational symmetry). Therefore, even though we have neglected all T_{mm} for $m > 3$ on the grounds that they are much more irrelevant in $1/\sqrt{N}$ than the terms we have kept, this still poses problems for calculating matrix elements of states including modes a_n where n is comparable to $\sqrt{N}$.

Constraints on non-local terms

Throughout this work we have assumed that the action, S_N contains no non-local terms. This claim is based on the premise that the Laughlin state is in the screening phase, and so has short-range correlations within the bulk. As such, this perturbation to the underlying CFT, our action in G_N, should depend only

on local degrees of freedom.

It is interesting now to assess this claim in light of the data. Consider some new action of the form

$$\tilde{S}_N = S_N + S_N^{(\text{non-local})} \tag{5.45}$$

where this extra contribution now contains anything which might be non-local. The simplest such terms which can couple the field at two arbitrarily separated positions are those with two integrals. The most well known of these which also respects our rotational invariance condition is the Benjamin-Ono term[81, 107], of the form

$$\begin{aligned} T_{\text{B-O}} &= \oint \frac{\mathrm{d}z}{2\pi i} \oint_{|z|>|w|} \frac{\mathrm{d}w}{2\pi i} \frac{zw}{(z-w)^2} : i\partial\varphi(z) i\partial\varphi(w) : \\ &= \sum_{n>0} n a_{-n} a_n. \end{aligned} \tag{5.46}$$

The coefficient of this term is expected to scale as N^{-1}.

However, this Benjamin-Ono term by itself does not respect translational invariance and therefore, to consider whether it appears or not, we create a new translationally invariant Benjamin-Ono term by combining it with T_{11}, such that the result commutes with a_{-1}. This has the form

$$\tilde{T}_{\text{B-O}} = \sum_{n>0} (n-1) a_{-n} a_n. \tag{5.47}$$

It is then possible for this term to appear in the expansion of S_N but with some unknown coefficient, $\frac{s_{\text{BO}}}{N}$, which cannot be fixed by translational symmetry. Therefore, if we include only this term in $S_N^{(\text{non-local})}$ for simplicity, we have one extra parameter we must fit.

In this vein we expand our new $\tilde{G}_N$, whose action is $\tilde{S}_N$, and attempt to fit this new coefficient. We take an N^{-2} expansion, neglecting any terms of order $N^{-5/2}$, and fit the coefficients, s_{22} and s_{BO} by using the $\left\{\Psi_{\langle 0|a_2} \middle| \Psi_{\langle 0|a_2}\right\}$ and $\left\{\Psi_{\langle 0|a_3} \middle| \Psi_{\langle 0|a_3}\right\}$ overlaps for calibration. I.e, we choose s_{22} and s_{BO} such that the

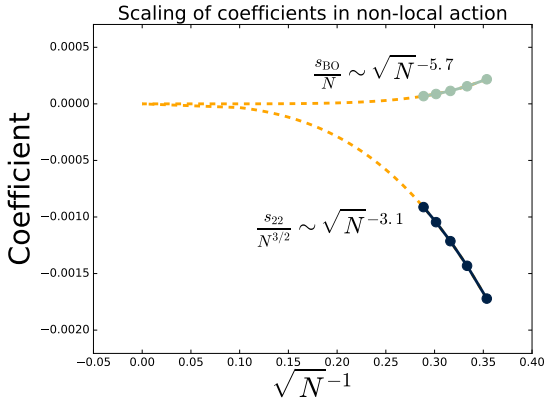

Figure 5.2: Naïve power law scaling of the coefficients of the Benjamin-Ono term (light blue) and the T_{22} term (dark blue) for $\nu = 1/2$ Laughlin when we expand the non-local metric, $\tilde{G}_N$, neglecting terms of order $N^{-5/2}$. We find that s_{22} scales as expected $\sim N^{-3/2}$ whilst the Benjamin-Ono term falls off faster than $N^{-5/2}$, which is the order of terms we neglect. This analysis does not rule out the existence of all non-local terms but is further evidence as to their insignificance.

numerically calculated normalisations of these two states agree exactly with our expression, $\tilde{G}_N$.

The result of the fit is shown in Fig. 5.2. It shows that the coefficient s_{22} scales approximately as expected, appearing very close to 3$^{\mathrm{rd}}$ order in the expansion, as corresponding to the scaling dimension of the T_{22} term. On the other hand, the Benjamin-Ono term falls of roughly as $N^{-5/2}$ or faster, which is the order of terms we are neglecting in this calculation. Therefore, this fit is as likely to come from the corrections we are neglecting as it is to be due to a non-zero Benjamin-Ono coefficient. This gives additional evidence supporting the notion that all terms should be local.

5.3.2 The Moore-Read State

Fitting the coefficients of S_N

We would also like to analyse these claims for the Moore-Read state. We proceed with fitting the coefficients of S_N in exactly the same manner as for the Laughlin

case, by minimising the Frobenius norm of deviations between the exact data and the results given by $G_N = R^{2L_0} e^{-S_N}$ where S_N is defined by Eq. 5.34. In this case, S_N is a function of four unknown couplings, $s_{\emptyset,01}, s_{22,\emptyset}, s_{\emptyset,12}$ and $s_{3,01}$, and we minimise

$$e_N = \| G_N(s_{\emptyset,01}, s_{22,\emptyset}, s_{\emptyset,12}, s_{3,01}) - O_N \|_F \,. \tag{5.48}$$

We once again minimise this in the normalised basis of states at $\Delta L = 4$ using a process of simulated annealing.

In this case we have truncated the expansion at fourth order (once again, this is due to an explosion of extra coefficients at subsequent orders with three new parameters required at fifth order). Therefore, we expect the errors on the coefficient $s_{\emptyset,01}$ to be N^{-2} whereas for the two coefficients, $s_{22,\emptyset}$ and $s_{\emptyset,12}$, the errors are of order N^{-1}. Finally, the error on $s_{3,01}$ is expected to be quite large; of order $\sqrt{N}^{-1}$. As such, these coefficients are expected to have much larger errors than those in the Laughlin case.

We should also note that we have four coefficients as opposed to only two in the Laughlin case. To some extent, this does make this description for the Moore-Read case less powerful as more numerical data is required. However, the dimension of the space of edge states is also much larger in the Moore-Read case as it replicates exactly the edge states from the Laughlin state, made purely from bosonic modes, in addition to fermionic and mixed states. For example, the $\Delta L = 4$ sub-space has dimension 5 in the Laughlin case and 10 in the Moore-Read case. There are therefore almost quadruple the number of distinct inner products one can consider at this angular momentum, which to some extent justifies the need for extra coefficients.

Thus, we perform fits for these coefficients at fillings $\nu = 1$ and $\nu = 1/2$ and show some extrapolations as a function of N in Fig. 5.3 (once again, we show a selection of the data, O_N, used to fit these coefficients in the following subsection, in tables 5.5 and 5.6, for the largest systems of $N = 18$). In the

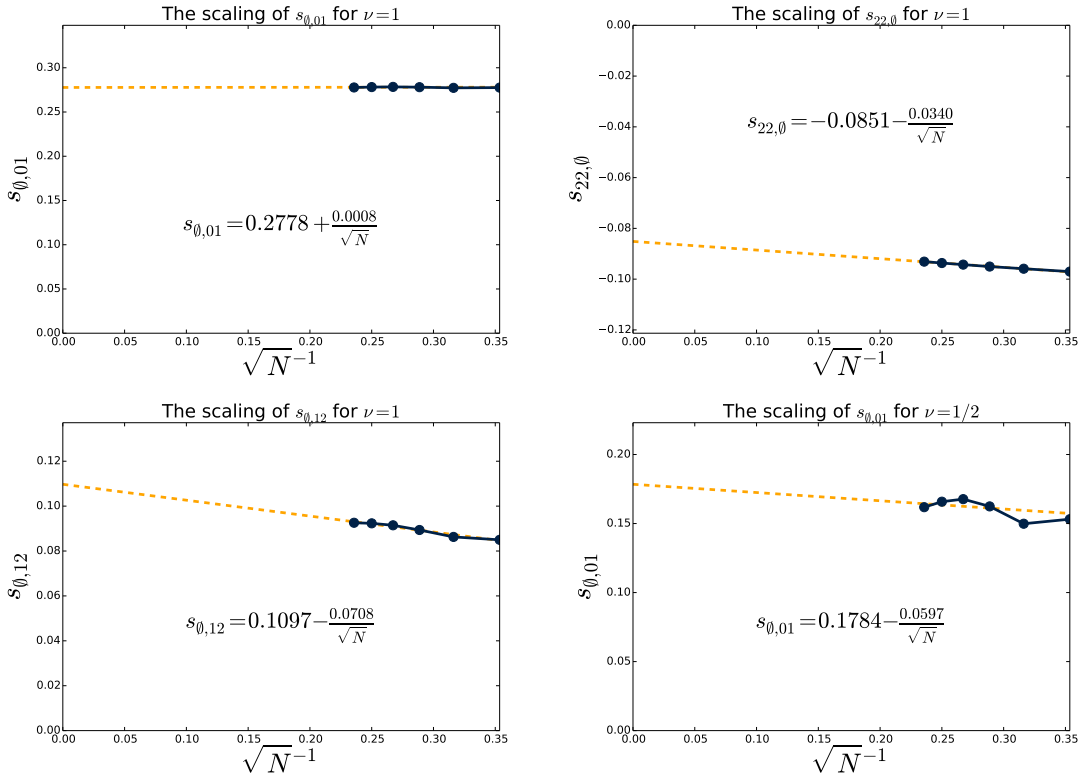

Figure 5.3: We calculate the values of coupling coefficients $s_{\emptyset,01}, s_{22,\emptyset}$ and $s_{\emptyset,12}$ which best describe the data for the Moore-Read edge states at filling $\nu = 1$ and also for $s_{\emptyset,01}$ at filling $\nu = 1/2$. These are shown by the dark blue points in the figures. We then perform a weighted least-squares fit of the variation of these coefficients with $\sqrt{N}^{-1}$ and find the forms given in each plot, as shown by the orange dashed curve. Each point is weighted according to the amount of error expected due to truncation. For example, we expect to calculate $s_{\emptyset,01}$ up to corrections of order N^{-2} and so we set this as the error on each point and then minimise the sum of squared residuals weighted by this error as for the Laughlin case detailed in Fig. 5.1.

$\nu = 1$ case each of the coefficients $s_{\emptyset,01}, s_{22,\emptyset}$ and $s_{\emptyset,12}$ appear to obey the scaling hypothesis with small sub-leading corrections of order $\sqrt{N}^{-1}$. Unfortunately, a similar extrapolation cannot be done for $s_{3,01}$ as the $\sqrt{N}^{-1}$ errors in the fits are too large. However, we do see that the values are small (less than 0.01 in each case, which is a similar size to the other coefficients) and so the effect of this term is not expected to be significant. We also present the extrapolation of the least irrelevant coefficient $s_{\emptyset,01}$ at $\nu = 1/2$. Again, this appears to obey the scaling

$\nu = 1$	$\Psi_{\langle 1,1,1,1\,;\,\emptyset\rvert}$	$\Psi_{\langle 2,1,1\,;\,\emptyset\rvert}$	$\Psi_{\langle 2,2\,;\,\emptyset\rvert}$	$\Psi_{\langle 3,1\,;\,\emptyset\rvert}$	$\Psi_{\langle 4\,;\,\emptyset\rvert}$	$\Psi_{\langle 1,1\,;\,\frac{1}{2},\frac{3}{2}\rvert}$	$\Psi_{\langle 2\,;\,\frac{1}{2},\frac{3}{2}\rvert}$	$\Psi_{\langle 1\,;\,\frac{1}{2},\frac{5}{2}\rvert}$	$\Psi_{\langle \emptyset\,;\,\frac{1}{2},\frac{7}{2}\rvert}$	$\Psi_{\langle \emptyset\,;\,\frac{3}{2},\frac{5}{2}\rvert}$
$\Psi_{\langle 1,1,1,1\,;\,\emptyset\rvert}$	24.0000	1.3333	0.0741	0.0741	0.0041	0.0000	0.0000	0.0000	0.0000	0.0000
	24.0000	**1.3333**	**0.0741**	**0.0741**	**0.0000**	**0.0000**	**0.0000**	**0.0000**	**0.0000**	**0.0000**
$\Psi_{\langle 2,1,1\,;\,\emptyset\rvert}$	1.3333	4.0113	0.4416	0.6603	0.0731	0.1199	0.0067	0.0133	0.0011	0.0004
	1.3333	**4.0124**	**0.4444**	**0.6667**	**0.0741**	**0.1185**	**0.0062**	**0.0123**	**0.0000**	**0.0000**
$\Psi_{\langle 2,2\,;\,\emptyset\rvert}$	0.0741	0.4416	7.8482	0.0731	0.8546	0.0133	0.2382	0.0015	0.0387	-0.0039
	0.0741	**0.4444**	**7.8522**	**0.0741**	**0.8889**	**0.0123**	**0.2371**	**0.0000**	**0.0340**	**-0.0031**
$\Psi_{\langle 3,1\,;\,\emptyset\rvert}$	0.0741	0.6603	0.0731	2.9181	0.6363	0.0200	0.0011	0.1935	0.0321	0.0107
	0.0741	**0.6667**	**0.0741**	**2.9216**	**0.6667**	**0.0185**	**0.0000**	**0.1895**	**0.0278**	**0.0093**
$\Psi_{\langle 4\,;\,\emptyset\rvert}$	0.0041	0.0731	0.8546	0.6363	3.6003	0.0022	0.0420	0.0428	0.4056	0.1369
	0.0000	**0.0741**	**0.8889**	**0.6667**	**3.5997**	**0.0000**	**0.0370**	**0.0370**	**0.4037**	**0.1346**
$\Psi_{\langle 1,1\,;\,\frac{1}{2},\frac{3}{2}\rvert}$	0.0000	0.1199	0.0133	0.0200	0.0022	2.5832	0.1435	0.2870	0.0239	0.0080
	0.0000	**0.1185**	**0.0123**	**0.0185**	**0.0000**	**2.5822**	**0.1440**	**0.2881**	**0.0185**	**0.0062**
$\Psi_{\langle 2\,;\,\frac{1}{2},\frac{3}{2}\rvert}$	0.0000	0.0067	0.2382	0.0011	0.0420	0.1435	2.5856	0.0159	0.3803	-0.2304
	0.0000	**0.0062**	**0.2371**	**0.0000**	**0.0370**	**0.1440**	**2.5777**	**0.0123**	**0.3834**	**-0.2300**
$\Psi_{\langle 1\,;\,\frac{1}{2},\frac{5}{2}\rvert}$	0.0000	0.0133	0.0015	0.1935	0.0428	0.2870	0.0159	1.4570	0.2402	0.0801
	0.0000	**0.0123**	**0.0000**	**0.1895**	**0.0370**	**0.2881**	**0.0123**	**1.4537**	**0.2451**	**0.0817**
$\Psi_{\langle \emptyset\,;\,\frac{1}{2},\frac{7}{2}\rvert}$	0.0000	0.0011	0.0387	0.0321	0.4056	0.0239	0.3803	0.2402	1.5792	-0.0032
	0.0000	**0.0000**	**0.0340**	**0.0278**	**0.4037**	**0.0185**	**0.3834**	**0.2451**	**1.5797**	**-0.0023**
$\Psi_{\langle \emptyset\,;\,\frac{3}{2},\frac{5}{2}\rvert}$	0.0000	0.0004	-0.0039	0.0107	0.1369	0.0080	-0.2304	0.0801	-0.0032	1.6294
	0.0000	**0.0000**	**-0.0031**	**0.0093**	**0.1346**	**0.0062**	**-0.2300**	**0.0817**	**-0.0023**	**1.6318**

Table 5.5: As in table 5.3 we show in row i and column j the inner product $\left\{\Psi_{\langle i\rvert}\middle\rvert\Psi_{\langle j\rvert}\right\}/R^{2\Delta L}$ where the angular momentum of these edge excitations is $\Delta L = 4$ and the system size is $N = 18$. The states $|i\rangle$ are defined by Eq. 4.44. This case is the Moore-Read state at filling $\nu = 1$. The upper value in each cell is calculated by taking the overlaps exactly in the physical space of monomials whilst the lower value in bold is calculated by using G_N using the extrapolations of $s_{\emptyset,01}$, $s_{22,\emptyset}$, $s_{\emptyset,12}$ and $s_{3,01}$ which we calculated in the previous section.

hypothesis, tending towards a constant value with a small sub-leading correction of order $\sqrt{N}^{-1}$. However, we note that the sub-sub-leading corrections for this fermionic case appear to remain appreciable for the values of $N \leq 18$ we present here.

Accuracy of the S_N expansion

Using the fits for the coefficients as described above we can compare with the overlaps we find numerically. In tables 5.5 and 5.6 we compare the exact overlaps

$\nu = 1/2$	$\Psi_{\langle 1,1,1,1\,;\,\emptyset\rangle}$	$\Psi_{\langle 2,1,1\,;\,\emptyset\rangle}$	$\Psi_{\langle 2,2\,;\,\emptyset\rangle}$	$\Psi_{\langle 3,1\,;\,\emptyset\rangle}$	$\Psi_{\langle 4\,;\,\emptyset\rangle}$	$\Psi_{\langle 1,1\,;\,\frac{1}{2},\frac{3}{2}\rangle}$	$\Psi_{\langle 2\,;\,\frac{1}{2},\frac{3}{2}\rangle}$	$\Psi_{\langle 1\,;\,\frac{1}{2},\frac{5}{2}\rangle}$	$\Psi_{\langle \emptyset\,;\,\frac{1}{2},\frac{7}{2}\rangle}$	$\Psi_{\langle \emptyset\,;\,\frac{3}{2},\frac{5}{2}\rangle}$
$\Psi_{\langle 1,1,1,1\,;\,\emptyset\rangle}$	24.0000	0.9428	0.0370	0.0370	0.0015	0.0000	0.0000	0.0000	0.0000	0.0000
	24.0000	**0.9428**	**0.0370**	**0.0370**	**0.0000**	**0.0000**	**0.0000**	**0.0000**	**0.0000**	**0.0000**
$\Psi_{\langle 2,1,1\,;\,\emptyset\rangle}$	0.9428	3.9899	0.3120	0.4673	0.0367	0.0871	0.0034	0.0068	0.0004	0.0001
	0.9428	**3.9898**	**0.3143**	**0.4714**	**0.0370**	**0.0817**	**0.0031**	**0.0062**	**0.0000**	**0.0000**
$\Psi_{\langle 2,2\,;\,\emptyset\rangle}$	0.0370	0.3120	7.8612	0.0367	0.6075	0.0068	0.1714	0.0005	0.0203	-0.0035
	0.0370	**0.3143**	**7.8606**	**0.0370**	**0.6285**	**0.0062**	**0.1633**	**0.0000**	**0.0170**	**-0.0015**
$\Psi_{\langle 3,1\,;\,\emptyset\rangle}$	0.0370	0.4673	0.0367	2.9096	0.4529	0.0103	0.0004	0.1295	0.0152	0.0051
	0.0370	**0.4714**	**0.0370**	**2.9116**	**0.4714**	**0.0093**	**0.0000**	**0.1273**	**0.0139**	**0.0046**
$\Psi_{\langle 4\,;\,\emptyset\rangle}$	0.0015	0.0367	0.6075	0.4529	3.6354	0.0008	0.0231	0.0203	0.2743	0.0857
	0.0000	**0.0370**	**0.6285**	**0.4714**	**3.6360**	**0.0000**	**0.0185**	**0.0185**	**0.2645**	**0.0882**
$\Psi_{\langle 1,1\,;\,\frac{1}{2},\frac{3}{2}\rangle}$	0.0000	0.0871	0.0068	0.0103	0.0008	2.3112	0.0908	0.1816	0.0107	0.0036
	0.0000	**0.0817**	**0.0062**	**0.0093**	**0.0000**	**2.3177**	**0.0917**	**0.1834**	**0.0093**	**0.0031**
$\Psi_{\langle 2\,;\,\frac{1}{2},\frac{3}{2}\rangle}$	0.0000	0.0034	0.1714	0.0004	0.0231	0.0908	2.3035	0.0071	0.2382	-0.1395
	0.0000	**0.0031**	**0.1633**	**0.0000**	**0.0185**	**0.0917**	**2.3075**	**0.0062**	**0.2381**	**-0.1429**
$\Psi_{\langle 1\,;\,\frac{1}{2},\frac{5}{2}\rangle}$	0.0000	0.0068	0.0005	0.1295	0.0203	0.1816	0.0071	1.2342	0.1446	0.0482
	0.0000	**0.0062**	**0.0000**	**0.1273**	**0.0185**	**0.1834**	**0.0062**	**1.2245**	**0.1484**	**0.0495**
$\Psi_{\langle \emptyset\,;\,\frac{1}{2},\frac{7}{2}\rangle}$	0.0000	0.0004	0.0203	0.0152	0.2743	0.0107	0.2382	0.1446	1.2474	-0.0015
	0.0000	**0.0000**	**0.0170**	**0.0139**	**0.2645**	**0.0093**	**0.2381**	**0.1484**	**1.2417**	**-0.0012**
$\Psi_{\langle \emptyset\,;\,\frac{3}{2},\frac{5}{2}\rangle}$	0.0000	0.0001	-0.0035	0.0051	0.0857	0.0036	-0.1395	0.0482	-0.0015	1.3021
	0.0000	**0.0000**	**-0.0015**	**0.0046**	**0.0882**	**0.0031**	**-0.1429**	**0.0495**	**-0.0012**	**1.3061**

Table 5.6: Similar to table 5.5 we show a comparison of the numerical calculations for the Moore-Read state (upper entry) with our approximation using G_N (lower entry in bold) for $N = 18$ and at filling fraction $\nu = 1/2$.

at system sizes of $N = 18$ and at $\Delta L = 4$ with those calculated with our inner product operator G_N, as a function of the coefficient fits we found in the previous section.

We find that the agreement is once again very good, though unsurprisingly not quite as accurate as the higher-order calculation we performed for the Laughlin state. The lack of a symmetry to constrain the coefficients of fermionic operators in G_N also hampers the agreement for fermionic or mixed states, which are noticeably less accurate than their purely bosonic counterparts.

5.4 Further Work

We recall that in the Laughlin case the coefficients involved in the inner product operator at fractional fillings were remarkably similar to the coefficients which can be calculated exactly for the integer quantum Hall effect. This suggests that yet further constraints could be imposed onto this description in order to constrain the values therein which we could not fix by the symmetries considered here alone. Such promising avenues for finding such analytic behaviour include exact Matrix Product state methods[135, 136] and large-N expansions of generating functions for the 2D Dyson gas[128]. It would also be interesting to analyse the claims of Ref. [34] in the context of further quantum Hall states, most notably the Read-Rezayi state. Furthermore, as previously mentioned, we can examine these claims rigorously in the integer quantum Hall effect[131] (which can be thought of as Laughlin at $\nu = 1$). We will also use a similar analysis to that presented here in the next chapter when considering the dynamics of edge modes.

CHAPTER 6

Effective Hamiltonians

I'm on the edge, the edge, the edge, the edge, the edge, the edge, the edge

— Lady Gaga [The Edge of Glory, 2011]

We have already seen that the low-energy dynamics of edge modes in the thermodynamic limit corresponds exactly to a chiral linear Luttinger liquid. For generic systems this linear picture is only true in the scaling limit of low energies and large system sizes. However, for the parent Hamiltonians discussed in Section 2.2.4 and in the presence of perfect quadratic confinement, the dispersion of the edge modes is linear regardless of system size all the way to high energies[61, 133, 137]. Away from these special cases one must consider the effect of *irrelevant* contributions[1], which introduce nonlinearities such as nontrivial dispersion or scattering processes between modes.

In this chapter we will consider exactly this non-ideal case, which can be characterised by anharmonic confinement or interactions and will, in general, have a far richer, nonlinear edge structure. This has been discussed in numerous works such as Refs. [1, 41, 80, 81, 106, 138–140]. To analyse these nonlinear effects we will take the ideal, linear case given by the parent Hamiltonian $\mathcal{H}_{\text{Parent}}$, and perturb it with $\delta\mathcal{H}$, thus moving it towards something more realistic. We then construct an effective field theory for the perturbed system. In doing so

[1] By irrelevant we mean that these contributions are small away from this "fixed point" at low energies and large system sizes and become smaller the closer we get to that point.

we generate a mapping from a perturbation acting upon the whole bulk of the droplet, $\delta\mathcal{H}$, onto a low-energy effective Hamiltonian which resides only on the edge.

In order to constrain the field theory, we conjecture it to be local and impose upon it the symmetries of the perturbation using a construction inspired by work from J. Dubail, N. Read and E. Rezayi[34] and revisited recently in the previous chapter[2]. We find that this procedure is especially fruitful as we can map symmetries of the perturbations, such as rotational and translational invariance, to powerful constraints on the effective Hamiltonian's form. We illustrate this mapping from bulk interactions to their effect on the edge for the Laughlin[19] and Moore-Read[22] quantum Hall states, though the procedure could in principle be generalised to more exotic quantum Hall states, such as the Read-Rezayi states[23] or any other state which can be expressed by a conformal field theory[35, 118].

We will see that this effective description of the edge dynamics is accurate for short-range interactions and confinements close to quadratic. These two conditions make our work particularly applicable to potential cold atom realisations of the quantum Hall effect where the interactions between atoms are generally short-range, perhaps even hard-core, the confinement can be readily tuned to a simple quadratic, and the number of particles can be quite small[42, 43, 45]. In this regime our effective theories prove to be extremely good at capturing the effects of finite size and non-ideal interactions on the edge behaviour.

We begin by introducing the concept of an effective Hamiltonian in section 6.1, describe how this can be expressed as a field theory on the edge of our system and discuss the effect of symmetries. We then use these powerful results in section 6.2 for the Laughlin and Moore-Read wavefunctions to propose generic theories for the edge dynamics induced by non-ideal bulk interactions. Finally, we present numerics in support of these claims in section 6.3, showing the excellent agreement

between finite-size exact diagonalisation and our effective edge theories.

6.1 An Effective Description

6.1.1 Effective Hamiltonians

We will use the powerful language of CFT to generate effective low-energy theories for quantum Hall edges. To do so we take a full Hamiltonian for the system of the form

$$\mathcal{H} = \mathcal{H}_{\text{Parent}} + \delta\mathcal{H} \tag{6.1}$$

and then diagonalise $\delta\mathcal{H}$ within the context of degenerate perturbation theory. In the construction of our physical states, each is labelled by some auxiliary state in the CFT $\Psi_{\langle v|}$. The state $|v\rangle$ is such that it describes a state with ΔL units of angular momentum with respect to the ground state. The parent Hamiltonian, with its parabolic confinement, is then such that the energies of these states are linear in this added angular momentum, $E_v \propto \Delta L$.

However, the subspaces at a given ΔL will be degenerate. For example, in the Laughlin case at $\Delta L = 2$ there are two states, $\Psi_{\langle 2|}$ and $\Psi_{\langle 1,1|}$. Once we impose our perturbation, $\delta\mathcal{H}$ on the system, this degeneracy will in general break, mixing the two states,

$$\delta\mathcal{H}\Psi_{\langle v|} = \sum_w H_{v,w}\Psi_{\langle w|}. \tag{6.2}$$

However, given the linearity of the description of these wavefunctions in terms of CFT (i.e, $\alpha\Psi_{\langle v|} + \beta\Psi_{\langle w|} = \Psi_{\langle v|\alpha+\langle w|\beta}$), we in fact have that

$$\delta\mathcal{H}\Psi_{\langle v|} = \Psi_{\langle v'|} \quad \text{where} \quad \langle v'| = \sum_w \langle w|H_{v,w}. \tag{6.3}$$

As such, there is an operator H which is the image of $\delta\mathcal{H}$ under a linear mapping from the physical space of states to the CFT which reproduces the mixing of the real states in the CFT language, i,e,

$$\delta\mathcal{H}\Psi_{\langle v|} = \Psi_{\langle v|H}. \tag{6.4}$$

This equation defines H.

In what follows we will consider the constraints imposed upon H by the symmetries of $\delta\mathcal{H}$. As usual in quantum mechanics, the symmetries of the Hamiltonian will be expressed as a vanishing commutation relation with some operator, $\mathcal{B}$, which encodes the particular symmetry. Consider then that this operator also has a mapping to the CFT,

$$\mathcal{B}\Psi_{\langle v|} = \Psi_{\langle v|B}. \tag{6.5}$$

In this way, the symmetry of $\delta\mathcal{H}$ can be simply mapped to a symmetry of H,

$$[\mathcal{B}, \delta\mathcal{H}] = 0 \quad \mapsto \quad [H, B] = 0. \tag{6.6}$$

This procedure allows us to impose strong constraints on the form of H.

It is worth noting a key consequence of the fact that the mapping is linear. Consider, for example that we perturb the trial wavefunction by two perturbations, $\delta\mathcal{H} = \delta\mathcal{H}_1 + \delta\mathcal{H}_2$. Given that our mapping to the CFT language is linear, each of these perturbations admits its own effective description and the two simply add,

$$\delta\mathcal{H} = \delta\mathcal{H}_1 + \delta\mathcal{H}_2 \quad \mapsto \quad H = H_1 + H_2. \tag{6.7}$$

Now consider that $\delta\mathcal{H}$ commutes with a set of operators $\{\mathcal{B}_1, \ldots, \mathcal{B}_n\}$ but that $\delta\mathcal{H}_2$ also has one extra symmetry, $\mathcal{B}_{n+1}$. The former statement implies that H commutes with each of B_1 to B_n. However, $\delta\mathcal{H}_2$ also commutes with $\mathcal{B}_{n+1}$ and, given that the mapping to the CFT language is linear, it must also be the case that $[H_2, B_{n+1}] = 0$. Therefore, the individual effective Hamiltonian satisfies symmetries that the whole might not.

This may seem like an obvious point but it is of crucial importance. Consider for example that $\delta\mathcal{H}_1$ is some confinement imposed on the system and $\delta\mathcal{H}_2$ corresponds to an interaction. In this case, $\delta\mathcal{H}_2$ possesses an extra symmetry compared to $\delta\mathcal{H}_1$, that of translational invariance, and this imposes extra constraints on the form of H_2. However, because the mapping $\delta\mathcal{H} \to H$ is linear,

the only part of the effective Hamiltonian that knows anything about the form of the interactions is H_2. Therefore, even when the generic perturbation to the system as a whole, $\delta\mathcal{H}$, does not possess translational symmetry, the fact that our mapping is linear means that we are still able to make strong statements about all the contributions to H arising from interactions.

6.1.2 Preliminary Examples

Harmonic Confinement

We begin with a simple example where the mapping $\delta\mathcal{H} \mapsto H$ can be performed exactly. In general, this will not be possible but this example provides a taste of the machinery involved in the subsequent calculations.

The perturbation we will consider is a harmonic confinement imposed upon the droplet. In the first quantised language this perturbation has the form

$$\delta\mathcal{H} = U_0 \sum_{i=1}^{N} \left|\frac{z_i}{R}\right|^2 . \tag{6.8}$$

We now wish to consider the effect of $\delta\mathcal{H}$ acting upon our wavefunction $\Psi_{\langle v|}$. At first glance this does not appear possible as the wavefunction $\Psi_{\langle v|}$ can only be holomorphic but the interaction contains $\bar{z}_i$ terms. However, we have already seen that this can be resolved using projection to the lowest Landau level, as discussed in Section 4.2.4, $\bar{z}_i \to 2{\ell_\mathrm{B}}^2\partial_i$.

In this way, we can reformulate our perturbation as a differential operator. Recalling that $R = \ell_B\sqrt{2mN}$ we find,

$$\delta\mathcal{H} = \frac{U_0}{m} + \frac{U_0}{mN}\sum_{i=1}^{N} z_i\partial_i \tag{6.9}$$

(where the constant term arises from the action of ∂_i on z_i itself). Thus, we find a constant energy shift plus an extra term which we can map into the CFT using the "Ward identity" Eq. 4.55 which gives

$$H = \frac{U_0}{mN}\left(L_0 + a_0 N\sqrt{m}\right) + U_0\frac{(mN - \tilde{m}) + 2}{2m} \tag{6.10}$$

where recall that $\tilde{m} = m$ for the Laughlin state and $m+1$ for Moore-Read.

Thus, we have our first effective Hamiltonian. In the space of neutral edge states (i.e, $a_0|v\rangle = 0$) this simply reduces to a linear model,

$$H = \frac{U_0}{mN} L_0 + \text{const} \tag{6.11}$$

where L_0 simply counts the conformal dimension, ΔL, of the state $|v\rangle$, and so

$$E = \frac{U_0}{mN} \Delta L + \text{const.} \tag{6.12}$$

This also proves that any perturbing confinement to the quantum Hall system which is quadratic gives only a linear contribution to the spectrum.

Harmonic Interactions

Consider the Harmonic interaction, which we take to have the form

$$\delta\mathcal{H} = V_0 \sum_{i \neq j} \left| \frac{z_i - z_j}{2\ell_B} \right|^2 . \tag{6.13}$$

This interaction is clearly very non-local, coupling particles with larger separations more than those which are close. In order to find the mapping of the operator in the CFT we must first convert it into a differential operator using projection to the lowest Landau level $\bar{z}_i \to 2\ell_B^2 \partial_i$. The result of this is that

$$\delta\mathcal{H} = NV_0 \sum_i z_i \partial_i - V_0 \sum_i z_i \sum_j \partial_j + V_0 N(N-1). \tag{6.14}$$

Therefore, we simply need the mapping of these operators into the CFT, as in Eqs. 4.55, 4.40 and 4.59. Collating these results we therefore find that

$$\begin{aligned} H = NV_0 \Big(L_0 - a_{-1}a_1 - \frac{1}{N\sqrt{m}} L_{-1}a_1 \Big) \\ + NV_0 \frac{mN^2 + (2-\tilde{m})N - 2}{2}. \end{aligned} \tag{6.15}$$

Note that this effective Hamiltonian is clearly non-local with the $L_{-1}a_1$ term being of the form

$$L_{-1}a_1 = \frac{1}{2} \oint \frac{\mathrm{d}z}{2\pi i} \oint \frac{\mathrm{d}w}{2\pi i} : (i\partial\varphi(w))^2 : zi\partial\varphi(z). \tag{6.16}$$

6.1.3 Local Field Theories

A priori, we know nothing about the form of H but we shall attempt to constrain it using a simple symmetry analysis. In what follows we shall use a local field theory description for H and then map the symmetries of the perturbation, $\delta\mathcal{H}$, into the CFT language in order to find symmetry constraints on the terms in H.

We begin by noting that our effective Hamiltonian operator, H, is a CFT operator which acts only within the space of edge states and so is supported along the edge. We then conjecture this Hamiltonian should be local, following from the work of Dubail, Read and Rezayi[34] who emphasised the importance of local field theories in the description of quantum Hall states. The motivations are then equivalent to those we saw in Chapter 5, that the bulk obeys a generalised screening hypothesis below $m_c \simeq 65$ and hence, the interactions between particles in the plasma decay exponentially, implying that the relevant physics be local.

Thus, we conjecture that our effective Hamiltonian, which by its definition is some operator supported along the edge of our droplet, should be local. This means that we take H to be of the form

$$H = \int \mathrm{d}x \sum_a h_a(x, \delta\mathcal{H})\Phi_a(x) \tag{6.17}$$

where x is the one-dimensional coordinate encircling the surface of the droplet and $\Phi_a(x)$ are local operators made up of the fields $\varphi(x)$ and $\chi(x)$ and which have associated coupling constants h_a that depend a priori on the position, x, and the perturbation, $\delta\mathcal{H}$. A non-local form would be an integral over multiple edge coordinates with local Hamiltonian densities depending in some non-trivial manner on each coordinate, thus coupling well-separated regions of space along our edge.

The mapping between this edge coordinate x and a complex planar coordinate z is given by $z = re^{ix/R}$ for any r (but physically we consider $r \simeq R$) and where R is the droplet's radius. Working with this planar coordinate proves to be a large

simplification. If we make this change of variables we find that

$$H = \sum_a \oint \frac{\mathrm{d}z}{2\pi i} h_a(z, \delta\mathcal{H}) \Big(\frac{z}{R}\Big)^{d_a - 1} \Phi_a(z) \tag{6.18}$$

where d_a is the scaling dimension of the field Φ_a (and we have also absorbed some constant factors into h_a). Given that we are interested in cases where the number of particles is finite but still large, we see that the effective Hamiltonian is an expansion in $\frac{1}{R}$ where R is large. As such, we may restrict ourselves to considering only contributions with a small scaling dimension, d_a, and still hope to gain an accurate picture for relatively large system sizes. Furthermore, in the scaling limit, for which $R \to \infty$, the behaviour is given simply by the term with the lowest scaling dimension, d_a.

It should be stressed that this locality conjecture is not a rigorous constraint on H. We have motivated it here on the idea that the bulk physics is local though exactly how this should transfer to the form of H is not fully understood (though we provide some further evidence in the integer quantum Hall effect in a future publication[131]). Therefore, we provide supporting numerical evidence in Section 6.3 which further substantiates that this local description is very accurate for at least short-range interactions. Nevertheless, the locality conjecture may incur some loss of generality when the perturbation we add to the Hamiltonian describes some long-range interactions, in which case one might no longer expect a local field theory to provide an ample description of the dynamics. However, without the powerful simplification that this conjecture imposes on the theory, it would be extremely difficult to make significant progress.

6.1.4 Symmetries

Number Conservation

We now move on to rigorous constraints on our Hamiltonian, of which we shall consider three. The first is the conservation of total number of particles in the

system. This is conservation of U(1) charge, as each particle possesses a charge of $\sqrt{m}$. The operator which counts this charge is a_0 and therefore, the particle number in the CFT language is $\hat{N} = a_0/\sqrt{m}$. As such, the Hamiltonian must commute with a_0,

$$[H, a_0] = 0. \tag{6.19}$$

The consequence of this is relatively simple and means that our Hamiltonian must obey the same underlying U(1) symmetry of the free boson CFT. For the field this symmetry manifests itself as a shift to the field under the action of the U(1) generator

$$\varphi(z) \to \varphi(z) + \delta\varphi_0. \tag{6.20}$$

As such, the individual operators $\Phi_a(z)$ can only involve $\varphi(z)$ as a derivative, i.e, $\partial^n\varphi(z)$ for $n > 0$. Note that there is no constraint on the statistics sector due to this conservation law.

Rotational Invariance

We will also consider perturbations $\delta\mathcal{H}$ which are rotationally invariant. Once again, this is a very reasonable constraint for interactions, though perhaps more restrictive for confining potentials. On a mathematical level, it is relatively simple to derive the concomitant commutation relation for this symmetry by noting that the Hamiltonian should leave the total amount of angular momentum in the system invariant. Recalling that the angular momentum relative to the ground state is equal to the conformal dimension of the state $\langle v|$, and this is measured by the operator L_0, we therefore have that

$$[H, L_0] = 0. \tag{6.21}$$

However, once again, it is perhaps simpler to consider this constraint from a more physical perspective. Our droplet is a disc, and this system is invariant under rotations. Our edge is the circle at the edge of this disc, and the rotation of

the bulk coordinate corresponds to a translation of the edge coordinate. Therefore, our edge Hamiltonian must be translationally invariant. This has a simple consequence that the coupling coefficients h_a which we introduced in Eq. 6.17 must be independent of x or z.

Translational Invariance

The final bulk symmetry we may consider is two-dimensional translational invariance. Of course, this symmetry is not applicable to confining potentials but it does provide very strong constraints on the forms of field theories which describe interaction perturbations. Such perturbations will be translationally invariant within the bulk, meaning that the perturbation commutes with the generator of translations,

$$\left[\delta\mathcal{H}\ ,\ \sum_i \partial_i\right] = 0. \tag{6.22}$$

where $\partial_i = \frac{\partial}{\partial z_i}$. We already know the mapping of the translation operator into the CFT from Eq. 4.59 and therefore, we arrive at the constraint that

$$\left[H, a_{-1} + \frac{1}{N\sqrt{m}} L_{-1}\right] = 0 \tag{6.23}$$

wherever H describes some translationally invariant perturbation, $\delta\mathcal{H}$.

Nevertheless, there is once again a simpler picture to keep in mind. Consider that our perturbation $\delta\mathcal{H}$ will induce dynamics on the edge states of our system. This is shown by another cartoon picture in Fig. 6.1. On the left of this figure the droplet is centred and the arrow indicates the dynamics induced by $\delta\mathcal{H}$ (there may be additional dynamics due to the parabolic confinement in $\mathcal{H}_{\text{parent}}$ which we ignore here). Now consider the right picture, where we shift the position of our droplet. The dynamics induced by $\delta\mathcal{H}$, assuming that it is a translationally invariant perturbation, should be identical, but now about a new origin. Therefore, there must be some decoupling of the centre-of-mass mode from the underlying field theory. If we reconsider our cartoon pictures for the edge modes in Fig. 2.4

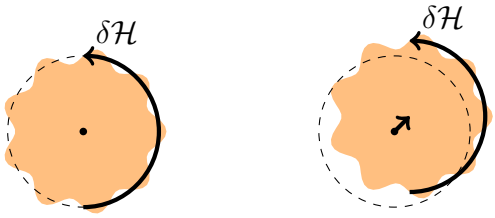

Figure 6.1: On the left we show a droplet with some edge excitation which is evolved by our translationally invariant perturbation, $\delta\mathcal{H}$. Given that $\delta\mathcal{H}$ is translationally invariant, this evolution will be about the centre of mass, and thus should be the same for the droplet on the right, whose centre of mass is slightly shifted. Crucially, $\delta\mathcal{H}$ cannot move this centre of mass.

---

then we see that the a_n edge mode creates n equally sized lobes of charge around the surface of the droplet. For $n \geq 2$ these cancel out, leading to no net shift of the centre-of-mass. The a_1 mode however, is equivalent to a shift of the droplet. As such, the field theory, H, cannot induce any dynamics on this edge mode. Therefore, a state $\Psi_{\langle v|}$ will have the same energy under $\delta\mathcal{H}$ as a shifted state $\Psi_{\langle v|a_1}$ and so

$$[H, a_1] = 0. \tag{6.24}$$

Now, of course, this does not immediately appear to agree with Eq. 6.23 but, in fact, the two are simply hermitian conjugates of each other, as we will demonstrate in Derivation 4. Therefore, these conditions together encode translational invariance *and* ensure that our effective Hamiltonian corresponds to some hermitian Hamiltonian in the physical space.

Derivation 4

As discussed in Chapter 5, our physical states $\Psi_{\langle v|}$ are not quite orthogonal under the same inner product as $|v\rangle$ but instead require some operator G_N which acts to give states non-zero overlaps. Therefore, consider matrix elements of our hermitian Hamiltonian, $\delta\mathcal{H}^\dagger = \delta\mathcal{H}$. Given that this Hamiltonian is hermitian we can act it either forward on the ket-state or backwards on the

bra-state, with the results that

$$\big\{\Psi_{\langle v|}\big|\delta\mathcal{H}\big|\Psi_{\langle w|}\big\} = \big\{\Psi_{\langle v|}\big|\Psi_{\langle w|H}\big\} = \big\{\Psi_{\langle v|H}\big|\Psi_{\langle w|}\big\}, \tag{6.25}$$

$$\implies \langle w|HG_N|v\rangle = \langle w|G_N H^\dagger|v\rangle. \tag{6.26}$$

Therefore, whilst we must have that $HG_N = (HG_N)^\dagger$ the effective Hamiltonian itself, H, need not be hermitian and is in fact not in general. In fact, the mapping we constructed from harmonic interactions in real space to an effective Hamiltonian, given by Eq. 6.15, was indeed non-hermitian. It need only have real eigenvalues which correspond to the real energy spectrum.

We can push this argument one step further. Consider the matrix element of some operator which might not be hermitian but similarly admits mappings into the CFT of the form

$$\mathcal{X}\big|\Psi_{\langle v|}\big\} = \big|\Psi_{\langle v|X}\big\}, \qquad \big\{\Psi_{\langle v|}\big|\mathcal{X} = \big\{\Psi_{\langle v|X^{\mathrm{H}}}\big| \tag{6.27}$$

where $X = X^{\mathrm{H}}$ only if $\mathcal{X}^\dagger = \mathcal{X}$. Therefore, considering the matrix elements of $\mathcal{X}$ in the CFT we see that the proper hermitian conjugation of operators (with respect to the physical space) is of the form

$$XG_N = G_N\big(X^{\mathrm{H}}\big)^\dagger \tag{6.28}$$

where $\dagger$ is the usual hermitian conjugation with respect to the CFT (i.e, $(a_n)^\dagger = a_{-n}$ for example).

Therefore, our particular case where $\mathcal{X} = \sum \partial_i$. We find that

$$\big(N\sqrt{m}a_{-1} + L_{-1}\big)G_N = G_N\big(X^H\big)^\dagger \tag{6.29}$$

which, by comparison with Eq. 5.15 for the translational symmetry consequence of the inner product operator, G_N, implies that

$$\big(X^H\big)^\dagger = \frac{a_{-1}}{2{\ell_{\mathrm{B}}}^2\sqrt{m}}. \tag{6.30}$$

This result can similarly be derived with no knowledge of the inner product by simply using projection to the lowest Landau level. Recall that $\bar{z}_i$ is equivalent to $2{\ell_\mathrm{B}}^2\partial_i$ and this works in reverse too, allowing us to replace $\sum_i \partial_i$ with $\sum_i \frac{\bar{z}_i}{2{\ell_\mathrm{B}}^2}$, which once mapped into the CFT is equivalent to Eq. 6.30. Therefore, we can take a "physical hermitian conjugate" of Eq. 6.23 to see that

$$\left[H, \left(a_{-1} + \frac{1}{N\sqrt{m}} L_{-1}\right)\right]^{\mathrm{H}} = \frac{1}{R^2}[a_1, H] = 0 \tag{6.31}$$

as required.

Confinement vs Interactions

To summarise the results of the preceding section, we have found the mapping of various symmetries of a general perturbation $\delta\mathcal{H}$ into our CFT language. They are as follows:

1. Number conservation implies charge conservation,

$$[H, a_0] = 0, \tag{6.32}$$

2. Rotational invariance implies translational invariance along the edge,

$$[H, L_0] = 0, \tag{6.33}$$

3. Translational invariance of $\delta\mathcal{H}$ implies a set of new constraints,

$$[H, a_1] = 0 \tag{6.34}$$

$$\left[H, a_{-1} + \frac{1}{N\sqrt{m}} L_{-1}\right] = 0. \tag{6.35}$$

Note that these are general symmetries which apply to H *regardless of our conjecture of locality.*

We are now in a position to consider any generic perturbation $\delta\mathcal{H}$, which we split up into a confining part $\delta\mathcal{H}_U$, and an interaction term, $\delta\mathcal{H}_V$. As discussed

previously, these individual perturbations will have mappings into the CFT of the form H_U and H_V which simply add,

$$\delta\mathcal{H}_U + \delta\mathcal{H}_V \mapsto H_U + H_V. \tag{6.36}$$

In the rotationally symmetric cases we will consider, H_U will then satisfy the first two symmetries, of number conservation and rotational invariance. However, we will find that we can constrain the form of H_V significantly more given that it must also satisfy the third symmetry, corresponding to bulk translational invariance.

6.2 Results

6.2.1 Confinement

We begin by considering the effect of number conservation and rotational symmetry on the form of effective Hamiltonians. This is the situation which corresponds to the part of our field theory which describes the effects of confinement on the droplet. We recall that number conservation forces H to commute with a_0, thus forcing $\varphi(z)$ to appear in H only as a derivative and that rotational invariance equates to one-dimensional translations along the edge, removing the possibility for our coupling coefficients, h_a, to depend on position, z.

Let us consider the effect of these symmetries for the Laughlin and Moore-Read wavefunctions. In the Laughlin case the statistics sector is trivial ($\chi = \mathbb{1}$) leaving only a theory made from the bosonic field. In general the fields $\Phi_a(z)$ have the form

$$\Phi_a(z) = (i\partial\varphi(z))^{m_1}\big(i\partial^2\varphi(z)\big)^{m_2}\cdots \tag{6.37}$$

for non-negative integers $m_1, m_2, \ldots$. Each term has a scaling dimension $d_a = m_1 + 2m_2 + \ldots$ and it is always assumed that they are normal ordered. Therefore, we can consider the first few most relevant terms (up to total derivatives) to be

$$H = \oint \frac{\mathrm{d}z}{2\pi i}\Big(\frac{v}{2}z(i\partial\varphi(z))^2 + gz^2(i\partial\varphi(z))^3\Big) + \mathcal{O}\big(R^{-3}\big). \tag{6.38}$$

The first of these terms is the usual chiral linear Luttinger liquid term, and by itself would lead to a dispersion $E = v\Delta L$. The second term is then a scattering term which, for example, might take the $n = 2$ mode (recall Fig. 2.4) and scatter this into two $n = 1$ modes. Note that this form of nonlinear Luttinger liquid has been studied at length in, for example, Refs. [106, 139].

We may also consider the consequences of these simple symmetries on the generic effective Hamiltonian describing a Moore-Read edge. In this case the statistics sector is a free fermion CFT with $\chi(z) = \psi(z)$. Therefore, our general fields have the form

$$\Phi_a(z) = (i\partial\varphi(z))^{m_1} \cdots \times (\psi(z))^{k_0}(\partial\psi(z))^{k_1} \cdots \tag{6.39}$$

where the m_i are once again any non-negative integer but $k_i \in \{0, 1\}$ due to fermionic exclusion. In this case the scaling dimension of a given term is $d_a = \sum_n nm_n + \sum_l \left(l + \frac{1}{2}\right)k_l$. As such, the first few most relevant terms will be

$$\begin{aligned} H = \oint \frac{\mathrm{d}z}{2\pi i} \Big(&-\frac{v_1}{2} z(\psi\partial\psi(z)) + \frac{v_2}{2} z(i\partial\varphi(z))^2 \\ &+ g_1 z^2 (i\partial\varphi(z))^3 + g_2 z^2 (i\partial\varphi\psi\partial\psi(z)) \Big) + \mathcal{O}\big(R^{-3}\big). \end{aligned} \tag{6.40}$$

In this Hamiltonian the first two terms are once again linear edge velocities which by themselves would simply give us the spectrum $E = v_1\Delta L_\psi + v_2\Delta L_\varphi$, giving the fermionic modes a velocity v_1 and the bosonic modes a velocity v_2. We then have two scattering terms, one exactly equivalent to the Laughlin scattering term, which scatters bosonic modes, and one coupling term which scatters a single bosonic mode into two fermions and vice versa.

6.2.2 Interacting Laughlin

Constructing H

We now consider the addition of two-dimensional translational symmetry to the effective Hamiltonian, which will allow us to describe the effects of interactions on

the edge dynamics. We will find that this symmetry is very restrictive, removing the majority of those terms which were present in those effective Hamiltonians describing confinement. Given these restrictions, we will need to go to rather high order (large d_a) to find the major contributing terms. In doing so we need to find a good basis of operators with which to work and then use those to construct linearly independent Hamiltonians H_a such that

$$H = \sum_a h_a H_a \tag{6.41}$$

where the H_a are individual blocks which satisfy the translational symmetry commutation relations and $h_a(\delta\mathcal{H})$ are coefficients which scale as $h_a \sim R^{1-d_a}$ where d_a is the scaling dimension of the leading term (the term with the lowest scaling dimension) in H_a. We will therefore use exactly the $T_{\mathbf{\Gamma}}$ used in the previous chapter, defined as

$$T_{\mathbf{\Gamma}} = \oint \frac{\mathrm{d}z}{2\pi i} z^{|\mathbf{\Gamma}|-1} \prod_{\gamma_i \in \mathbf{\Gamma}} i\partial^{\gamma_i}\varphi(z). \tag{6.42}$$

Once again, we must then be careful to only construct the individual H_a from linearly independent $T_{\mathbf{\Gamma}}$.

Restricting to interactions we must now find individual effective Hamiltonians, H_a, which satisfy the commutation relations Eqs. 6.24 and 6.23, which we recall to have the form

$$[H_a, a_1] = 0, \tag{6.43}$$

$$\left[H_a, a_{-1} + \frac{1}{N\sqrt{m}} L_{-1}\right] = 0. \tag{6.44}$$

By inspecting Eq. 6.44 we note that we will need to expand H_a in powers of $\frac{1}{N\sqrt{m}}$ of the form

$$H_a = H_a^{(0)} + \frac{H_a^{(1)}}{N\sqrt{m}} + \frac{H_a^{(2)}}{(N\sqrt{m})^2} + \dots. \tag{6.45}$$

Note here that the expansion in powers of $1/N$ can be compared to our overall expansion of the effective Hamiltonian in powers of $1/R$. To relate the two we recall that the radius varies as the square root of the particle number, $R =$

$\ell_B\sqrt{2mN}$. Therefore, if $H_a^{(0)}$ is made up from terms of scaling dimension d_a this tells us that $H_a^{(1)}$ can be made only from terms with a scaling dimension $d_a + 2$ or smaller. In general, $H_a^{(n)}$ is a combination of terms with scaling dimension $d_a + 2n$ or smaller. Furthermore, recalling than h_a scales as R^{1-d_a} and given that $R \sim \sqrt{N}$ we note that the overall coefficient in front of any $H_a^{(n)}$ must vary as $\sqrt{N}^{1-d_a-2n}$.

Using this expansion, we find from Eqs. 6.43 and 6.44 that the leading order terms in any H_a are those which satisfy the simple relations

$$[H_a^{(0)}, a_1] = [H_a^{(0)}, a_{-1}] = 0. \tag{6.46}$$

For example, of the terms listed in table 5.1 those which satisfy both of these constraints are T_{22} and T_{33}. A summary of these leading terms up to a scaling dimension of 9 is provided in table 6.1. The majority of these are simple bilinear terms, which will predominantly modify the dispersion of the edge modes (see below), though we will also find at $d_a = 9$ that there is a three-body scattering term.

Nevertheless, the leading terms do not tell the whole story and we must generate the sub-leading terms via Eq. 6.44, which necessarily generates interesting nonlinear scattering terms. This ladder of sub-leading corrections are generated by the constraints

$$[H_a^{(n)}, a_1] = 0 \qquad \forall n, \tag{6.47}$$

$$[H_a^{(n)}, a_{-1}] = [L_{-1}, H_a^{(n-1)}] \tag{6.48}$$

with the former equation from Eq. 6.43 latter arising from Eq. 6.44.

The Leading Contributions

Let us consider this in greater detail for the least irrelevant term with leading contribution T_{22}. To see that this satisfies the leading order requirements for a

d_a	$H_a^{(0)}$
4	T_{22}
6	T_{33}
8	T_{44}
9	$T_{333} + T_{332} - \frac{1}{3}T_{222}$
⋮	⋮

Table 6.1: The first few leading contributions to the effective Hamiltonian for the Laughlin case which commute with both a_1 and a_{-1} and whose effects are suppressed by factors of R^{1-d_a}. We note that the first three are bilinears in the bosonic modes, which means that their primary effect is on the dispersion of edge modes. The final example at $d_a = 9$ is a trilinear, which corresponds to some three-body scattering of bosonic modes.

translationally invariant effective Hamiltonian, Eq. 6.46, consider that in terms of bosonic modes this term has the form

$$T_{22} = \oint \frac{\mathrm{d}z}{2\pi i} z^3 \big(i\partial^2\varphi\big)^2 = -2\sum_{n>0}(n^2-1)a_{-n}a_n. \tag{6.49}$$

Therefore, it is clear that the $n = \pm 1$ modes are absent from this term. We then proceed to apply Eqs. 6.47 and 6.48 to produce the sub-leading terms $H_a^{(n)}$. We first consider Eq. 6.47 in the context of the individual fields,

$$[i\partial^n\varphi(z), a_1] = -\delta_{n,1}. \tag{6.50}$$

Therefore, in order to satisfy this condition, we must have that $n > 1$, and so we only consider $T_{\boldsymbol{\gamma}}$ where $\boldsymbol{\gamma}$ contains integers greater than or equal to 2 such as T_{222}, T_{33}, T_{2222} and so on.

We then consider Eq. 6.48, recalling that L_{-1} acts to differentiate the fields of the CFT[2], and so this constraint becomes

$$[H_{22}^{(1)}, a_{-1}] = \oint \frac{\mathrm{d}z}{2\pi i} z^3 \partial\Big(\big(i\partial^2\varphi\big)^2\Big). \tag{6.51}$$

[2] Simply consider that $[L_{-1}, \varphi(z)] = \partial\varphi(z)$.

We must now consider which terms might appear in $H_{22}^{(1)}$. Recall that by scaling arguments the pool of terms which might appear is restricted to those with a scaling dimension $d_{22} + 2 = 6$ or smaller. This therefore includes T_{22}, T_{33} or T_{222}. A priori, any of these might appear in $H_{22}^{(1)}$ but, given that T_{22} and T_{33} commute with a_{-1} their coefficients are unconstrained by this equation. Initially, this appears worrying as it suggests that

$$H_{22}^{(1)} = \alpha T_{22} + \beta T_{33} + \gamma T_{222} \tag{6.52}$$

where we are unable to say anything about α and β. However, in practice this is not a problem as T_{22} and T_{33} are also permissible $H_a^{(0)}$ terms, exactly because they commute with a_{-1}. Therefore, whatever the values of α and β, these coefficients can be combined with h_{22} and h_{33}, thus yielding no new coefficients. This argument is indicative of a more general principle. When considering what terms might appear in any $H_a^{(n)}$ where $n > 0$ one should first remove any terms which commute with a_{-1} and therefore produce their own $H_{a'}^{(0)}$ to avoid adding unnecessary extra coefficients.

Therefore, returning to our example, we note that $H_{22}^{(1)}$ should be made up of only T_{222}. To find how much of this term is present, consider once again the commutation of the mode with the field, which in this case is

$$[i\partial^n \varphi(z), a_{-1}] = \partial^{n-1}(z^{-2}). \tag{6.53}$$

Therefore, if we state that $H_{22}^{(1)} = \alpha T_{222}$ then we find by evaluating Eq. 6.51 that

$$\alpha = \frac{1}{2}. \tag{6.54}$$

Thus,

$$H_{22} = T_{22} + \frac{1}{2N\sqrt{m}} T_{222} + \dots. \tag{6.55}$$

In fact, this procedure can be continued easily to all orders, with the result that

$$\boxed{H_{22} = T_{22} + \sum_{n=1}^{\infty} \frac{8}{(N\sqrt{m})^n} \frac{(2n+1)!!}{(2n+4)!!} T_{2^n}} \tag{6.56}$$

where 2^n refers to the partition containing n copies of 2.

We can also consider this picture for the H_a whose leading contribution is T_{33}. For this root the first sub-leading correction as calculated using Eq. 6.48 has the form

$$H_{33} = T_{33} + \frac{5}{2N\sqrt{m}} T_{332} - \frac{15}{2N\sqrt{m}} T_{222} + \dots . \tag{6.57}$$

In general, this contribution is made from the terms $T_{332^{n-2}}$ and T_{2^n} of the form

$$\boxed{H_{33} = T_{33} + \sum_{n=1}^{\infty} \left(\frac{\alpha_n}{(N\sqrt{m})^n} T_{332^n} + \frac{\beta_n}{(N\sqrt{m})^n} T_{2^{n+2}} \right),} \tag{6.58}$$

where the coefficients, α_n and β_n, satisfy the recursive relation

$$\alpha_n = \frac{2n+3}{2n} \alpha_n, \tag{6.59}$$

$$\beta_n = \frac{2n+1}{2n+4} \beta_{n-1} - \frac{6(2n+1)}{(n+1)(n+2)} \alpha_n, \tag{6.60}$$

for all $n > 0$ and where $(\alpha_0, \beta_0) = (1, 0)$. A similar procedure can be repeated to fix all the H_a, leaving only h_a as free parameters which depend on the bulk interactions and cannot be fixed by symmetry only.

6.2.3 Interacting Moore-Read

Effective Hamiltonians for the Moore-Read state follow an extremely similar pattern to that we have seen for the Laughlin state. Once again, the imposition of bulk translational symmetry on the effective Hamiltonian prompts us to search for individual, independent contributions, $H_a = H_a^{(0)} + \frac{1}{N\sqrt{m}} H_a^{(1)} + \dots$, which satisfy the commutation relations in Eqs. 6.47 and 6.48. The sole difference is that the individual terms, $H_a^{(n)}$, for the expansions in $\frac{1}{N\sqrt{m}}$ are some terms expressed in terms of both the bosonic field, $\varphi(z)$ and the fermionic field, $\psi(z)$.

We begin once again by recalling that our basis of possible operators,

$$T_{\mathbf{\Gamma},\mathbf{\Xi}} = \oint \frac{\mathrm{d}z}{2\pi i} z^{|\mathbf{\Gamma}|+|\mathbf{\Xi}|+\frac{l(\mathbf{\Xi})}{2}-1} \prod_{\gamma_i \in \mathbf{\Gamma}} i\partial^{\gamma_i} \varphi(z) \prod_{\xi_i \in \mathbf{\Xi}} \partial^{\xi_i} \psi(z), \tag{6.61}$$

d_a	$H_a^{(0)}$
2	$T_{\emptyset,01}$
3	
4	$T_{22,\emptyset}$ $T_{\emptyset,12}$
5	$T_{3,01} + 3T_{2,01}$
6	$T_{33,\emptyset}$ $T_{\emptyset,23}$
⋮	⋮

Table 6.2: The leading contributions to the effective Hamiltonian in the Moore-Read case. These contributions occur at order R^{1-d_a} and are mostly diagonal in the basis defined by Eq. 4.44, and so primarily affect the dispersion. However, there are scattering terms at order R^{-4} which couple the fermionic edge states with the bosonic modes.

has been discussed at length in the previous chapter. We then restrict the wide array of possible linearly independent terms in Table 5.2 to those which satisfy the symmetries of our Hamiltonian. Recall that to first order this entails searching for $H_a^{(0)}$ which commute with both a_1 and a_{-1}. In the Laughlin case this was extremely restrictive. However, in this Moore-Read case the constraint is somewhat less powerful due to the fact that the centre of mass mode commutes with terms of purely fermionic nature. As such, there are more contributions than previously, as provided in table 6.2.

Finding all the sub-leading contributions is then a case of applying the commutation relation in Eq. 6.48 to generate the ladder of terms, $H_a^{(1)}$, $H_a^{(2)}$ and so on. As before, the situation is relatively simple, with L_{-1} acting as a derivative on the fields within each $T_{\mathbf{\Gamma},\mathbf{\Xi}}$ on the right and a_{-1} seeing only bosonic fields on the left. Applying this procedure, one then finds that the three leading terms for Moore-Read hamiltonians have the form

$$\boxed{H_{\emptyset,01} = T_{\emptyset,01} + \sum_{n=1}^{\infty} \frac{1}{(N\sqrt{m})^n} \frac{(2n-1)!!}{(2n)!!} T_{2^n,01},} \tag{6.62}$$

$$\boxed{H_{22,\emptyset} = T_{22,\emptyset} + \sum_{n=1}^{\infty} \frac{8}{(N\sqrt{m})^n} \frac{(2n+1)!!}{(2n+4)!!} T_{2^{n+2},\emptyset},} \tag{6.63}$$

$$\boxed{H_{\emptyset,12} = T_{\emptyset,12} + \sum_{n=1}^{\infty} \frac{1}{(N\sqrt{m})^n} \frac{(2n+1)!!}{(2n)!!} T_{2^n,12}.} \tag{6.64}$$

Therefore, each of the terms which, to leading order, simply change the dispersion of the fermionic modes (i.e, those of the form $H_{\emptyset,\Xi}$) necessarily have sub-leading contributions which couple the bosonic and fermionic excitations, suppressed by a factor of $\frac{1}{N\sqrt{m}}$.

6.3 Numerical Analysis

We once again stress that the claim of locality which was so instrumental in calculating these allowed contributions to our Hamiltonian was a conjecture based primarily on the understanding of the Laughlin state as a plasma in its screening phase (for $\frac{1}{\nu} \lesssim 65$). As such, we present thorough numerical evidence to further motivate this claim by comparing the results of these local effective Hamiltonians, which we hope will provide a very accurate description of the low-energy physics, with exact numerical results. For this particular work, we have made the relevant code openly available[141], which is based in part on the open source package DiagHam[142].

To assess our effective Hamiltonians we will take H to be simply a sum of the first few, least irrelevant terms from the field theoretic considerations we have made, including their coupling coefficients, h_a, which we cannot fix by symmetry alone. These Hamiltonians are then simple to diagonalise, being phrased in terms of second quantised operators. We then perform the exact numerics by generating the full edge states in a basis of single-particle states, the monomial basis, by using their expression in terms of Jack polynomials[82–84]. We then exactly diagonalise the interaction within reduced subspaces of edge states at fixed angular

momentum to find the eigenstates and eigenvalues, and compare to the effective Hamiltonians, $H(h_a)$, by fitting the coupling coefficients to the data.

6.3.1 Confinement

We will initially consider the simpler case of confinement where the perturbation is simply a single-body term in the Hamiltonian. Recall then that we cannot use translational invariance to significantly constrain the final form of the effective Hamiltonian so we simply take the first few least irrelevant contributions,

$$H = \oint \frac{\mathrm{d}z}{2\pi i}\Big(\frac{v}{2}z(i\partial\varphi(z))^2 + gz^2(i\partial\varphi(z))^3\Big) + \mathcal{O}\big(R^{-3}\big). \tag{6.65}$$

We will use this to consider a relatively steep edge confinement of $U = U_0(r/R)^8$ and fit the coefficients v and g by simply matching the exact and effective spectra. To perform this fitting we minimise a loss function, as in the inner products case, specifically taking

$$\mathcal{L}(v,g) = \sum_i \big(E_i^{\text{eff.}}(v,g) - E_i^{\text{exact}}\big)^2 \tag{6.66}$$

where E_i^{eff} are the eigenvalues of our effective Hamiltonian, H, and E_i^{exact} are the corresponding eigenvalues of our perturbation, $\delta\mathcal{H}$. We can then choose which eigenvalues to use in this loss function and we include only the eigenvalues at $\Delta L = 5$. The simulated annealing method used for finding the coefficients within the inner product is once again useful to avoid becoming stuck in a local minimum. We find the results in Fig. 6.2 for the $\nu = 1/3$ Laughlin state containing $N = 10$ particles, which shows a very good match.

We also consider the Moore-Read case. Once again, without translational invariance the resulting effective Hamiltonian cannot be significantly simplified, which leaves us with the following least irrelevant terms,

$$\begin{aligned} H = \oint \frac{\mathrm{d}z}{2\pi i}\Big(&-\frac{v_1}{2}z(\psi\partial\psi(z)) + \frac{v_2}{2}z(i\partial\varphi(z))^2 \\ &+g_1z^2(i\partial\varphi(z))^3 + g_2z^2(i\partial\varphi\psi\partial\psi(z))\Big) + \mathcal{O}\big(R^{-3}\big). \end{aligned} \tag{6.67}$$

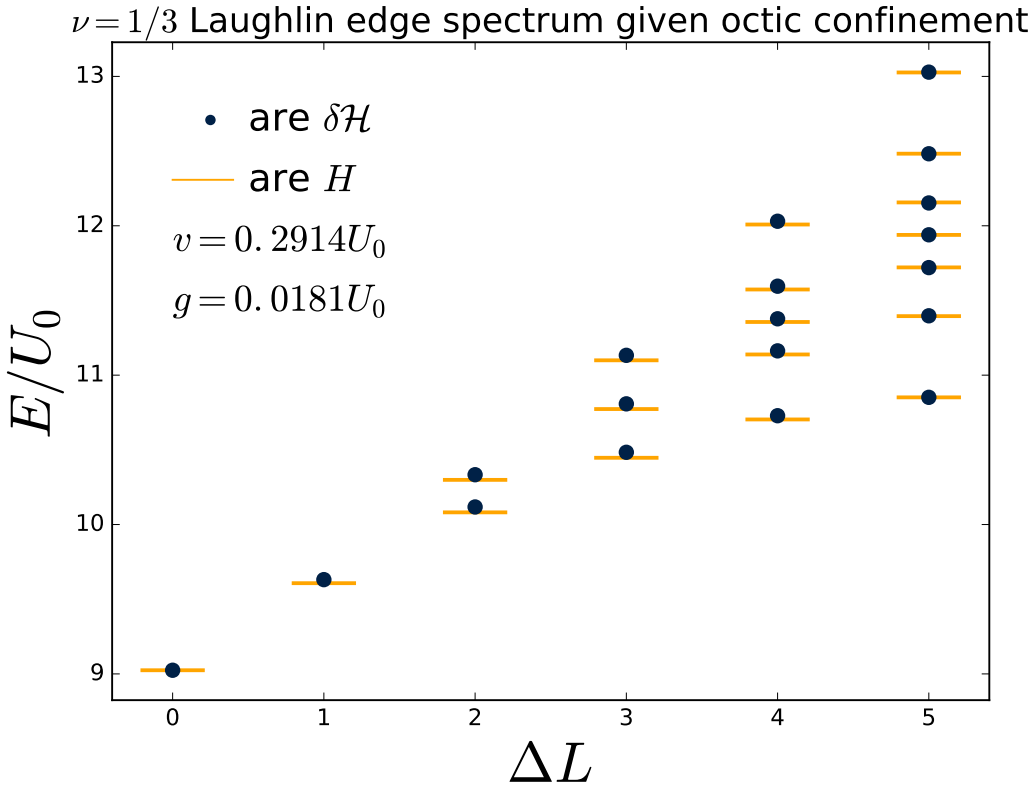

Figure 6.2: A comparison of our effective Hamiltonian with fit parameters g and v with the exact spectrum for an $N = 10$ Laughlin state at $\nu = 1/3$ confined purely by a weak octic confinement $U = U_0 \sum_i (r_i/R)^8$ (i.e, there is no additional quadratic confinement).

Once again, we check this against exact numerical results for a Moore-Read droplet confined by radial potential of the form $U_0(r/R)^8$ and fit the coefficients by minimising the discrepancy between the exact eigenvalues and those predicted by the effective Hamiltonian. The results are given in Fig. 6.3 and show good agreement once again.

6.3.2 Interacting Laughlin

For the Laughlin state perturbed by nontrivial interactions we shall employ a simple two-parameter effective Hamiltonian, including only the two least irrelevant

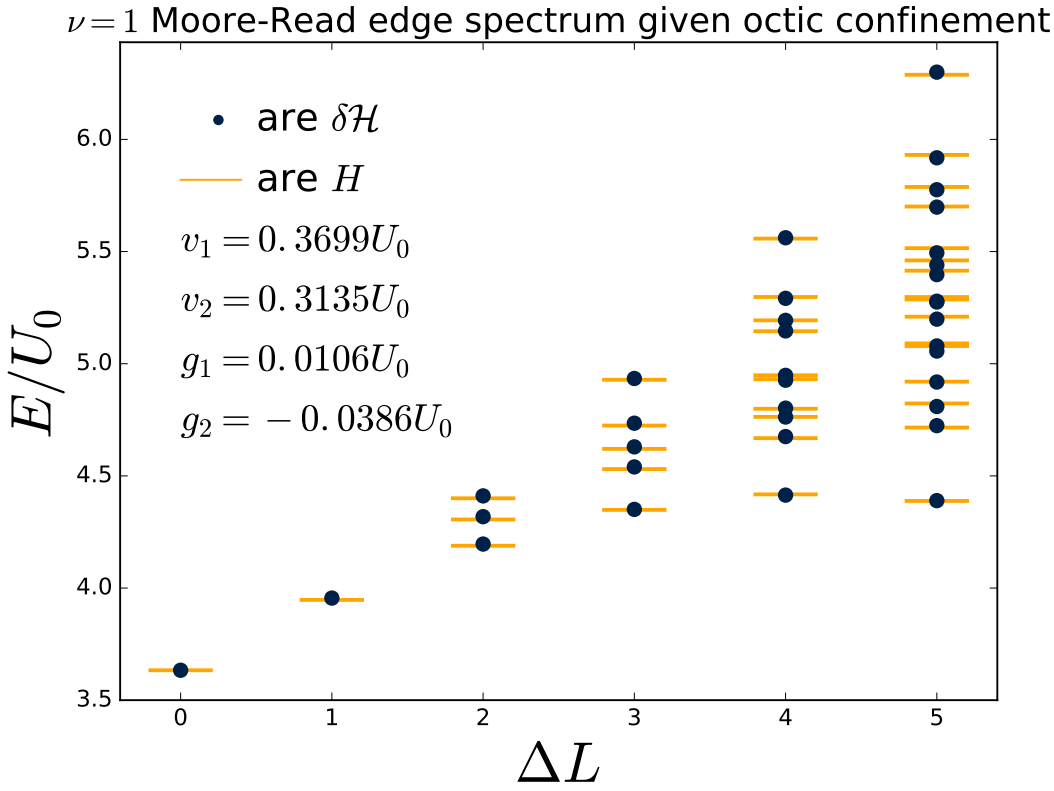

Figure 6.3: A comparison of our effective Hamiltonian with fit parameters v_1, v_2, g_1 and g_2 with the exact spectrum for a $\nu = 1$ Moore-Read state confined by a weak octic confinement $U = U_0 \sum_i (r_i/R)^8$ when $N = 14$. Once again, the quadratic confinement was set to zero for these results.

contributions,

$$H = h_{22}H_{22} + h_{33}H_{33}. \tag{6.68}$$

This should replicate the matrix elements of the Hamiltonian as calculated numerically up to corrections of order R^{-7}.

We then note that, given this form for the effective Hamiltonian, certain matrix elements will constrain the coefficients h_{22} and h_{33} exactly. Specifically, consider the element $\langle 2|H|2\rangle$ where $|2\rangle = a_{-2}|0\rangle$ as defined in Eq. 4.38. The only non-zero contribution to this comes from T_{22} contained in H_{22}. Not only is this true for the truncated expansion, but we expect it to hold true at every order. Furthermore, the only local terms which we expect can contribute to the matrix element $\langle 3|H|3\rangle$, even in an infinite-order expansion, are T_{22} and T_{33}. Therefore,

these two matrix elements should determine h_{22} and h_{33} exactly, and these are what we use to fit these coefficients.

Note that to find the effective Hamiltonian H from the data requires one to also calculate the overlaps of the wavefunctions. To see this, recall that the states in the quantum Hall language are not orthogonal, i.e,

$$\left\{\Psi_{\langle v|}\middle|\Psi_{\langle w|}\right\} = \langle w|G_N|v\rangle \tag{6.69}$$

where we have discussed the form of G_N at length in Chapter 5. Furthermore,

$$\left\{\Psi_{\langle v|}\middle|\delta\mathcal{H}\middle|\Psi_{\langle w|}\right\} = \langle w|HG_N|v\rangle. \tag{6.70}$$

Therefore, we can calculate the matrices G_N and (HG_N), and therefore we find the effective Hamiltonian by

$$H = (HG_N)G_N^{-1}. \tag{6.71}$$

Coefficient Scaling

Upon fitting the coefficients it is important to check that the scaling arguments made previously hold. These claimed that the coefficients h_a should scale as R^{1-d_a}. Then, given that the radius scales as the square root of particle number, N, this means that

$$h_a \sim \sqrt{N}^{1-d_a}. \tag{6.72}$$

To check that this scaling is borne out in the data, we fit the parameters for a variety of system sizes for fillings $\nu = 1$ and $\nu = 1/2$ and plot the results in Figs. 6.4a and 6.4b. The exact results will depend upon the interaction and filling and in these examples we take the interaction to be the first Haldane pseudopotential for $\nu = 1$ and the second Haldane pseudopotential at $\nu = 1/2$. We see that the results appear to be consistent with the scaling hypothesis, with h_{22} varying in the large-N limit as $h_{22} \sim \sqrt{N}^{-3}$, exactly as expected. h_{33} is less clear. For the integer case it also appears to vary as expected, $h_{33} \sim \sqrt{N}^{-5}$, but

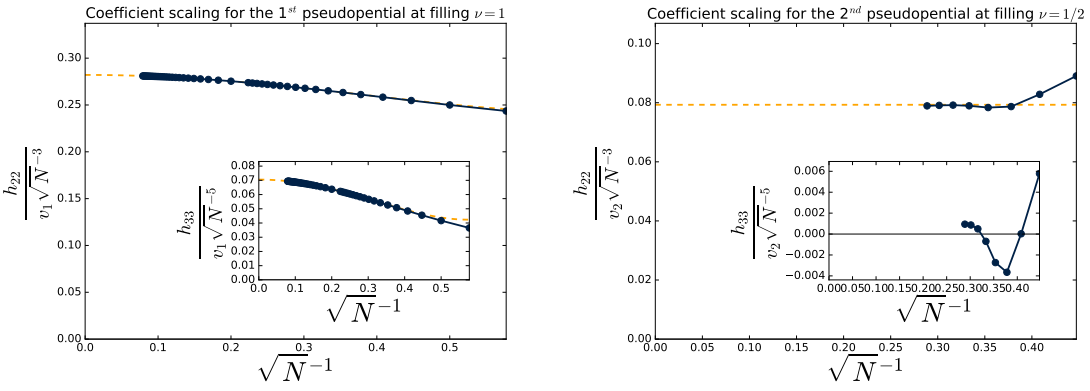

(a) (b)

Figure 6.4: In (a) we perturb the integer quantum Hall effect at $\nu = 1$ with a first pseudopotential, V_1, and find the scaling of the coefficients h_{22} and h_{33} in the effective Hamiltonian. In both cases the coefficients appear to obey the scaling hypothesis well, varying as $h_a \sim \sqrt{N}^{1-d_a}$ where $d_{22} = 4$ and $d_{33} = 6$. In (b) we perturb the Laughlin wavefunction at $\nu = 1/2$ by the second pseudopotential. Plotted is the value we fit for h_{22} (which we expect to scale as $v_2\sqrt{N}^{-3}$) in the effective Hamiltonian as N is varied, which appears to converge very quickly to some constant$/\sqrt{N}^{3}$. Unfortunately, h_{33}, which is expected to vary as $\sqrt{N}^{-5}$, does not converge for this range of system sizes but does appear to decay at least as quickly as $\sqrt{N}^{-5}$, if not faster, as required by the scaling hypothesis.

at $\nu = 1/2$ it appears that sub-leading corrections to this coefficient are large enough that the value does not converge for the range of N we can reach with exact methods. Nevertheless it does not appear to fall off slower than $\sqrt{N}^{-5}$, so this also appears consistent with scaling arguments.

Effective Hamiltonian Spectra

Perhaps the most crucial check that our effective Hamiltonians describe the true behaviour of quantum Hall edges is that they faithfully reproduce the spectrum of edge states. Therefore, we take the Hamiltonian in Eq. 6.68 and fit values for h_{22} and h_{33} based on the method described above. We then plot the agreement for the case of exponential repulsion between particles,

$$V = w_0 \sum_{i<j} \exp\left(-\left|\frac{z_i - z_j}{2\ell_B^2}\right|^2\right), \tag{6.73}$$

at a variety of filling fractions in figures 6.5, 6.6 and 6.7. In each case we find that this two-parameter fit is very good.

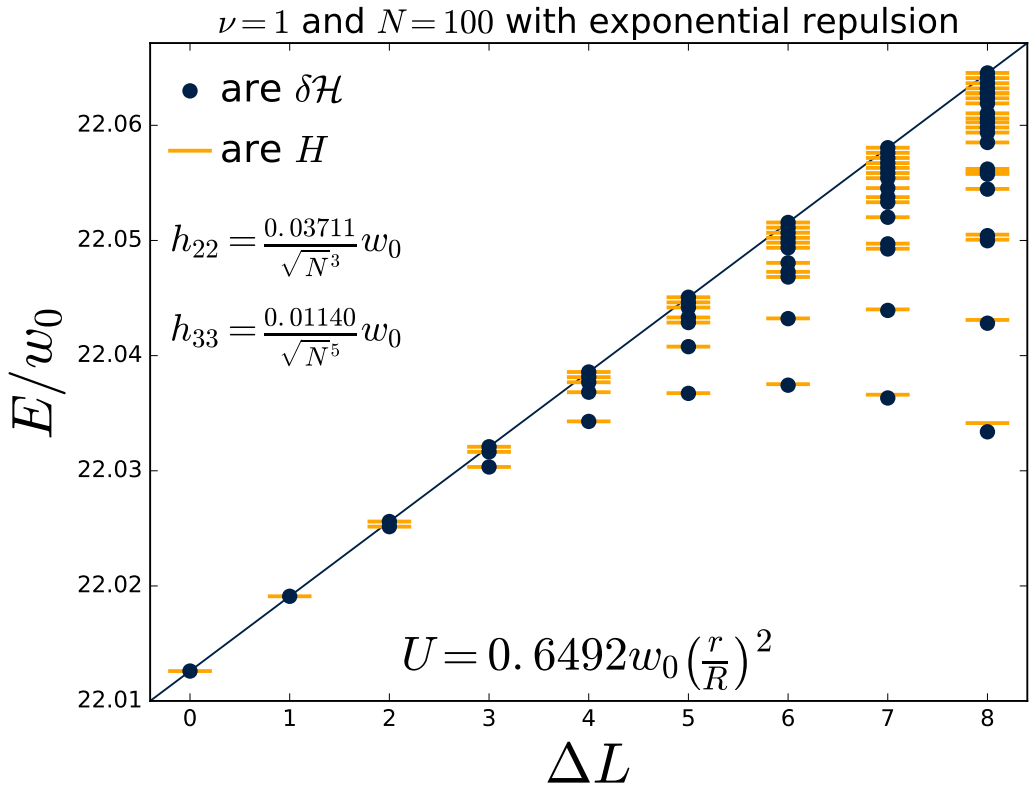

Figure 6.5: A comparison of our 2-parameter effective Hamiltonian with the exact edge spectrum for a $\nu = 1$ quantum Hall state perturbed by exponential repulsive interactions in Eq. 6.73 in the limit where w_0 is small. Recall that, because we expect the only terms in H which contribute to the matrix elements we use to fit h_{22} and h_{33} are H_{22} and H_{33}, we expect that the fits to these coefficients are exact for these systems at these particle numbers. We find that the subsequent agreement is extremely good, capturing the distinct characteristics of the spectrum and matching most points extremely closely.

Note that in these plots the linear slope is a free parameter of the parent Hamiltonian derived from the confinement, which we always take as quadratic. Therefore, in each plot we add an arbitrary harmonic potential (specified in each figure) which produces the accompanying linear slope. The repulsive interactions then cause the energies to decrease with respect to this linear edge as angular momentum is increased. This is because these excited states allow the particles

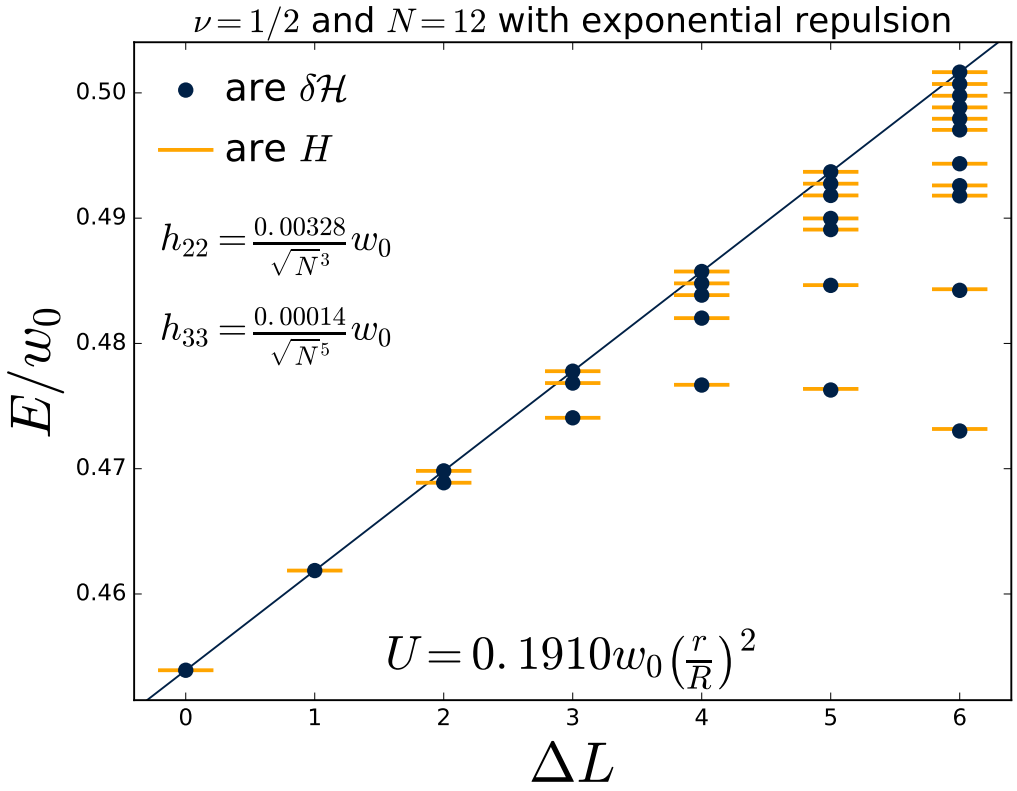

Figure 6.6: A comparison of numerical results for a $\nu = 1/2$ Laughlin state perturbed by exponential interactions with our 2-parameter effective Hamiltonians. As with the integer quantum Hall case, the agreement is excellent.

to avoid each other more successfully, increasing their average separations. The states which then lie exactly on the Luttinger liquid line are those edge states which correspond simply to translations of the original circular droplet as a whole, i.e, the states $a_{-1}^{\Delta L}|0\rangle$.

Constraints on non-local terms

Throughout the preceding text we have assumed that the only terms which contribute to H are local. However, this is a conjecture based on the Laughlin state being in a screening phase for $m \lesssim 65$, which makes correlations short range. However, for sufficiently long-range interactions we expect non-local terms to also contribute. One such example is the harmonic interaction, for which we can find the effective Hamiltonian exactly as presented in Eq. 6.15 and which contains

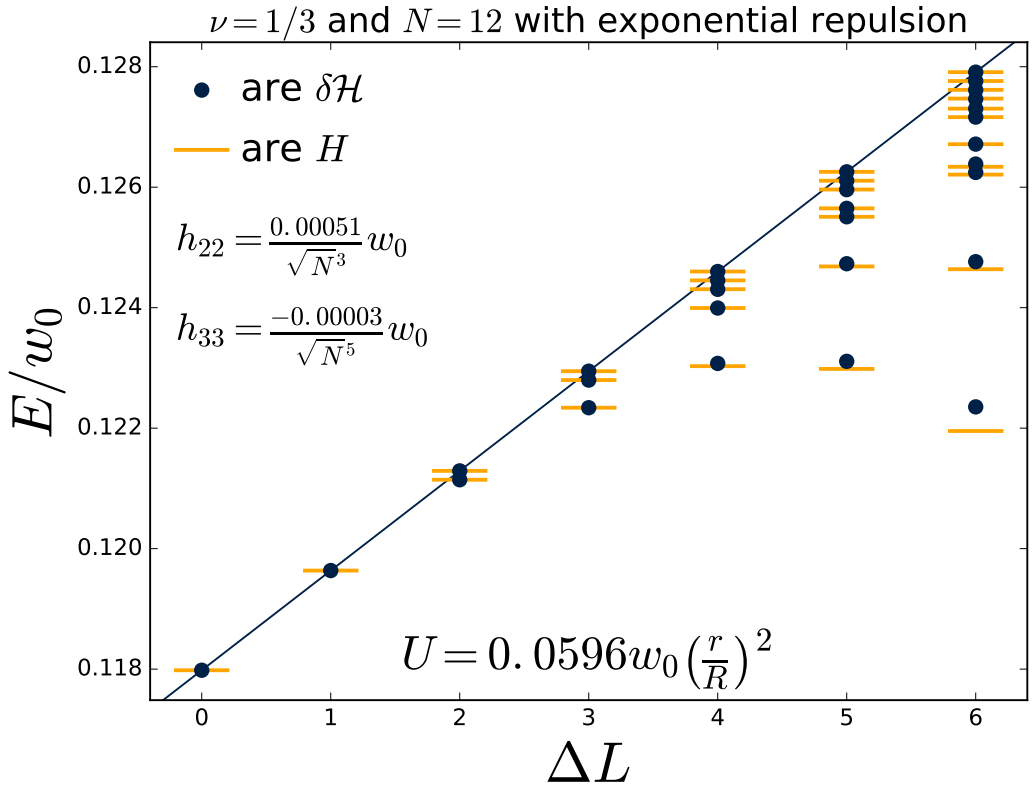

Figure 6.7: A final comparison of numerical results with our effective description for the $\nu = 1/3$ Laughlin state, which once again shows excellent agreement.

non-local contributions.

However, this is a special case of an interaction which actually grows with separation. In a more general setting, one of the most well-known non-local terms we might expect to contribute is the Benjamin-Ono term[80, 81, 107], which has the form

$$T_{\text{B-O}} = \oint \frac{\mathrm{d}z}{2\pi i} \oint_{|z|>|w|} \frac{\mathrm{d}w}{2\pi i} \frac{zw}{(z-w)^2} : i\partial\varphi(z) i\partial\varphi(w) := \sum_{n>0} n a_{-n} a_n \tag{6.74}$$

and has the lowest scaling dimension possible for such a double-integral term. Therefore, to ascertain the likelihood that non-local terms might appear we insert it into the Hamiltonian and attempt to fit its coefficient. We will then analyse the scaling of the resulting coefficient.

Therefore, we take the ultra-simple Hamiltonian

$$H = g_{\text{B-O}}\left(T_{\text{B-O}} - \frac{1}{2}T_{11}\right) + g_{22}T_{22} + \dots \tag{6.75}$$

and fit these two coefficients. Note that the inclusion of the T_{11} here ensures that the overall Benjamin-Ono term which we have inserted here obeys the leading condition of translational symmetry, i.e,

$$[a_1, H_a^{(0)}] = [a_{-1}, H_a^{(0)}] = 0. \tag{6.76}$$

The terms that we throw away in Eq. 6.75 are then either off-diagonal (terms which are generated by this Benjamin-Ono term to satisfy translational invariance at all orders) or of order $N^{-5/2}$. We then fit the coefficients $g_{\text{B-O}}$ and g_{22} with the first two non-trivial diagonal elements, $\langle 2|H|2\rangle$ and $\langle 3|H|3\rangle$.

The fits for the coefficients are plotted in Fig. 6.8 for the case of an exponential interaction at $\nu = 1/2$. We see that the scaling of g_{22} is very close to the expected $\sqrt{N}^{-3}$ whereas the Benjamin-Ono coefficient does not scale in a manner which can even be approximated by a power law. Nevertheless, we see that it is always much smaller than g_{22} despite the fact that it is expected to be roughly $\sqrt{N}$ times larger. Therefore, it is unlikely that the Benjamin-Ono term contributes to our effective Hamiltonian, or at least its effects are much smaller than expected by simple scaling arguments.

Couplings for Pseudopotentials

We now look at what the values for the couplings, h_{22} and h_{33}, look like for the first few Haldane pseudopotentials. In theory, each pseudopotential has associated with it an effective Hamiltonian,

$$V_k \Psi_{\langle \boldsymbol{\lambda}|} = \Psi_{\langle \boldsymbol{\lambda}|H_k}, \tag{6.77}$$

and therefore, given that any interaction can be formed from a sum of pseudopotentials, i.e, $V = \sum_k v_k V_k$, the effective Hamiltonian of such an interaction is

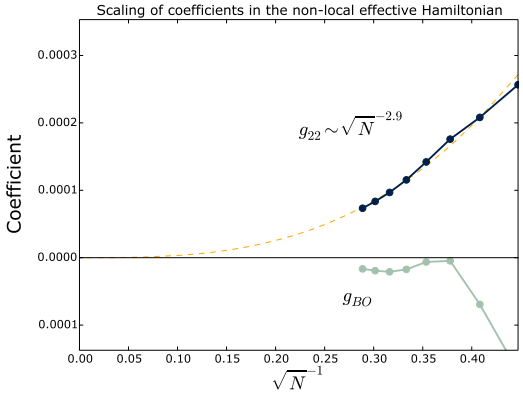

Figure 6.8: We assume for the moment that the Hamiltonian might contain non-local terms and fit them taking the form in Eq. 6.75 for H and taking exponential interactions between the particles at filling $\nu = 1/2$. We see that the Benjamin-Ono coefficient is consistently smaller than g_{22} despite scaling arguments suggesting that it should be $\sim \sqrt{N}$ times larger. As such, any contribution this term makes to the dynamics are much smaller than expected. Clearly this does not prevent any non-local term being present at any order in the expansion but it does provide evidence against this most likely contribution.

---

simply

$$H = \sum_k v_k H_k. \tag{6.78}$$

Recall that the parent Hamiltonian at $\nu = 1/m$ is constructed from all the pseudopotential V_k with $k < m$ and so these annihilate all our wavefunctions at these filling fractions. Therefore, knowledge of the coupling coefficients within the H_k of Eq. 6.78 for $k \geq m$ is all we require to be able to build the effective Hamiltonian for any interaction.

Unfortunately, as we have already seen in Fig. 6.4b for example, fitting some of these coefficients can be difficult or simply unreliable for the system sizes we are able to compute exactly. Therefore, we fit only the leading order contribution, h_{22} for each and give the values in table 6.3 for the pseudopotentials contributing to the interactions at $\nu = 1/2$.

However, whilst our data for fractional fillings remains too small to form a reliable conclusion about the sub-leading corrections to the effective Hamiltonian, we can perform this analysis extremely reliably for $\nu = 1$, where we consider N

Pseudopotential	$h_{22}^{\nu=1/2}$
V_2	0.079 ± 0.007
V_4	0.074 ± 0.020
V_6	0.087 ± 0.036

Table 6.3: The leading coupling coefficient for the effective Hamiltonian of various pseudopotentials at fractional fillings $\nu = 1/2$. For the case at half filling the convergence to a constant appears robust and the errors are very small. Similar extrapolations could not be made reliably for the case at $\nu = 1/3$ given the inferior convergence in this case.

Pseudopotential	$h_{22}^{(3)}$	$h_{22}^{(4)}$	$h_{22}^{(5)}$	$h_{33}^{(5)}$
V_1	0.282 ± 0.001	0.000 ± 0.002	-0.179 ± 0.016	0.071 ± 0.001
V_3	0.423 ± 0.001	0.001 ± 0.017	-0.633 ± 0.187	0.247 ± 0.001
V_5	0.529 ± 0.001	0.004 ± 0.014	-1.268 ± 0.156	0.485 ± 0.001
V_7	0.617 ± 0.001	0.010 ± 0.010	-2.088 ± 0.135	0.771 ± 0.005
V_9	0.694 ± 0.006	0.014 ± 0.278	-2.982 ± 5.472	1.103 ± 0.189

Table 6.4: The coupling coefficients for the first few contributing pseudopotentials at filling $\nu = 1$. We note that the higher-order coefficients are larger relative to the lower order coefficients for the higher pseudopotentials (which are the pseudopotentials that are more important for less local interactions), i.e, $\left|h_{22}^{(3)}/h_{22}^{(5)}\right|$ is smaller for V_k where k is larger. Furthermore, we note that the coefficient of h_{22} at order $\sqrt{N}^{-4}$ is very small relative to the coefficients at fractional powers of N. This is in good agreement with our calculation for the asymptotic behaviour of the exponential potential shown in a future publication [131], which predicts vanishing coefficients at even order (i.e, at order $\sqrt{N}^{-2n}$).

as high as 160. Thus, we fit the effective Hamiltonian to 5^{th} order, expanding the leading coupling coefficient as

$$h_{22} = \frac{h_{22}^{(3)}}{\sqrt{N}^3} + \frac{h_{22}^{(4)}}{\sqrt{N}^4} + \frac{h_{22}^{(5)}}{\sqrt{N}^5} + \mathcal{O}\left(\sqrt{N}^{-6}\right) \tag{6.79}$$

and considering only the leading order for $h_{33} = h_{33}^{(5)}/\sqrt{N}^5 + \mathcal{O}\left(\sqrt{N}^{-6}\right)$. Each of these coefficients is shown in table 6.4.

6.3.3 Interacting Moore-Read

The spectra for the Moore-Read state are more complex than those for the Laughlin state. For example, consider the subspace of states with $\Delta L = 5$ units of angular momentum added with respect to the ground state. In the Laughlin case, this is a 7-dimensional subspace but in the Moore-Read case there are 16 states. As such, the matrix, $\delta\mathcal{H}$, which our effective Hamiltonian, H, must reproduce includes over four times as many matrix elements. Nevertheless, as we shall see, an effective Hamiltonian containing only three terms (and thus three fit parameters) can still provide an extremely good description of the resulting behaviour. Thus, in the resulting discussion we will take the effective Hamiltonian to include the three least irrelevant terms

$$H = h_{\emptyset,01}H_{\emptyset,01} + h_{22,\emptyset}H_{22,\emptyset} + h_{\emptyset,12}H_{\emptyset,12}. \tag{6.80}$$

Note that to leading order, each term of this Hamiltonian is purely fermionic or bosonic, and hence the modes appear to decouple. However, one should recall that to first order each of these fermionic terms (as given in Eqs. 6.62 and 6.64) will couple the bosonic and fermionic edge channels.

As in the Laughlin case, we will fit the coupling coefficients in Eq. 6.80 by comparison with particular matrix elements. Specifically $\langle 2;\emptyset|H|2;\emptyset\rangle$ will fit the coefficient $h_{22,\emptyset}$. Additionally, we use $\left\langle \emptyset;\frac{3}{2}\frac{1}{2}\middle|H\middle|\emptyset;\frac{3}{2}\frac{1}{2}\right\rangle$ and $\left\langle \emptyset;\frac{5}{2}\frac{1}{2}\middle|H\middle|\emptyset;\frac{5}{2}\frac{1}{2}\right\rangle$ together to fit the coefficients $h_{\emptyset,01}$ and $h_{\emptyset,12}$. We present a scaling analysis of the resulting fit coefficients for the bosonic $\nu = 1$ Moore-Read state perturbed by exponential interactions in Fig. 6.9. As these plots show, the scaling hypothesis appears to work well even for these relatively small system sizes. The convergence for the least irrelevant contribution, $h_{\emptyset,01}$ is very good and is shown to vary as $\sqrt{N}^{-1}$ as expected by scaling arguments. Less clear are the forms of scaling for $h_{22,\emptyset}$ and $h_{\emptyset,12}$ which do not converge so convincingly over the system sizes we are able to access though still appear to fall off no faster than the $\sqrt{N}^{-3}$ required.

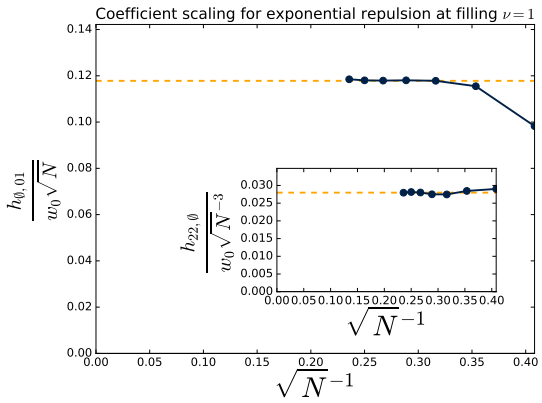

Figure 6.9: We consider the Moore-Read state at $\nu = 1$ perturbed by an exponential repulsive interaction, Eq. 6.73, and fit the coupling coefficients, $h_{\emptyset,01}, h_{22,\emptyset}$ and $h_{\emptyset,12}$ at a variety of system sizes, N. We then plot the variation of $h_{\emptyset,01}$ and $h_{22,\emptyset}$ with N, which are expected to vary as $\sqrt{N}^{-1}$ and $\sqrt{N}^{-3}$ respectively based on scaling arguments. The convergence to this scaling behaviour is quite good for both $h_{\emptyset,01}$ and $h_{22,\emptyset}$. However, the convergence is unclear for the coefficient $h_{\emptyset,12}$, whose scaling behaviour we do not show here, as we cannot reach large enough N with these exact methods for the value to converge. Nevertheless, the scaling hypothesis does not appear to be incompatible with any of this data.

Effective Hamiltonian Spectra

One again, the most crucial check of our effective theory is that they are able to reproduce the spectra of the corresponding systems. As such, we calculate the spectrum numerically for Moore-Read states containing $N = 16$ particles at filling $\nu = 1$. The data when the interactions we perturb with are exponentially repulsive (i.e, the same as in Eq. 6.73) is shown in Fig. 6.10 alongside a comparison to the effective Hamiltonian, $H(h_{\emptyset,01}, h_{22,\emptyset}, h_{\emptyset,12})$, where these coupling coefficients are fit using the procedure described above.

This comparison shows very good agreement between the exact numerical data and our low energy effective theories. Notably, the renormalisation of the velocity of the fermionic modes is indeed borne out by the data, with the lowest energy modes in Fig. 6.10 corresponding to cases where all of the angular momentum goes into the excitation of fermionic edge modes. Their velocity is reduced by the presence of interactions.

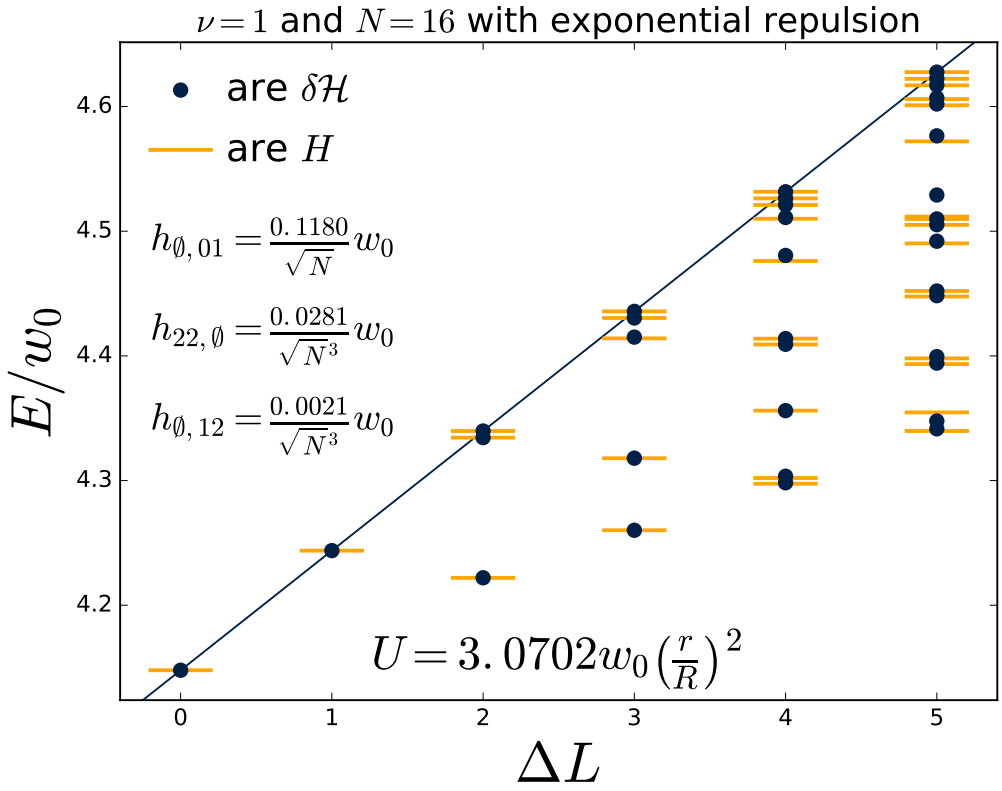

Figure 6.10: We show the spectrum for the Moore-Read state containing $N = 16$ particles at filling $\nu = 1$ perturbed by an exponential repulsive interaction, Eq. 6.73. The three coupling coefficients in the effective Hamiltonian, H, are fit using the process described above and provide a very accurate fit to the numerically calculated spectrum (the dots corresponding to the spectrum of $\delta\mathcal{H}$ whilst the orange lines are the spectra of H). As in the Laughlin case, the gradient of this linear Luttinger liquid slope (the blue line corresponding to an unperturbed droplet) is a free parameter of the parent Hamiltonian arising from the assumption of quadratic confinement.

However, we show here data only for the $\nu = 1$ Moore-Read state as smaller filling fractions do not converge sufficiently to be described by our effective theories at the system sizes we can reach with these exact methods. We suspect that this is due to a larger correlation length in these systems[143], which therefore requires higher order terms to be included in H to provide an adequate description of the data at small system sizes. This point is also true for the Laughlin state, whose agreement with our low energy theories also worsens as the filling fraction decreases. We present an illustration of this point in Fig. 6.11.

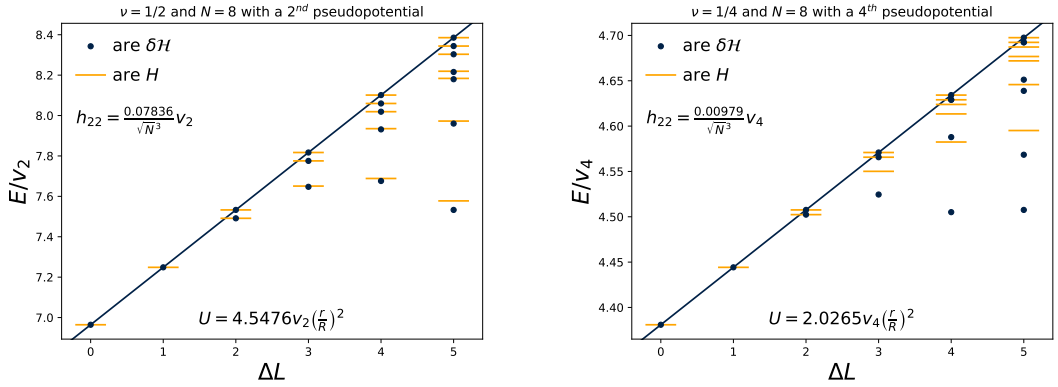

Figure 6.11: A pair of plots showing the spectrum for the Laughlin quantum Hall edge when the bulk interactions are the first non-vanishing pseudopotentials at filling fractions $\nu = 1/2$, $1/3$ and $1/4$, (i.e, at filling $1/m$ we add the pseudopotential V_k) and the system size is $N = 8$. The effective Hamiltonian we fit is simply $H = g_{22}T_{22}$, with the coefficient fit using only the data at $\Delta L = 2$. The blue points are the numerical data and the orange levels are the result of diagonalising the effective Hamiltonian. This data shows that the agreement becomes worse as the filling fraction decreases, with the agreement very poor for $\nu = 1/4$. To describe this case well one would require higher order terms in the effective Hamiltonian.

6.4 Future Work

We have found accurate theories describing the behaviour of quantum Hall edges relatively close to the Luttinger liquid fixed point. However, the present analysis does not cover the full behaviour of the resulting theories. It would be extremely interesting to analyse the consequences of the remaining terms in greater details, considering for example the implications on the hydrodynamics of the systems, perhaps along similar lines to previous works[80, 106, 139] which have, among other things, considered the potential for shockwaves along the edge. Furthermore, the line of reasoning we use in this paper is readily applicable to any other quantum Hall wavefunction which can be expressed in terms of conformal blocks, which might indicate further interesting results in, for example, the Read-Rezayi states. Finally, given that these results depend intimately on our conjecture of locality and that this is not fully understood, it would be worth exploring exactly

how and why the Hamiltonian can be claimed to be local, something which we partially consider for the integer quantum Hall effect in a future publication[131].

Part III

Concluding Remarks

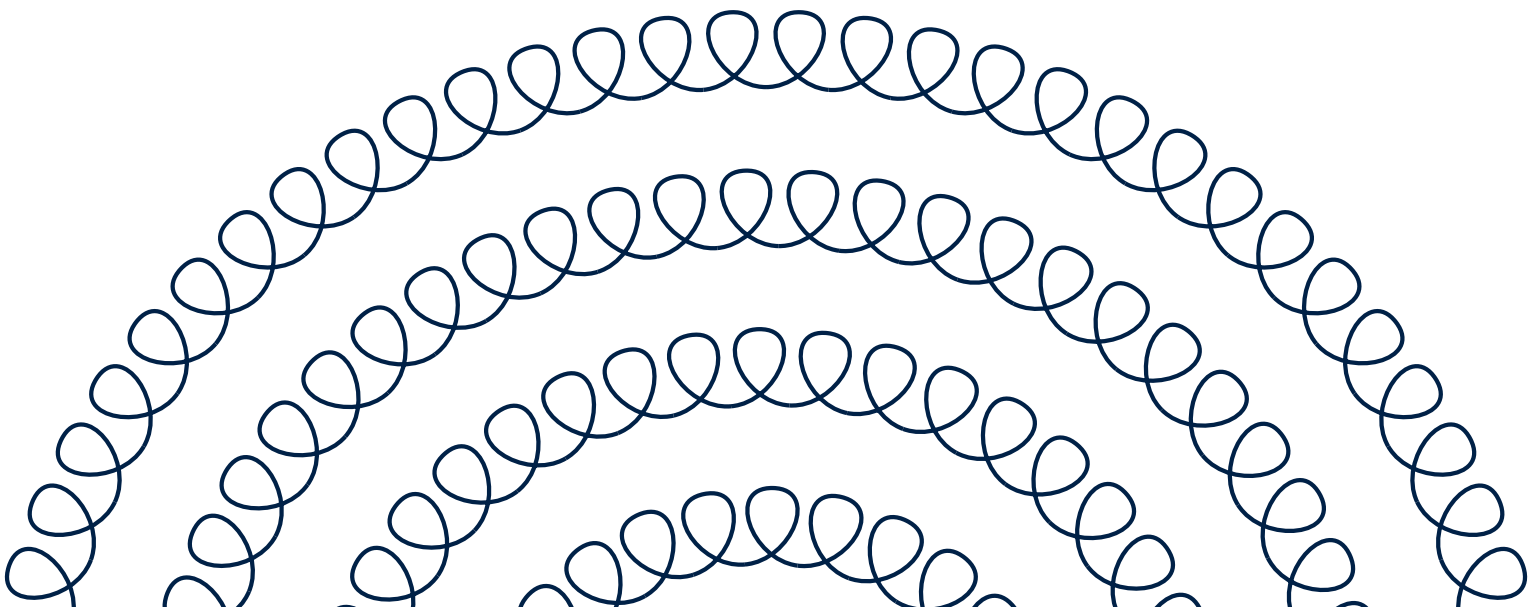

CHAPTER 7

Summary and outlook

That's beyond our borders; you must never go there, Simba.

— Mufasa [The Lion King, 1994]

This thesis has considered a variety of problems in quantum Hall edge physics. We have found the exact solution for the edge behaviour in a particularly extreme limit, finding that the eigenstates correspond to Jack polynomials with a strange dispersion relation. We have also looked in detail at the validity of conjectures regarding the edge state inner products for two particularly important quantum Hall states. Finally, we have produced highly accurate effective descriptions of the dynamics of edge states in cases close to the Luttinger liquid fixed point corresponding to low energies and large system sizes.

More specifically, in Chapter 3 we provided an analytic solution for the edge excitations of Laughlin states in a steep confinement limit. We found that the eigenfunctions are the Jack polynomials analogous to the Calogero-Sutherland model, but the eigenenergies are wildly different from that model. The dispersion even suggests novel new behaviour such as the possibility for counter-propagating edge modes, a phenomenon which arises due to the correlation of the outermost particles with the bulk droplet.

We have also provided an in-depth analysis of the inner products of quantum Hall edge states in both the Laughlin and Moore-Read states. We find that the form for the inner product conjectured in Ref. [34] agrees very well with the

numerical data, especially for larger system sizes. We are also able to fit values of the coefficients involved in this expansion which cannot be constrained by using exact methods. The values determined for certain expansion coefficients match simple analytic forms which may suggest that additional physical constraints are present.

Finally, we looked at the behaviour of quantum Hall edge states in anharmonic traps and in the presence of short-range interactions, generating highly accurate descriptions of the dynamics using a local field theory approach. We showed that these theories are extremely accurate by providing numerical comparison to the low energy structure of both the Laughlin and Moore-Read states. These effective theories show that the addition of bulk translational symmetry causes surprising simplifications in the nonlinear Luttinger liquid expansion. Furthermore, these local descriptions of the edge behaviour are at odds with alternative proposals for the edge state behaviour relying on non-local models such as the quantum Benjamin-Ono equation[81].

To summarise, the methods presented in this thesis shed light on the physics of quantum Hall edges in certain situations though there are, of course, a number of open questions remaining within the field. For example, we have not discussed problems such as the effects of long-range interactions or considered edges with disorder, where translational invariance can no longer be assumed along the boundary. Furthermore, we have focused only on states which admit a construction in terms of conformal field theories, leaving interesting questions regarding the behaviour of systems without such a description, such as the Jain series and the anti-Pfaffian[124, 144]. Additionally, there is a great deal of interesting work on analysing the physics of nonlinear one-dimensional systems that we have barely touched upon in this work[80, 81, 105, 106, 139, 140]. These are rich and interesting problems which will surely continue to produce intriguing results.

Bibliography

[1] Richard Fern and Steven H. Simon. "Quantum Hall edges with hard confinement: Exact solution beyond Luttinger liquid". *Physical Review B* ***95*** (2017), 201108(R).

[2] R. Fern, R. Bondesan, and S. H. Simon. "Structure of edge-state inner products in the fractional quantum Hall effect". *Physical Review B* ***97*** (2018), 155108.

[3] Richard Fern, Roberto Bondesan, and Steven H. Simon. "Effective Edge State Dynamics in the Fractional Quantum Hall Effect". *arXiv:1805.04108* (2018).

[4] Steven H. Simon. *The Oxford Solid State Basics*. OUP Oxford, 2013.

[5] Horst L. Stormer. "Nobel Lecture: The fractional quantum Hall effect". *Reviews of Modern Physics* ***71*** (1999), 875–889.

[6] James Binney and David Skinner. *The Physics of Quantum Mechanics*. OUP Oxford, 2013.

[7] Xiao-Gang Wen. *Quantum Field Theory of Many-Body Systems: From the Origin of Sound to an Origin of Light and Electrons*. OUP Oxford, 2007.

[8] Mikio Nakahara. *Geometry, Topology and Physics, Second Edition*. CRC Press, 2003.

[9] F. Duncan M. Haldane. "Nobel Lecture: Topological quantum matter". *Reviews of Modern Physics* ***89*** (2017), 040502.

[10] Jiannis K. Pachos. *Introduction to Topological Quantum Computation*. Cambridge University Press, 2012.

[11] Xiao-Gang Wen. "Theory of the Edge States in Fractional Quantum Hall Effects". *International Journal of Modern Physics B* ***06*** (1992), 1711–1762.

[12] John David Jackson. *Classical Electrodynamics*. Wiley, 2012.

[13] M V Berry. "Classical adiabatic angles and quantal adiabatic phase". *Journal of Physics A: Mathematical and General* ***18*** (1985), 15–27.

[14] N. D. Mermin. "The topological theory of defects in ordered media". *Reviews of Modern Physics* ***51*** (1979), 591–648.

[15] M. Z. Hasan and C. L. Kane. "Colloquium: Topological insulators". *Reviews of Modern Physics* ***82*** (2010), 3045–3067.

[16] Di Xiao, Ming-Che Chang, and Qian Niu. "Berry phase effects on electronic properties". *Reviews of Modern Physics* ***82*** (2010), 1959–2007.

[17] Alexei Kitaev. "Anyons in an exactly solved model and beyond". *Annals of Physics* ***321*** (2006), 2–111.

[18] D. J. Thouless, M. Kohmoto, M. P. Nightingale, and M. den Nijs. "Quantized Hall Conductance in a Two-Dimensional Periodic Potential". *Physical Review Letters* ***49*** (1982), 405–408.

[19] R. B. Laughlin. "Anomalous Quantum Hall Effect: An Incompressible Quantum Fluid with Fractionally Charged Excitations". *Physical Review Letters* ***50*** (1983), 1395–1398.

[20] V. J. Goldman and B. Su. "Resonant Tunneling in the Quantum Hall Regime: Measurement of Fractional Charge". *Science* ***267*** (1995), 1010–1012.

[21] Daniel Arovas, J. R. Schrieffer, and Frank Wilczek. "Fractional Statistics and the Quantum Hall Effect". *Physical Review Letters* ***53*** (1984), 722–723.

[22] Gregory Moore and Nicholas Read. "Nonabelions in the fractional quantum hall effect". *Nuclear Physics B* ***360*** (1991), 362–396.

[23] N. Read and E. Rezayi. "Beyond paired quantum Hall states: Parafermions and incompressible states in the first excited Landau level". *Physical Review B* ***59*** (1999), 8084–8092.

[24] E. H. Rezayi and N. Read. "Non-Abelian quantized Hall states of electrons at filling factors 12/5 and 13/5 in the first excited Landau level". *Physical Review B* ***79*** (2009).

[25] B. I. Halperin. "Quantized Hall conductance, current-carrying edge states, and the existence of extended states in a two-dimensional disordered potential". *Physical Review B* ***25*** (1982), 2185–2190.

[26] Chetan Nayak, Steven H. Simon, Ady Stern, Michael Freedman, and Sankar Das Sarma. "Non-Abelian anyons and topological quantum computation". *Reviews of Modern Physics* ***80*** (2008), 1083–1159.

[27] David Aasen, Michael Hell, Ryan V. Mishmash, Andrew Higginbotham, Jeroen Danon, Martin Leijnse, Thomas S. Jespersen, Joshua A. Folk, Charles M. Marcus, Karsten Flensberg, and Jason Alicea. "Milestones Toward Majorana-Based Quantum Computing". *Physical Review X* ***6*** (2016), 031016.

[28] A. R. Calderbank and Peter W. Shor. "Good quantum error-correcting codes exist". *Physical Review A* ***54*** (1996), 1098–1105.

[29] C. L. Kane and Matthew P. A. Fisher. "Edge-State Transport". *Perspectives in Quantum Hall Effects*. Wiley-VCH Verlag GmbH, 1996, pp. 109–159.

[30] X. G. Wen. "Chiral Luttinger liquid and the edge excitations in the fractional quantum Hall states". *Physical Review B* ***41*** (1990), 12838–12844.

[31] A. M. Chang. "Chiral Luttinger liquids at the fractional quantum Hall edge". *Reviews of Modern Physics* ***75*** (2003), 1449–1505.

[32] Xiao-Gang Wen, Yong-Shi Wu, and Yasuhiro Hatsugai. "Chiral operator product algebra and edge excitations of a fractional quantum Hall droplet". *Nuclear Physics B* ***422*** (1994), 476–494.

[33] C. W. J. Beenakker. "Edge channels for the fractional quantum Hall effect". *Physical Review Letters* ***64*** (1990), 216–219.

[34] J. Dubail, N. Read, and E. H. Rezayi. "Edge-state inner products and real-space entanglement spectrum of trial quantum Hall states". *Physical Review B* ***86*** (2012), 245310.

[35] Philippe Di Francesco, Pierre Mathieu, and David Sénéchal. *Conformal Field Theory*. Springer New York, 1997.

[36] A. M. Chang, L. N. Pfeiffer, and K. W. West. "Observation of Chiral Luttinger Behavior in Electron Tunneling into Fractional Quantum Hall Edges". *Physical Review Letters* ***77*** (1996), 2538–2541.

[37] M. Grayson, D. C. Tsui, L. N. Pfeiffer, K. W. West, and A. M. Chang. "Continuum of Chiral Luttinger Liquids at the Fractional Quantum Hall Edge". *Physical Review Letters* ***80*** (1998), 1062–1065.

[38] L. Saminadayar, D. C. Glattli, Y. Jin, and B. Etienne. "Observation of the $e/3$ Fractionally Charged Laughlin Quasiparticle". *Physical Review Letters* ***79*** (1997), 2526–2529.

[39] R de-Picciotto, M Reznikov, M Heiblum, V Umansky, G Bunin, and D Mahalu. "Direct observation of a fractional charge". *Physica B: Condensed Matter* ***249-251*** (1998), 395–400.

[40] F. E. Camino, Wei Zhou, and V. J. Goldman. "Realization of a Laughlin quasiparticle interferometer: Observation of fractional statistics". *Physical Review B* ***72*** (2005), 075342.

[41] Nigel R. Cooper and Steven H. Simon. "Signatures of Fractional Exclusion Statistics in the Spectroscopy of Quantum Hall Droplets". *Physical Review Letters* ***114*** (2015), 106802.

[42] N. Regnault and Th. Jolicoeur. "Quantum Hall Fractions in Rotating Bose-Einstein Condensates". *Physical Review Letters* ***91*** (2003), 030402.

[43] Anders S. Sørensen, Eugene Demler, and Mikhail D. Lukin. "Fractional Quantum Hall States of Atoms in Optical Lattices". *Physical Review Letters* ***94*** (2005), 086803.

[44] N.R. Cooper. "Rapidly rotating atomic gases". *Advances in Physics* ***57*** (2008), 539–616.

[45] Nigel R. Cooper and Jean Dalibard. "Reaching Fractional Quantum Hall States with Optical Flux Lattices". *Physical Review Letters* ***110*** (2013), 185301.

[46] Nathan Gemelke, Edina Sarajlic, and Steven Chu. "Rotating Few-body Atomic Systems in the Fractional Quantum Hall Regime". *arXiv:1007.2677* (2010).

[47] Immanuel Bloch, Jean Dalibard, and Wilhelm Zwerger. "Many-body physics with ultracold gases". *Reviews of Modern Physics* ***80*** (2008), 885–964.

[48] J. Eisert, M. Friesdorf, and C. Gogolin. "Quantum many-body systems out of equilibrium". *Nature Physics* ***11*** (2015), 124–130.

[49] Alexander L. Gaunt, Tobias F. Schmidutz, Igor Gotlibovych, Robert P. Smith, and Zoran Hadzibabic. "Bose-Einstein Condensation of Atoms in a Uniform Potential". *Physical Review Letters* ***110*** (2013), 200406.

[50] Markus Greiner, Olaf Mandel, Tilman Esslinger, Theodor W. Hänsch, and Immanuel Bloch. "Quantum phase transition from a superfluid to a Mott insulator in a gas of ultracold atoms". *Nature* ***415*** (2002), 39–44.

[51] Belén Paredes, Artur Widera, Valentin Murg, Olaf Mandel, Simon Fölling, Ignacio Cirac, Gora V. Shlyapnikov, Theodor W. Hänsch, and Immanuel Bloch. "Tonks–Girardeau gas of ultracold atoms in an optical lattice". *Nature* ***429*** (2004), 277–281.

[52] M. Schreiber, S. S. Hodgman, P. Bordia, H. P. Luschen, M. H. Fischer, R. Vosk, E. Altman, U. Schneider, and I. Bloch. "Observation of many-body localization of interacting fermions in a quasirandom optical lattice". *Science* ***349*** (2015), 842–845.

[53] S. M. Girvin. "The Quantum Hall Effect: Novel Excitations And Broken Symmetries". *Aspects topologiques de la physique en basse dimension. Topological aspects of low dimensional systems*. Springer Berlin Heidelberg, 2002, pp. 53–175.

[54] A. H. MacDonald. "Introduction to the Physics of the Quantum Hall Regime". *arXiv:cond-mat/9410047* (1994).

[55] Ady Stern. "Anyons and the quantum Hall effect—A pedagogical review". *Annals of Physics* ***323*** (2008), 204–249.

[56] Richard E. Prange and Steven M. Girvin, eds. *The Quantum Hall Effect*. Springer New York, 1990.

[57] L. D. Landau and E. M. Lifshitz. *Quantum Mechanics: Non-Relativistic Theory*. Elsevier, 1981.

[58] Milton Abramowitz and Irene A. Stegun. *Handbook of Mathematical Functions*. Courier Corporation, 1964.

[59] Klaus von Klitzing. "The quantized Hall effect". *Reviews of Modern Physics* ***58*** (1986), 519–531.

[60] D. C. Tsui, H. L. Stormer, and A. C. Gossard. "Two-Dimensional Magnetotransport in the Extreme Quantum Limit". *Physical Review Letters* ***48*** (1982), 1559–1562.

[61] F. D. M. Haldane and E. H. Rezayi. "Finite-Size Studies of the Incompressible State of the Fractionally Quantized Hall Effect and its Excitations". *Physical Review Letters* ***54*** (1985), 237–240.

[62] Fenner Harper. "The Hofstadter model and other fractional chern insulators". PhD thesis. 2015.

[63] J. Fröhlich and A. Zee. "Large scale physics of the quantum hall fluid". *Nuclear Physics B* ***364*** (1991), 517–540.

[64] V L Pokrovsky and A L Talapov. "A simple model for fractional Hall effect". *Journal of Physics C: Solid State Physics* ***18*** (1985), L691–L694.

[65] S. A. Trugman and S. Kivelson. "Exact results for the fractional quantum Hall effect with general interactions". *Physical Review B* ***31*** (1985), 5280–5284.

[66] Alain Lascoux. *Symmetric Functions and Combinatorial Operators on Polynomials, Issue 99*. American Mathematical Soc., 2003.

[67] Peter Borwein and Tamas Erdelyi. *Polynomials and Polynomial Inequalities*. Springer Science and Business Media, 1995.

[68] I. G. Macdonald. *Symmetric Functions and Hall Polynomials*. Oxford University Press, 2015.

[69] Gabor Szegő. *Orthogonal Polynomials, Volume 23*. American Mathematical Soc., 1939.

[70] Henry Jack. "I.—A class of symmetric polynomials with a parameter". *Proceedings of the Royal Society of Edinburgh. Section A. Mathematical and Physical Sciences* ***69*** (1970), 1–18.

[71] Richard P Stanley. "Some combinatorial properties of Jack symmetric functions". *Advances in Mathematics* ***77*** (1989), 76–115.

[72] P. Fendley, F. Lesage, and H. Saleur. "Solving 1D plasmas and 2D boundary problems using Jack polynomials and functional relations". *Journal of Statistical Physics* ***79*** (1995), 799–819.

[73] Katsuhisa Mimachi and Yasuhiko Yamada. "Singular vectors of the Virasoro algebra in terms of Jack symmetric polynomials". *Communications in Mathematical Physics* ***174*** (1995), 447–455.

[74] Harley Flanders. *Differential Forms with Applications to the Physical Sciences*. Courier Corporation, 1963.

[75] Bill Sutherland. "Exact Results for a Quantum Many-Body Problem in One Dimension". *Physical Review A* ***4*** (1971), 2019–2021.

[76] V. Pasquier. "A lecture on the Calogero-Sutherland models". *Integrable Models and Strings*. Springer Berlin Heidelberg, 2005, pp. 36–48.

[77] Jan Felipe van Diejen and Luc Vinet, eds. *Calogero-Moser-Sutherland Models*. Springer New York, 2000.

[78] Yoshio Kuramoto and Yusuke Kato. *Dynamics of One-Dimensional Quantum Systems*. Cambridge University Press, 2009.

[79] Z.N.C. Ha. "Fractional statistics in one dimension: view from an exactly solvable model". *Nuclear Physics B* ***435*** (1995), 604–636.

[80] E. Bettelheim, Alexander G. Abanov, and P. Wiegmann. "Nonlinear Quantum Shock Waves in Fractional Quantum Hall Edge States". *Physical Review Letters* ***97*** (2006).

[81] P. Wiegmann. "Nonlinear Hydrodynamics and Fractionally Quantized Solitons at the Fractional Quantum Hall Edge". *Physical Review Letters* ***108*** (2012).

[82] B. Andrei Bernevig and F. D. M. Haldane. "Generalized clustering conditions of Jack polynomials at negative Jack parameter α". *Physical Review B* ***77*** (2008), 184502.

[83] B. Andrei Bernevig and F. D. M. Haldane. "Properties of Non-Abelian Fractional Quantum Hall States at Filling $\nu = k/r$". *Physical Review Letters* ***101*** (2008), 246806.

[84] B. Andrei Bernevig and F. D. M. Haldane. "Model Fractional Quantum Hall States and Jack Polynomials". *Physical Review Letters* ***100*** (2008), 246802.

[85] B. Andrei Bernevig and F. D. M. Haldane. "Clustering Properties and Model Wave Functions for Non-Abelian Fractional Quantum Hall Quasielectrons". *Physical Review Letters* ***102*** (2009), 066802.

[86] B. Andrei Bernevig and N. Regnault. "Anatomy of Abelian and Non-Abelian Fractional Quantum Hall States". *Physical Review Letters* ***103*** (2009), 206801.

[87] B Andrei Bernevig, Victor Gurarie, and Steven H Simon. "Central charge and quasihole scaling dimensions from model wavefunctions: toward relating Jack wavefunctions to $\mathcal{W}$-algebras". *Journal of Physics A: Mathematical and Theoretical* ***42*** (2009), 245206.

[88] Ki Hoon Lee, Zi-Xiang Hu, and Xin Wan. "Construction of edge states in fractional quantum Hall systems by Jack polynomials". *Physical Review B* ***89*** (2014), 165124.

[89] Christine Berkesch Zamaere, Stephen Griffeth, and Steven V Sam. "Jack Polynomials as Fractional Quantum Hall States and the Betti Numbers of the $(k+1)$-Equals Ideal". *Communications in Mathematical Physics* ***330*** (2014), 415–434.

[90] Benoit Estienne and B. Andrei Bernevig. "Spin-singlet quantum Hall states and Jack polynomials with a prescribed symmetry". *Nuclear Physics B* ***857*** (2012), 185–206.

[91] Th Jolicoeur and J G Luque. "Highest weight Macdonald and Jack polynomials". *Journal of Physics A: Mathematical and Theoretical* ***44*** (2011), 055204.

[92] Benoit Estienne, Nicolas Regnault, and Raoul Santachiara. "Clustering properties, Jack polynomials and unitary conformal field theories". *Nuclear Physics B* ***824*** (2010), 539–562.

[93] Benoit Estienne, B. Andrei Bernevig, and Raoul Santachiara. "Electron-quasihole duality and second-order differential equation for Read-Rezayi and Jack wave functions". *Physical Review B* ***82*** (2010), 205307.

[94] Benoit Estienne and Raoul Santachiara. "Relating Jack wavefunctions to WA_{k-1} theories". *Journal of Physics A: Mathematical and Theoretical* ***42*** (2009), 445209.

[95] Wendy Baratta and Peter J. Forrester. "Jack polynomial fractional quantum Hall states and their generalizations". *Nuclear Physics B* ***843*** (2011), 362–381.

[96] J. M. Caillol, D. Levesque, J. J. Weis, and J. P. Hansen. "A Monte Carlo study of the classical two-dimensional one-component plasma". *Journal of Statistical Physics* ***28*** (1982), 325–349.

[97] S. M. Girvin, A. H. MacDonald, and P. M. Platzman. "Magneto-roton theory of collective excitations in the fractional quantum Hall effect". *Physical Review B* ***33*** (1986), 2481–2494.

[98] R. Morf and B. I. Halperin. "Monte Carlo evaluation of trial wave functions for the fractional quantized Hall effect: Disk geometry". *Physical Review B* ***33*** (1986), 2221–2246.

[99] G. S. Boebinger, A. M. Chang, H. L. Stormer, and D. C. Tsui. "Magnetic Field Dependence of Activation Energies in the Fractional Quantum Hall Effect". *Physical Review Letters* ***55*** (1985), 1606–1609.

[100] T. W. B. Kibble and Frank H. Berkshire. *Classical Mechanics*. Imperial College Press, 2004.

[101] Victor G. Kac. *Infinite dimensional Lie algebras*. Cambridge University Press, 1990.

[102] S.-i. Tomonaga. "Remarks on Bloch's Method of Sound Waves applied to Many-Fermion Problems". *Progress of Theoretical Physics* ***5*** (1950), 544–569.

[103] Thierry Giamarchi. *Quantum Physics in One Dimension*. Oxford University Press, 2003.

[104] Jan von Delft and Herbert Schoeller. "Bosonization for beginners - refermionization for experts". *Annalen der Physik* ***7*** (1998), 225–305.

[105] Adilet Imambekov, Thomas L. Schmidt, and Leonid I. Glazman. "One-dimensional quantum liquids: Beyond the Luttinger liquid paradigm". *Reviews of Modern Physics* ***84*** (2012), 1253–1306.

[106] Tom Price and Austen Lamacraft. "Quantum Hydrodynamics in One Dimension beyond the Luttinger Liquid". *arXiv:1509.08332* (2015).

[107] Alexander G. Abanov and Paul B. Wiegmann. "Quantum Hydrodynamics, the Quantum Benjamin-Ono Equation, and the Calogero Model". *Physical Review Letters* ***95*** (2005), 076402.

[108] William Fulton. *Young Tableaux*. Cambridge University Press, 1996.

[109] P. Di Francesco, M. Gaudin, C. Itzykson, and F. Lesage. "Laughlin's wave functions, Coulomb gases and expansions of the discriminant". *International Journal of Modern Physics A* ***09*** (1994), 4257–4351.

[110] M. E. J. Newman and G. T. Barkema. *Monte Carlo Methods in Statistical Physics*. Clarendon Press, 1999.

[111] Jainendra Jain. *Composite Fermions*. Cambridge University Press, 2007.

[112] Tobias F. Schmidutz, Igor Gotlibovych, Alexander L. Gaunt, Robert P. Smith, Nir Navon, and Zoran Hadzibabic. "Quantum Joule-Thomson Effect in a Saturated Homogeneous Bose Gas". *Physical Review Letters* ***112*** (2014), 040403.

[113] Paul Ginsparg. "Applied Conformal Field Theory". *arXiv:hep-th/9108028* (1988).

[114] Sylvain Ribault. "Conformal field theory on the plane". *arXiv:1406.4290* (2014).

[115] Dmitry Green. "Strongly Correlated States in Low Dimensions (Thesis)". *arXiv preprint cond-mat/0202455* (2002).

[116] Steven H. Simon, E. H. Rezayi, N. R. Cooper, and I. Berdnikov. "Construction of a paired wave function for spinless electrons at filling fraction $\nu = 2/5$". *Physical Review B* ***75*** (2007), 075317.

[117] E. Ardonne, N. Read, E. Rezayi, and K. Schoutens. "Non-abelian spin-singlet quantum Hall states: wave functions and quasihole state counting". *Nuclear Physics B* ***607*** (2001), 549–576.

[118] T. H. Hansson, M. Hermanns, S. H. Simon, and S. F. Viefers. "Quantum Hall physics: Hierarchies and conformal field theory techniques". *Reviews of Modern Physics* ***89*** (2017), 246401.

[119] M. Storni, R. H. Morf, and S. Das Sarma. "Fractional Quantum Hall State at $\nu = 5/2$ and the Moore-Read Pfaffian". *Physical Review Letters* ***104*** (2010), 076803.

[120] Edward H. Rezayi. "Landau Level Mixing and the Ground State of the $\nu = 5/2$ Quantum Hall Effect". *Physical Review Letters* ***119*** (2017), 026801.

[121] Edward H. Rezayi and Steven H. Simon. "Breaking of Particle-Hole Symmetry by Landau Level Mixing in the $\nu = 5/2$ Quantized Hall State". *Physical Review Letters* ***106*** (2011), 116801.

[122] A. A. Zibrov, C. Kometter, H. Zhou, E. M. Spanton, T. Taniguchi, K. Watanabe, M. P. Zaletel, and A. F. Young. "Tunable interacting composite fermion phases in a half-filled bilayer-graphene Landau level". *Nature* ***549*** (2017), 360–364.

[123] Sung-Sik Lee, Shinsei Ryu, Chetan Nayak, and Matthew P. A. Fisher. "Particle-Hole Symmetry and the $\nu = 5/2$ Quantum Hall State". *Physical Review Letters* ***99*** (2007), 236807.

[124] Michael Levin, Bertrand I. Halperin, and Bernd Rosenow. "Particle-Hole Symmetry and the Pfaffian State". *Physical Review Letters* ***99*** (2007), 236806.

[125] N. Read and E. Rezayi. "Quasiholes and fermionic zero modes of paired fractional quantum Hall states: The mechanism for non-Abelian statistics". *Physical Review B* ***54*** (1996), 16864–16887.

[126] Martin Greiter, Xiao-Gang Wen, and Frank Wilczek. "Paired Hall state at half filling". *Physical Review Letters* ***66*** (1991), 3205–3208.

[127] S. M. Girvin and Terrence Jach. "Formalism for the quantum Hall effect: Hilbert space of analytic functions". *Physical Review B* ***29*** (1984), 5617–5625.

[128] A Zabrodin and P Wiegmann. "Large-N expansion for the 2D Dyson gas". *Journal of Physics A: Mathematical and General* ***39*** (2006), 8933–8963.

[129] J. Dubail, N. Read, and E. H. Rezayi. "Real-space entanglement spectrum of quantum Hall systems". *Physical Review B* ***85*** (2012), 115321.

[130] Hui Li and F. D. M. Haldane. "Entanglement Spectrum as a Generalization of Entanglement Entropy: Identification of Topological Order in Non-Abelian Fractional Quantum Hall Effect States". *Physical Review Letters* ***101*** (2008), 010504.

[131] Roberto Bondesan, Richard Fern, and Steven H. Simon. "Future Publication".

[132] Parsa Bonderson, Victor Gurarie, and Chetan Nayak. "Plasma analogy and non-Abelian statistics for Ising-type quantum Hall states". *Physical Review B* ***83*** (2011), 075303.

[133] N. Read. "Conformal invariance of chiral edge theories". *Physical Review B* ***79*** (2009), 245304.

[134] S. Kirkpatrick, C. D. Gelatt, and M. P. Vecchi. "Optimization by Simulated Annealing". *Science* ***220*** (1983), 671–680.

[135] Michael P. Zaletel and Roger S. K. Mong. "Exact matrix product states for quantum Hall wave functions". *Physical Review B* ***86*** (2012).

[136] B. Estienne, Z. Papić, N. Regnault, and B. A. Bernevig. "Matrix product states for trial quantum Hall states". *Physical Review B* ***87*** (2013).

[137] M. Milovanović and N. Read. "Edge excitations of paired fractional quantum Hall states". *Physical Review B* ***53*** (1996), 13559–13582.

[138] Andrea Cappelli, Carlo A. Trugenberger, and Guillermo R. Zemba. "$W_{1+\infty}$ Dynamics of Edge Excitations in the Quantum Hall Effect". *Annals of Physics* ***246*** (1996), 86–120.

[139] Tom Price and Austen Lamacraft. "Fine structure of the phonon in one dimension from quantum hydrodynamics". *Physical Review B* ***90*** (2014), 241415(R).

[140] Tom Price, Dmitry Kovrizhin, and Austen Lamacraft. "Nonlinear Luttinger liquid: Exact result for the Green function in terms of the fourth Painlevé transcendent". *SciPost Physics* ***2*** (2017), 005.

[141] *Effective Hamiltonians Code*. `https://github.com/richardfern57/FQHEEffectiveHamiltonians`.

[142] *The DiagHam Package*. `http://nick-ux.lpa.ens.fr/diagham/wiki/`.

[143] B. Estienne, N. Regnault, and B. A. Bernevig. "Correlation Lengths and Topological Entanglement Entropies of Unitary and Nonunitary Fractional Quantum Hall Wave Functions". *Physical Review Letters* ***114*** (2015), 186801.

[144] J. K. Jain. "Composite-fermion approach for the fractional quantum Hall effect". *Physical Review Letters* ***63*** (1989), 199–202.